Aggregation and fragmentation in reaction-diffusion systems posed in heterogeneous domains

Aggregation and fragmentation in reaction-diffusion systems posed in heterogeneous domains

Oleh Krehel

Printed by Print service Technische Universiteit Eindhoven

CIP-DATA LIBRARY TECHNISCHE UNIVERSITEIT EINDHOVEN

Oleh Krehel

Aggregation and fragmentation in reaction-diffusion systems posed in heterogeneous domains / by Oleh Krehel.

A catalogue record is available from the Eindhoven University of Technology Library

ISBN: 978-90-386-3707-5

Key Words and Phrases: Colloidal transport, microstructures, periodic homogenization, effective coefficients, upscaled equations, aggregation, deposition, error estimates

MSC (2010): 35B27, 74S05, 74Q99

PACS (2010): 82.30.Nr, 82.40.Ck, 82.30.Lp, 87.15.nr

Aggregation and fragmentation in reaction-diffusion systems posed in heterogeneous domains

PROEFSCHRIFT

ter verkrijging van de graad van doctor aan de
Technische Universiteit Eindhoven, op gezag van de
rector magnificus, prof.dr.ir. C.J. van Duijn, voor een
commissie aangewezen door het College
voor Promoties in het openbaar te verdedigen
op maandag 13 oktober 2014 om 16.00 uur

door

Oleh Krehel

geboren te Lviv, Oekraïne

Dit proefschrift is goedgekeurd door de door de promotoren en de samenstelling van de promotiecommissie is als volgt:

voorzitter:	prof.dr. E.H.L. Aarts
1^e promotor:	prof.dr. M.A. Peletier
copromotor:	dr.habil. A. Muntean
leden:	prof.dr.ir. B. Koren
	prof.dr. P. Knabner (Friedrich-Alexander-Universität Erlangen-Nürnberg)
	prof.dr. F. Legoll (Ecole des Ponts ParisTech)
	dr.ir. J.T. Padding
	dr. F.J. Vermolen (Delft University of Technology)

Abstract

Aggregation and fragmentation mechanisms play a major role in the reactive transport of colloidal particles especially in relation to contaminant transport in porous media. In this thesis, we treat the aggregation and fragmentation in the context of reaction-diffusion-advection systems. We use multiscale concepts to develop a mathematical and numerical framework that can be useful in forecasting the transport of colloids. The focus of our research lies on the modeling, analysis and simulation of multiscale reaction-diffusion systems taking place in heterogeneous media.

We investigate the processes first at the pore level and then try to predict their behavior on the observable macroscopic scales. As microstructure model, we consider arrays of periodically distributed pores (i.e. cells with prescribed inner geometry). We show the well-posedness of the microscopic system and then apply both formal and rigorous periodic homogenization techniques to derive the corresponding upscaled system together with explicit formulae for the effective transport and reaction constants.

Within our modeling framework, we additionally treat the Soret and Dufour effects, as the transport of colloidal particles can be influenced by the temperature gradients occurring in the medium, while the particles themselves carry heat and influence the temperature distribution. This combination of transport terms results in a cross-diffusion-like system, for which we prove the well-posedness and study its numerical (*a priori*) analysis.

We show that our class of models is able to predict within the experimental range the effect of colloid deposition on the transport of matter in soils. Essentially, we have recovered the experimental results obtained by M. Elimelech and collaborators in [61].

This thesis sets up a modeling framework which can be helpful in further multiscale investigations of colloidal transport in heterogeneous media.

Contents

Chapter 1

Introduction

1.1 Background

Particles with sizes less than 1 μm are typically classified as colloids. If many such colloids are present within a flow passing through confined regions, then their interaction and dispersion affects the transport properties of the flow in a non-trivial manner. As a rule of thumb, the stronger the colloidal interactions, the more complex the flow behavior [31]. The analogy goes beyond non-living particles – inspiration from the experimental and theoretical understanding of colloidal systems has become nowadays a tool to explore living systems like pedestrian flows (see e.g. [90]), growth of collagen networks (see e.g. [78]), and transport in plant tissues (see e.g. [20]). If the host media are heterogeneous, then challenges appear for both experimental and theoretical approaches; see for instance [38] and [108].

This thesis focuses on the modeling, analysis and simulation of the transport of colloids in heterogeneous domains (for instance, in porous media), with a particular emphasis on *aggregation*, *fragmentation*, *deposition*, and the effects induced by the presence of *coupled fluxes*.

It is worth noting that most of our considerations can be used to handle similar aspects for conceptually different modeling scenarios (like the dynamics of crowds within corridors or the self-assembly of polymeric networks). To fix ideas and also to be able to validate our modeling approach, we study the case of the transport and interaction of populations of finitely many size classes of colloidal particles in porous media composed of arrays of periodically distributed pores (microstructures). Paying special attention to aggregation effects between size classes, and hence, to the granularity of the flow, this thesis can be seen as a follow up research along the lines open in recent multiscale works, e.g., cf. [35], [59], [108], and [38].

The main mathematical difficulties encountered in this framework are due to

- the presence of coupled fluxes (i.e. due to the Soret and Dufour effects);
- the nonlinearity of the Smoluchowski production term;
- the non-dissipative feature of the deposition component of the model;

- the coupling induced by the structure of the production term by Henry's law.

Our working techniques, facing these difficulties, include basic estimates like L^∞, energy and positivity estimates, as well as fixed-point arguments, two-scale convergence and compactness for periodic media together with *a priori* error estimates on FEM Galerkin approximates very much in the spirit of V. Thomée; see for instance [121] and references cited therein.

We look for a mathematically well-posed class of reaction-diffusion systems that is able to describe at low spatial scales the motion, interaction, and deposition of populations of colloids as well as their interplay with heat conduction effects in media with microstructures. As ultimate goal, we wish to have an upscaled version of such a model that is flexible enough to recover experimental data, in a numerically efficient way in 2D and 3D situations. Once the trust in such an upscaled model and numerical approximation tool is reached, multiscale finite elements (MsFEM, see e.g. [56], [17]) way of thinking can introduce fluctuations (microstructure information) back into the model equations improving this way the chance of obtaining better predictions when highly heterogeneous media are involved.

1.2 Synopsis of the thesis

The thesis is structured as follows:

Chapter 2 is devoted to the basic modeling of colloidal interactions, treated at the pore scale. This is the place where the main reaction kinetics that couples the system of equations is described in detail, including various parameters of the continuous medium that influence these interactions. We also use this place to discuss a prominent example of group formation in a particular type of a pedestrian flow.

In Chapter 3, we focus on the deposition of colloids on grain surfaces within a porous medium. We extend our microscopic model from Chapter 2 by adding immobile species that live on the grain surface and describe their evolution. We apply formal asymptotic homogenization techniques to the extended model. As a result, we obtain an upscaled model with effective coefficients that depend on the information from the microscopic scale. We perform simulation studies for this basic model and compare the model output (profiles of colloidal populations) with the experimental data by M. Elimelech and collaborators (see [60], [61]).

In Chapter 4, we further extend the model from Chapter 3 by coupling the existing microscopic system with heat conduction, leading the way to nonlinearly coupled flux-like terms called in the literature *the Soret and Dufour effects* (see e.g. [46]).

We study the well-posedness of this further extended system, and ensure the positivity and L^∞ bounds on the concentrations and temperature. We are able to prove here the global-in-time existence of solutions. As next step, we proceed

with the averaging. We use two-scale convergence in the spirit of [1] (see also [95], [13], [86], [24]) to derive rigorously the corresponding upscaled system.

Chapter 5 presents the discretization techniques required to solve our problem and comments on the details of using and extending the simulation platforms DUNE [7] and deal.II [5] to cope with the structure of our model equations. Also, here we point out a few relevant implementation details.

The role of Chapter 6 is to ensure that the the discretization schemes used in this thesis (cf. Chapter 2 and Chapter 3) lead actually to convergent finite element Galerkin approximates. To this end, we prove the semi-discrete error bounds for the FEM discretization of the thermal diffusion problem, followed by the fully discrete error analysis.

Note that the Chapters 2 - 6 can be read independently. We conclude the thesis with Chapter 7, where we show a few conclusions of this work. Furthermore, we point out a few open issues and possible future research directions.

Chapter 2

Modeling Aggregation and Fragmentation in Homogeneous Media

2.1 Introduction

Small particles with sizes within the range $1 - 10^3$ nm are typically referred to as colloids. A few concrete examples of materials that fall in this size range are fine clay particles, iron oxides, humid substances, bacteria and viruses (see e.g. [31], [80], [58]). Natural colloids have been found in large amounts in waters of diverse geological environments [119]. They are mobile in groundwater and thus can play an important role in the transport of contaminants [122]. Similarly, they are important for the efficiency of drug delivery designs [87].

In suspensions, such populations of particles interact via basic attraction and repulsion mechanisms (explained in detail in e.g. [31]) which finally lead to clusters – groups of particles sticking together and having a joint evolution. These clusters are subjected to aggregation and fragmentation depending on their distribution and the configuration of the medium in which they are suspended.

This Chapter discusses the mechanisms of colloidal aggregation and fragmentation at the level of populations of colloids having a discrete distribution of sizes. Although theoretically it is possible to handle the case of an infinite number of sizes, we focus our attention to the practical case of finitely many size classes. The main reason is that straightforward discretizations of the Becker-Döring and/or Smoluchowski systems are natural mathematical models to describe the evolution of a finite number of populations of colloids with distinct sizes [67].

Throughout this thesis, $N \in \mathbb{N}$ denotes the maximum size class allowed. In the coming Chapters, this N should be seen as a fixed large number (for instance, $N \approx 1000$ for collagen). Note however, that in most practical situations a small value of N is sufficient. In other cases, it is legitimate to wonder what happens when this threshold N goes to infinity. We do not touch this aspect here.

The Chapter is organized as follows. We present in Section 2.2 the basic modeling of aggregation and fragmentation in homogeneous media of finitely many discrete size classes. This is the bulk of the Chapter. The case of a heterogeneous

media is much more complex and is addressed in the reminder of the thesis. In Section 2.2, we decide to list a number of practical approximations of interaction convolution integrals, their moments, etc. The list is far from exhaustive, but it gives nevertheless a general impression on these common facts. We called them "practical approximations" mainly because of their use and general acceptance in the engineering community. We will used them in Chapter 3 to recover the experimental data from [60]. Also, it is worth mentioning that these choices are used in our implementations discussed in Chapter 5. Note however that the mathematical analysis in Chapter 4 and the numerical analysis in Chapter 6 do not rely on the precise structure of these particular approximations.

We close this part with an example of the application of the modeling methodology to a particular crowd dynamics scenario. We study group formation in pedestrian flows moving in the dark, recovering this way the same cooperation pattern as reported in [25]. The details of this example are explained in [90].

2.2 Background on aggregation and fragmentation of colloids with finitely many discrete size classes

2.2.1 Population balance equations (PBE)

The foundations of aggregation modeling were laid down in the classical work of Smoluchowski [115]. Here we assume that the colloidal population consists of identical particles, called *primary particles*, some of which form aggregate particles that are characterized by the number of primary particles that they contain – i.e. we have u_1 particles of size 1, u_2 particles of size 2, etc. We refer to each particle of size i as a member of the i^{th} species.

The fundamental assumption: aggregation is a second-order rate process [31], i.e. rate of collision is proportional to concentrations of the colliding species. Thus A_{ij} – the number of aggregates (of size $i+j$) formed from particles of sizes i and j per unit time and volume equals:

$$A_{ij} := \alpha_{ij}\beta_{ij}u_i u_j. \tag{2.1}$$

Here β_{ij} is the *collision kernel* – a rate constant determined by *the transport mechanisms* that bring the particles in close contact, while $\alpha_{ij} \in [0,1]$ is the *collision efficiency* – fraction of collisions that finally form an aggregate. α_{ij} are determined by *particle-particle interactions*.
For example, when $\alpha = 0$, the particles are fully stable and no aggregation occurs. And when $\alpha = 1$, the particles are fully destabilized and every collision results in an aggregation. In ([119]) α has been suggested to be of order $10^{-4} - 10^{-6}$ in natural groundwaters and $10^{-1} - 10^{0}$ in seawater for hydrous oxides of Si, Al, and Fe.

From (2.1) it follows that the rate of change of concentration of k-sized aggregates is

$$\frac{du_k}{dt} = \frac{1}{2}\sum_{i+j=k} \alpha_{ij}\beta_{ij}u_i u_j - u_k \sum_{i=1}^{\infty} \alpha_{ki}\beta_{ki}u_i, \tag{2.2}$$

where $u_k(0)$ are prescribed. The first term represents the gain in the k^{th} species by collisions of $i+j=k$. The second term represents the loss of k^{th} species due to collisions with others.

2.2.2 Modeling of β_{ij}

The collision kernel β_{ij} is determined by a combination of three main transport mechanisms:

Perikinetic (cf. [115]):

$$\beta_{ij} := \frac{2kT}{3\mu}\frac{(d_i + d_j)^2}{d_i d_j}; \tag{2.3}$$

Orthokinetic (cf. [115]):

$$\beta_{ij} := \frac{1}{6}G(d_i + d_j)^3; \tag{2.4}$$

Sedimentation (cf. [39]):

$$\beta_{ij} := \frac{\pi g}{72\mu}(\rho_s - \rho)(d_i + d_j)^3(d_i - d_j). \tag{2.5}$$

Perikinetic aggregation results from that fact that colloids, due to their size, undergo Brownian motion. The derivation of (2.3) can be obtained by considering the rate of diffusion of spherical particles to a fixed sphere. Each particle captured by the central sphere is removed from the suspension resulting in a concentration gradient. After the steady-state is established, we can derive the number of particles contacting the fixed sphere in unit time as the product of surface area, diffusion and concentration. Then, it only remains to use the mutual diffusion coefficient instead of the regular one since the central sphere is also in motion.

Orthokinetic aggregation results when the fluid in which they are suspended is subjected to shear. The movement of fluid brings more particles into contact, resulting in aggregation.

Another mechanism that contributes to aggregation is the differential sedimentation - the process when particles of different size are settling from a suspension. Larger particles are sedimenting faster than smaller ones, and capture them as they are falling. A comparison of perikinetic, orthokinetic and sedimentation aggregation rates is given in Figure 2.1.

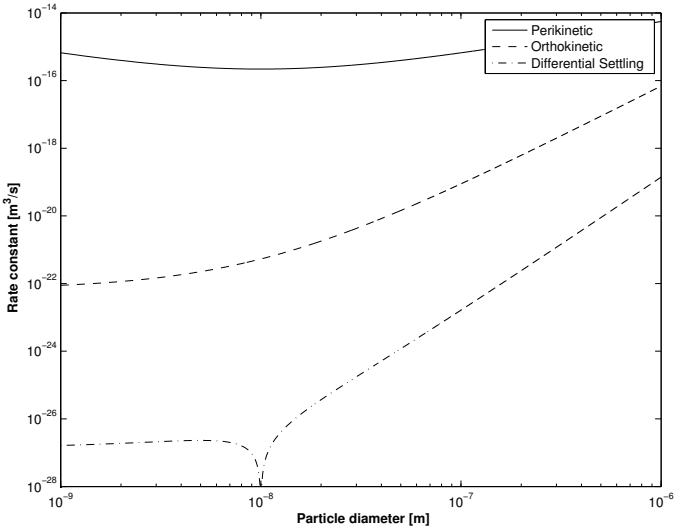

FIGURE 2.1: Comparison of rates for perikinetic, orthokinetic and sedimentation aggregation mechanisms at room temperature in water. d_0=8e-9 m, G=50 1/s.

In (2.3)-(2.5), d_i is the diameter of the i^{th} species, k is the Boltzmann constant, T is the absolute temperature, μ is the dynamic viscosity, G is the local shear rate, ρ is the density of fluid, ρ_s is the density of the aggregate, g is gravitation acceleration. Smoluchowski considered only the case of uniform laminar shear, i.e. $G = \mathrm{d}u/\mathrm{d}x$. Camp and Stein [19] have derived for a more general case a mean velocity gradient:

$$\overline{G} := \sqrt{\frac{\epsilon}{\nu}}, \tag{2.6}$$

where ϵ is the power input per unit mass of fluid and ν is the kinematic viscosity. $\overline{G}$ can be inserted in place of G in (2.4). The relations (2.3) and (2.4) suggest that a coupling of (2.2) to heat conduction equation or the Navier-Stokes equation is possible. We discuss the influence of heat on the colloidal transport in Chapter 4. While a one-way coupling through G being the solution of a Navier-Stokes system is possible, it is beyond the scope of this thesis to investigate the influence of colloidal particles on the flow of the fluid that they are dispersed in.

2.2.3 Fractal dimension

Except for the special case of liquid droplets that coalesce on aggregation, forming a sphere of equivalent volume, aggregates generally have a porous structure – they take up much greater volume than the number of primary particles that constitute them.

Aggregates are typically recognized as *fractal objects* see e.g. [85]. Due to the fractal structure of the aggregates the collision diameters are larger than that of volume-equivalent spheres. Self-similarity of the aggregate results in a power-law relationship between the size and mass of the aggregate. The collision diameter can thus be calculated as:

$$d_i = d_0 i^{\frac{1}{D_F}}, \tag{2.7}$$

where D_F is called the fractal dimension. For geometric reasons, it holds that $1 < D_F \leq 3$. Note that $D_F = 3$ corresponds to entirely compact aggregates, such as coalesced spheres. The lower D_F the more porous is the structure of the aggregate. Typical experimental values of D_F range from 1.8 to 2.1, depending on the transport mechanism and stability of particles.

2.2.4 Colloidal stability

The collision efficiency α_{ij} and its reciprocal – the stability ratio W_{ij} depend on the interaction potential $V_{ij}(h)$ of particles i and j at distance h. The stability ratio was calculated by Fuchs [40]:

$$W_{ij} = 2\int_0^\infty \frac{e^{V_{ij}(h)/kT}}{(\rho+2)^2} d\rho, \text{ where } \quad \rho = \frac{h}{d_i + d_j}. \tag{2.8}$$

The theory of colloid stability of hydrophobic (lyophobic) colloid dispersions most commonly accepted is that proposed by Derjaguin and Landau [28] and Verway and Overbeek [125]. Based on this theory, the total potential energy V for the interaction for a two particle system is given by

$$V = V_R + V_A, \tag{2.9}$$

where V_R is the potential energy of repulsion, V_A is the potential energy of attraction.

The potential energy of repulsion can be calculated approximately as indicated by by Reerink and Overbeek [109]:

$$\begin{aligned} V_R^{aa} &= 3.469 \times 10^{19} \varepsilon (kT)^2 (a\gamma^2/v^2) e^{-\tau\rho} \\ &= 4.62 \times 10^{-6} (a\gamma^2/v^2) e^{-\tau\rho} = C\, e^{-\tau\rho}, \end{aligned} \tag{2.10}$$

where

$$\begin{aligned} &\gamma = (e^z - 1)/(e^z + 1), \qquad z = ve\psi_\sigma/2kT, \\ &\tau = \kappa a \qquad u = H_0/a, \end{aligned} \tag{2.11}$$

In (2.10)-(2.11), ε - dielectric constant of the suspension, a - particle radius, v - valency,

κ - reciprocal Debye-Hückel double-layer thickness, H_0 - particle separation, and ψ_σ is Stern potential.

For the repulsion between two unequal spheres of radii a and b, we take

$$V_R^{ab} = \frac{2b}{a+b} \times V_R^{aa}, \quad b > a. \tag{2.12}$$

The potential energy of attraction for two spherical particles of equal size has been given by Hamaker (see [50], [120]) as

$$V_A^{aa} = -\frac{A}{12}\left(\frac{1}{x^2+2x} + \frac{1}{x^2+2x+1} + 2ln\frac{x^2+2x}{x^2+2x+1}\right), \tag{2.13}$$

where $x = \rho/2$.

In (2.13), A is the Hamaker constant (tabulated in [80, A9.1]), which for particles of first material immersed in a liquid medium of second material is given by:

$$A = (\sqrt{A_{11}} - \sqrt{A_{22}})^2. \tag{2.14}$$

V_A^{ab} for unequal spheres can be calculated as in (2.12)

2.2.5 Fragmentation / breakage mechanism

The discrete coagulation-fragmentation equation is described in [117], for instance, as follows:

$$\begin{aligned}\frac{du_k}{dt} =& \frac{1}{2}\sum_{i+j=k}\beta_{ij}u_iu_j - u_k\sum_{i=1}^{N}\beta_{ki}u_i \\ &- b_ku_k + \sum_{i=k}^{N} d_{ki}b_iu_i,\end{aligned} \tag{2.15}$$

where b_k - fragmentation rate of flocs of size k, d_{ki} - breakage distribution defining the volume fraction of the fragments of size k coming from i-sized particles (see e.g. [64], [101] for details). We denote by N the largest size class that we consider. Although (2.15) is just a system of ODEs, i.e. there's no space component involved, it still is challenging to solve numerically, since N can be very large, reaching millions in some cases. To see this, consider an aggregate as a lattice for primary particles. Allowing for the aggregate to be 200 primary particles-wide in each direction (which is allowable by the $1-1000$ nm colloidal range), the largest aggregate can contain 200^3 primary particles. A few methods to reduce the amount of unknowns to make the system (2.15) computationally tractable are discussed in Chapter 5.

2.2.6 The advection-diffusion-reaction equations

Different aggregates have varying size, which allows us to prescribe different diffusion coefficients D_k to the species according to Einstein-Stokes relation (see,

e.g. [30]). The advection rates c_k can also be influenced by the particle size (c.f. [84], [114]) The resulting transport equation is:

$$\begin{aligned}\frac{du_k}{dt} =&\nabla \cdot (D_k \nabla u_k - c_k u_k) + \frac{1}{2} \sum_{i+j=k} \beta_{ij} u_i u_j - u_k \sum_{i=1}^{N} \beta_{ki} u_i \\ &- b_k u_k + \sum_{i=k}^{N} d_{ki} b_i u_i.\end{aligned} \tag{2.16}$$

The system (2.16) has to be completed by the appropriate initial and boundary conditions. These equations are discussed in more detail in Chapter 3. It is worth noting that equations (2.16) (the so-called Smoluchowski system) can be derived rigorously from an interacting particle system as described in [47].

2.3 Application to the modeling of group formation in pedestrian flows

Inspired by the modeling of charged colloids transport in porous media (see e.g. [68, 106]), we consider now a system of reaction-diffusion equations describing the aggregation and fragmentation (dissolution) of social groups (groups of pedestrians); the ith variable in the vector of unknowns represents the specific size of the subgroup i (density of the i-mer u_i). Here u_1 – density of crowds of group size one (individuals), u_2 – density of groups of size two, and so on until u_N are the corresponding Radon-Nikodym derivatives of suitable measures (see the Appendix of [90]).

The following equations describe our system:

$$\partial_t u_1 + \nabla \cdot (-d_1 \nabla u_1) = -u_1 \sum_{i=1}^{N-1} \beta_i u_i + \sum_{i=2}^{N} \alpha_i u_i - \beta_1 u_1 u_1 + \alpha_2 u_2 \tag{2.17}$$

$$\partial_t u_2 + \nabla \cdot (-d_2 \nabla u_2) = \beta_1 u_1 u_1 - \beta_2 u_2 u_1 + \alpha_3 u_3 - \alpha_2 u_2 \tag{2.18}$$

$$\vdots$$

$$\partial_t u_{N-1} + \nabla \cdot (-d_{N-1} \nabla u_{N-1}) = \beta_{N-2} u_{N-2} u_1 - \tag{2.19}$$

$$- \beta_{N-1} u_{N-1} u_1 + \alpha_N u_N - \alpha_{N-1} u_{N-1} \tag{2.20}$$

$$\partial_t u_N + \nabla \cdot (-d_N \nabla u_N) = \beta_{N-1} u_{N-1} u_1 - \alpha_N u_N. \tag{2.21}$$

This system of partial differential equations indicates that groups diffuse inside Ω. If the groups meet each other, then they start to interact via the mechanism suggested by the right-hand side of the system (aggregation or fragmentation being the only allowed interaction behaviors). Note that the aggregation mechanism in (2.17)-(2.21) is a simplification of the Smoluchowski mechanism in which species aggregate only if one of them is of size one (the Becker-Döering dynamics). From the modeling point of view, it means that only individuals

are allowed to join a group, i.e. two groups that meet keep going their separate ways. We take as boundary conditions

$$u_1 = 0 \qquad \text{on } \Gamma_D \tag{2.22}$$

$$-d_1 \nabla u_1 \cdot n = 0 \qquad \text{on } \partial\Omega \setminus \Gamma_D \tag{2.23}$$

$$-d_i \nabla u_i \cdot n = 0 \qquad \text{on } \partial\Omega, i \in \{2, \dots, N\}, \tag{2.24}$$

while the initial conditions at $t = 0$ are

$$u_1 = M \qquad \text{in } \Omega \tag{2.25}$$

$$u_i = 0 \qquad \text{in } \Omega, i \in \{2, \dots, N\}. \tag{2.26}$$

These boundary conditions model the following scenario: only the population of size one is allowed to exit, all the other groups need to split in smaller groups close to Γ_D. In (2.26), $M > 0$ denotes the initial density of individuals, the total number [of pedestrians] in the system being $\int_\Omega \sum_{i=1}^N i u_i$. The total mass at $t = 0$ is $M|\Omega|$. Note that (2.25) indicates that, initially, groups are not yet formed. Group formation happens here immediately after the initial time. As transport mechanism, we have chosen to use Fickian diffusion fluxes to model the mesoscopic erratic motion of the crowd [with all its N group structures] inside the corridor Ω.

Similarly to the case of moving colloidal particles in porous media (cf. for instance [68] and references cited therein), we take as reference diffusion coefficients the ones given the Stokes-Einstein relation, i.e. the diffusion coefficient of the social conglomeration is inversely proportional to its size as described by $d_i := \frac{1}{\sqrt{i}}$ (which would correspond to the colloidal particles diffusion in 2D) for any $i \in \{1, \dots, N\}$; see for instance [30]. In contrast to the case of transport in porous media, we assume that no heterogeneities are present inside Ω. Consequently, the diffusion coefficients are taken here to be independent of the space and time variables. If heterogeneities were present (like it is nearly always the case e.g. in shopping malls), then one needs to introduce concepts like local porosity and porosity measures as in [33]; see [22] for a related scenario discussing stochastically interacting self propelled particles within a heterogeneous media with dynamic obstacles. We restrict ourselves here to the case of homogeneous corridors.

We take the degradation (dissociation, group splitting) coefficients $\alpha_i > 0$ ($i \in \{2, \dots, N\}$) as being given constants, while for the aggregation coefficients we use the concept of *social threshold*. We define

$$\beta_i := \begin{cases} i & i < T \\ 1 & i \geq T, \end{cases} \tag{2.27}$$

where $T \in (0, \infty)$ is the social threshold. Essentially, using (2.27) we expect that the choice of T essentially limits the size of groups that can be formed by means of this Becker-Döring-like model. In other words, even if large values of

N are allowed (say mimicking $N \to \infty$) most likely groups of sizes around $\lfloor T \rfloor$ will be created; here $\lfloor p \rfloor$ denotes the integer part of $p \in \mathbb{R}$. For an analysis of Becker-Döring-like models see e.g. [118].

For the numerical examples illustrated here, we consider $N = 20$ species waking inside the corridor $\Omega = (0,1) \times (0,1)$. On the boundary $\partial\Omega$, we design the door $\Gamma_D = \{(x,y) : x = 0, y \in [0.4, 0.6]\}$, while the rest of the boundary $\partial\Omega \setminus \Gamma_D$ is considered to be impermeable, i.e. the pedestrians cannot penetrate the wall $\partial\Omega \setminus \Gamma_D$.

The goal of our simulation scenarios is to provide insight into whether it's beneficial to group up when exiting the building, or it's better to go alone. To see this we compare the exiting flux of people averaged over large time for various values of the social threshold T.

To solve the system numerically, we use the library DUNE and rely on a 2D Finite Element method discretization (with linear Lagrange elements) for the space variable, with implicit time-stepping. Note that we allow only crowds of size one, i.e. u_1, to exit the door. For larger group sizes the door in impenetrable. Such groups need to dissociate first and then attempt to exit. We choose constant degradation coefficients and take as reference values $\alpha_i = 0.7$ ($i \in \{1, \dots, N\}$).

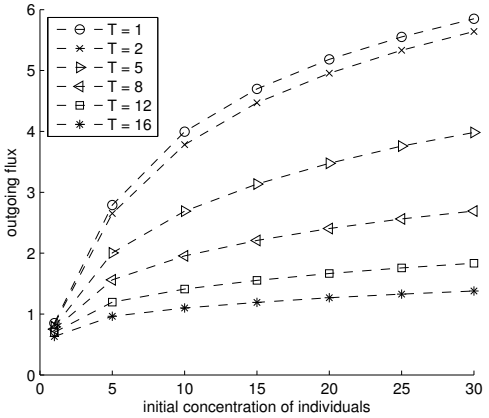

FIGURE 2.2: Outgoing flux with respect to initial density.

As we can see from Figure 2.2, the outgoing flux (close to the steady state[1]) exhibits a polynomial behavior with respect to the initial number of people, where the polynomial exponent is influenced by the choice of the threshold T. It seems than the higher the threshold, the smaller is the polynomial power. This effect is rather dramatic – it indicates that, regardless the threshold size, behaving/moving gregariously is less efficient that performing random walks.

Figure 2.3 shows that there's no apparent saturation for the outgoing flux with respect to the mass: the growth goes on in a polynomial fashion. The linear

[1]The mass exiting the system is re-inserted into Ω following a uniform distribution.

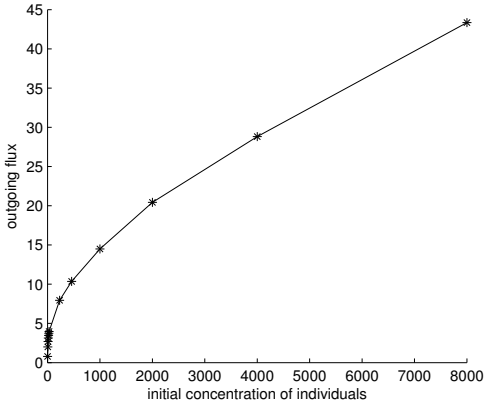

FIGURE 2.3: Outgoing flux for $T = 5$ *versus* large initial data $M \to \infty$.

behavior has been obtained by setting to zero the aggregation and degradation coefficients.

In Figure 2.4, we see that the influence of variable diffusion coefficients is marginal; since a lot of mass exchange is happening in terms of species u_1, setting all the other coefficients $d_2, \ldots, d_N$ to be lower than $d_1 = 1$ (i.e. bigger groups move somewhat slower than individuals) does not affect the output too much. Probably, the effect of diffusion could be stronger as soon as the effective diffusion coefficients are allowed to degenerate with locally vanishing u_i; this is a situation that can be foreseen in a modified setting [48].

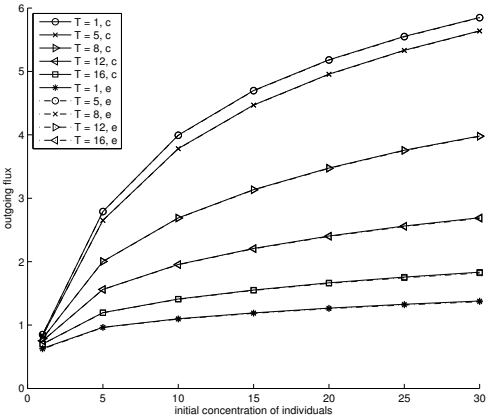

FIGURE 2.4: Homogeneous diffusion (c) and Stokes-Einstein diffusion (e). Note that the profiles are overlapping very closely.

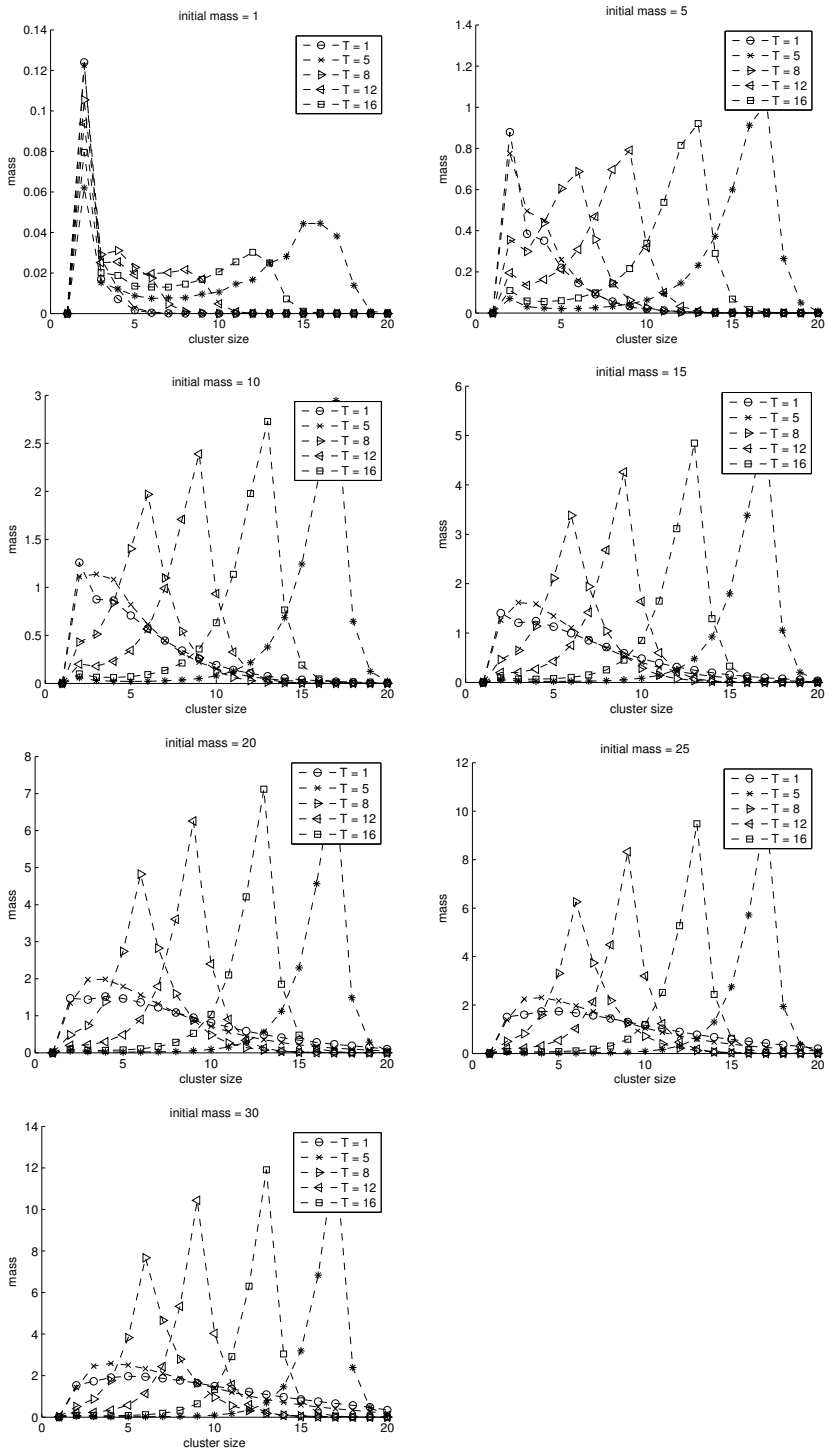

FIGURE 2.5: Steady-state mass distributions. Pile-up effect around group size T.

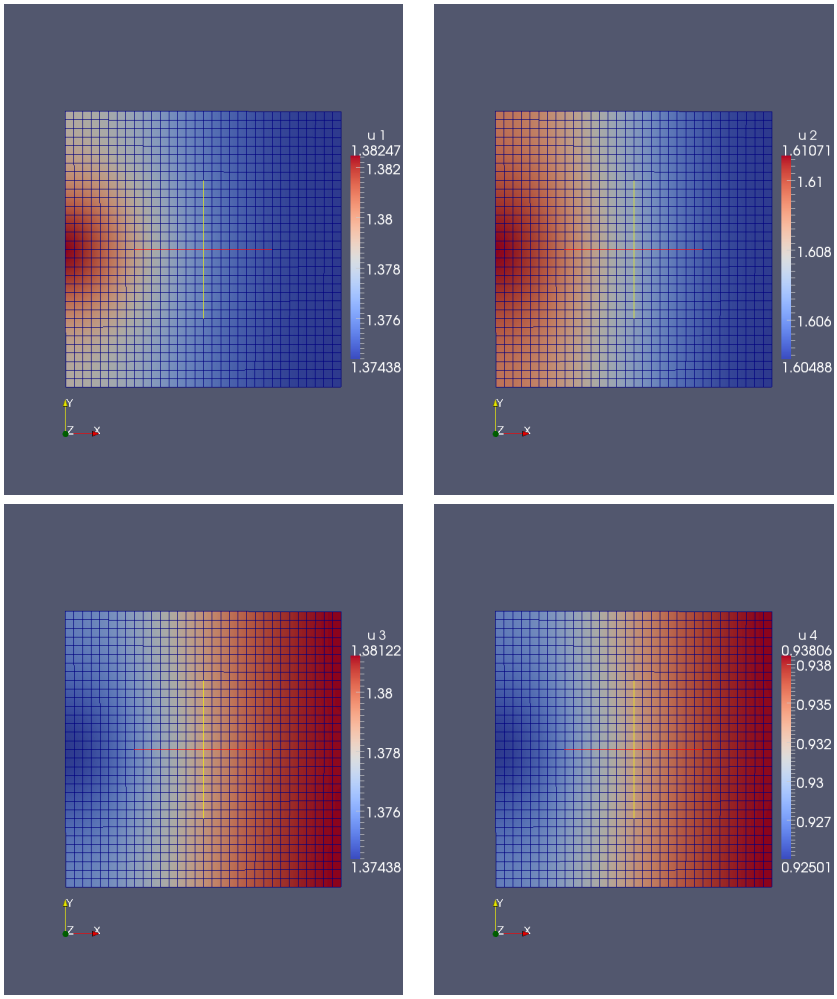

FIGURE 2.6: Clusters behavior close to the exit. The case of u_1–u_4.

In Figure 2.6, we see the mass escaping from the clusters u_1–u_4 in the neighborhood of the exit. Note the dramatic change in u_1 compared to what happens with the other group sizes. It is visible that large group have to stay in the queue until the small groups exit.

On the other hand, we can see in Figure 2.7 how the crowd breakage directly influences the outward flux. Essentially, a faster splitting of the groups tends to increase the averaged outgoing (evacuation) flux. This effect is due to our choice of boundary conditions at the exit.

Our results here are in agreement with the results of [25], which use a lattice model to investigate pedestrian flows. Their cellular automata model uses a 2D lattice with any number of individuals allowed to occupy each site. At each time

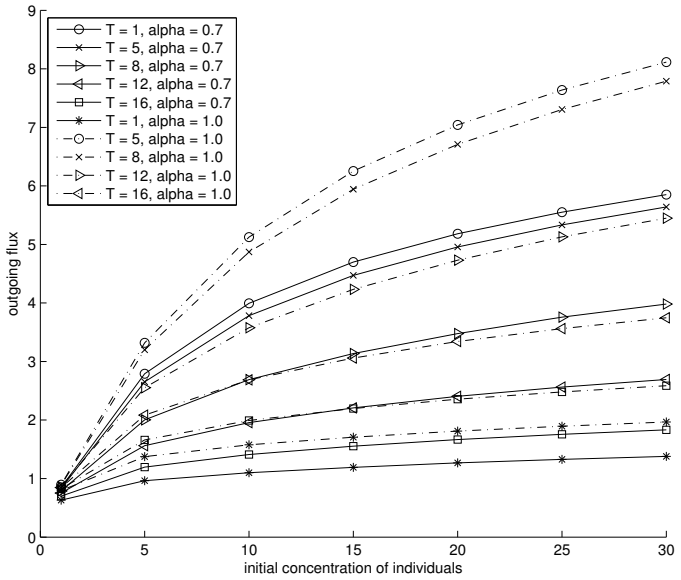

FIGURE 2.7: Comparison of outgoing flux for different values of degradation coefficients α.

tick, the probability of each individual moving in one of four directions is based on the amount of individuals in these directions and the social threshold.

A challenging question is to derive the mean field limit of the lattice model and compare it to our model. Another interesting question is the coupling of the lattice model and our model within a single multiscale network. More discussions on these topics are given in [90]. It is also of interest to try derive the reaction coefficients from a psychological point of view using cognitive group dynamics [26].

Chapter 3

Modeling Deposition of Colloids in Porous Media

3.1 Introduction

The dynamics of colloidal particles plays a significant functional role in a number of technological and biological applications, such as waste water treatment, food industry, printing, design of drug delivery; see e.g. [100, 110]. The existing literature on colloids and their dynamics is huge. Here we only mention that the self-assembly of collagen structures (basic component of the mechanics of the human body) together with secondary nucleation effects have recently been treated in [78], starting off from an interacting particle system for colloids. A detailed discussion of the main principles of aggregation mechanisms can be found in [102], while a thorough analysis of the aggregation in terms of ordinary differential equations can be found e.g. in [18].

The central topic of this chapter is the treatment of the aggregation and deposition of colloids in porous media (particularly, soils) that has been recently shown to be a dominant factor in estimating contaminant transport; see [122]. Essentially, one supposes that that the presence of colloidal aggregation strongly affects the deposition rates on the pore (grain) boundary. Similar aggregation (group formation, cooperation) patterns can emerge also in pedestrian flows strongly affecting their viscosity [90]. Previous investigations on contaminant dynamics in soils, yet not accounting explicitly for aggregation, can be found, for instance, in [65] and [123].

Our aim here is to study the influence of multiscale aggregation and deposition on the colloidal dynamics in a saturated porous medium mimicking a column experiment performed by Johnson, Sun and Elimelech and reported in [61]. For more information on this experimental context, we refer the reader also to Refs. [79, 60]. To get more theoretical insight in this column experiment, we proceed as follows: As departure point, we assume that at the pore scale we can model the aggregation of colloids by the Smoluchowski equation. Consequently, the colloidal mass is distributed between different size clusters. We treat these clusters as different species involved in a coupled diffusion-advection-reaction system. This modeling procedure allows for different material properties to be varied

between the different species, specifically the rates of diffusion, aggregation, deposition as well as the advection velocities. As next step, we apply the periodic homogenization methodology to give insight into the effective coefficients of the upscaled model equations. Finally, for a set of reference parameters, we solve the upscaled equations for different choices of microstructures and investigate the influence of aggregation on both transport and deposition of the colloidal mass, validating in the same time our methodology and numerical platform by means of the results from [61].

The outline of the chapter is as follows: In Section 3.2 we set up a microscopic pore-scale model for aggregation, diffusion and deposition of populations of colloidal particles. In Section 3.3 the microscopic model is nondimensionalized. One of the small dimensionless numbers pointed out therein (denoted by ε) connects a ratio of characteristic time scales of the process to the relevant microscopic and macroscopic length scales arising in the system. In Section 3.4 we use the concept of two-scale asymptotic expansions to obtain in the limit of small ε an equivalent macroscopic model together with the corresponding effective coefficients. We conclude the chapter with a few numerical multiscale experiments and discussions on further work (cf. Section 3.5 and Section 3.6).

3.2 Microscopic model

The foundations of the modeling of colloids aggregation and fragmentation were laid down in the classical work of Smoluchowski [115]. A nice overview can be found, for instance, in [31]. The role of this section is to introduce our modeling Ansatz on the second order kinetics describing the colloidal cluster growth and decline, the functional structure of the deposition rate, as well as the assumptions on the microscopic diffusion coefficients for the clusters.

3.2.1 Aggregation and fragmentation of clusters

We assume that the colloidal population consists of identical particles, called primary particles, some of which form aggregate particles that are characterized by the number of primary particles that they contain – i.e. we have u_1 particles of size 1, u_2 particles of size 2, etc. We refer to each particle of size i as a member of the i^{th} species (or of the $i-$cluster).

The fundamental assumption behind this modeling strategy is that aggregation can be perceived as a second-order rate process, i.e. the rate of collision is proportional to concentrations of the colliding species. Thus A_{ij} – the number of aggregates of size $i+j$ formed from the collision of particles of sizes i and j per unit time and volume, equals:

$$A_{ij} := \gamma_{ij} u_i u_j, \text{ with} \tag{3.1}$$

$$\gamma_{ij} := \alpha_{ij} \beta_{ij}. \tag{3.2}$$

Here β_{ij} is the collision kernel – rate constant determined by the transport mechanisms that bring the particles in close contact, while $\alpha_{ij} \in [0,1]$ is the

collision efficiency – the fraction of collisions that finally form an aggregate. The coefficients α_{ij} are determined by a combination of particle-particle interaction forces, both DLVO (i.e. double-layer repulsion and van der Waals attraction) and non-DLVO, e.g. steric interaction forces (see [28], [50]).

A typical choice for α_{ij} and β_{ij} can be found in for instance in [68]. The interaction rates (written in the spirit of balance of populations balances as reaction rates) should then satisfy

$$R_i(u) = \frac{1}{2}\sum_{i+j=k} \alpha_{ij}\beta_{ij}u_i u_j - u_k \sum_{i=1}^{\infty} \alpha_{ki}\beta_{ki}u_i, \tag{3.3}$$

where $u = (u_1, \ldots, u_N, \ldots)$ is the vector of the concentrations for each size class $i \in \{1, \ldots, N\}$ for a fixed choice of N.

3.2.2 Diffusion coefficients for clusters

We take the diffusivity d_1 of the monomers as a baseline. All the other diffusivities are here assumed to depend on d_1 in agreement with the Einstein-Stokes relation

$$d_i = \frac{kT}{6\pi\eta r_i}. \tag{3.4}$$

The cluster diffusion coefficients d_i arising in (3.4) are designed for the diffusion of spherical particles through liquids at low Reynolds number. In (3.4), T denotes the absolute temperature, k is the Boltzmann factor, η is the dynamic viscosity, while r_i is the aggregate (i-mer, i-cluster) radius. Note the following dependence of the aggregate radius r_i on the number of monomers contained in the i-cluster:

$$r_i = i^{\frac{1}{D_F}} r_1, \tag{3.5}$$

with D_F being a dimensionless parameter called the fractal dimension of the aggregate [85]. D_F indicates how porous the aggregate is. For instance, a completely non-porous aggregate in three dimensions, such as coalesced liquid drops, would have $D_F = 3$. Combining (3.4) and (3.5), we obtain:

$$d_i = \frac{1}{i^{\frac{1}{D_F}}} d_1, \qquad\qquad i \in \{1, \ldots, N\}. \tag{3.6}$$

3.2.3 Deposition rate of colloids on grain surfaces

The colloidal species u_i, defined in Ω (see Figure 3.1), can deposit on the grain boundary of the solid matrix $\Gamma \subset \partial\Omega$, transforming into an immobile species v_i, defined on Γ. This means that the colloids of different size can be present both in the bulk and on the boundary. The boundary condition for Γ then looks like:

$$-d_i \nabla u_i \cdot n = F_i(u_i, v_i). \tag{3.7}$$

The structure of F_i can be quite complex, as seen e.g. in [89], but at this stage, we assume the deposition rate F_i to be linear, which is also a valid modeling choice under certain conditions (c.f. [61]). Namely we take

$$F_i(u_i, v_i) = a_i u_i - b_i v_i, \tag{3.8}$$

this resembles the structure of Henry's law acting in the context of gas exchange at liquid interfaces [9]. In Section 3.5 we will also consider a non-linear choice of F_i.

3.2.4 Setting of the microscopic model equations

Collecting the modeling assumptions from Section 3.2.1, Section 3.2.2, and Section 3.2.3, we see that the microscopic system to be tackled in this context is as follows:

Find $(u_1, \dots, u_N, v_1, \dots, v_N)$ satisfying

$$\partial_t u_i + \nabla \cdot (-d_i \nabla u_i) = R_i(u) \qquad \text{in } \Omega, \tag{3.9}$$
$$\partial_t v_i = a_i u_i - b_i v_i \qquad \text{on } \Gamma, \tag{3.10}$$

with the boundary conditions

$$-d_i \nabla u_i \cdot n = a_i u_i - b_i v_i \qquad \text{on } \Gamma, \tag{3.11}$$
$$-d_i \nabla u_i \cdot n = 0 \qquad \text{on } \Gamma_N, \tag{3.12}$$
$$u_i = u_{iD} \qquad \text{on } \Gamma_D, \tag{3.13}$$

and the initial conditions

$$u_i(0, x) = u_i^0(x) \qquad \text{for } x \in \Omega, \tag{3.14}$$
$$v_i(0, x) = v_i^0(x) \qquad \text{for } x \in \Gamma. \tag{3.15}$$

3.3 Nondimensionalization

Let τ, χ, d, u_0, v_0, and a_0 be reference quantities. We choose the scaling $t := \tau\tilde{t}$, $x := \chi\tilde{x}$, $d_i := d\tilde{d}_i$, $u_i := u_0\tilde{u}_i$, $v_i := v_0\tilde{v}_i$, $a_i := a_0\tilde{a}_i$, and $b_i := \frac{a_0 u_0}{v_0}\tilde{b}_i$. As reference quantities, we select $\chi := L$, $d := d_1$, $u_0 := \max\{u_{i0}, u_{iD} : i \in \{1, \dots, N\}\}$, and $v_0 := \max\{v_{i0} : i \in \{1, \dots, N\}\}$.

Note that we need to distinguish between u_0 and v_0 since they have different dimensions, i.e. volume and surface concentration, respectively. After substituting these scaling relations into (3.9)-(3.15) and dropping the tildes, we obtain:

$$\partial_t u_i + \frac{\tau d}{L^2} \nabla \cdot (-d_i \nabla u_i) = \tau u_0 \beta_{11} R_i(u) \tag{3.16}$$
$$-d_i \nabla u_i \cdot n = \frac{a_0 L}{d}(a_i u_i - b_i v_i) \tag{3.17}$$
$$\partial_t v_i = \frac{\tau a_0}{v_0} u_0 (a_i u_i - b_i v_i). \tag{3.18}$$

Here $\tilde{R}_i(u)$ is a rescaled version of (3.3):

$$\tilde{R}_i(u) = \frac{1}{\beta_{11}} \left(\frac{1}{2} \sum_{i+j=k} \alpha_{ij}\beta_{ij}u_i u_j - u_k \sum_{i=1}^{\infty} \alpha_{ki}\beta_{ki}u_i \right). \tag{3.19}$$

This nondimensionalization procedure involves three relevant dimensionless numbers. We denote by ε our first dimensionless number, viz.

$$\varepsilon := \frac{a_0 L}{d}. \tag{3.20}$$

For our particular scenario, the dimensionless number ε takes a small value (here $\varepsilon \approx$ 7.61e-7). We refer to ε as the *homogenization parameter*. The factor ε is used to take the different scalings of surfaces and volumes into account and thus to allow for a reasonable and meaningful homogenized model, see ([54, p. 130]). It can be seen as the ratio of the characteristic time scales of deposition of particles and macroscopic diffusion. In Section 3.4 we treat ε as the ratio of characteristic micro-macro length scales, $\varepsilon = \frac{l_{pore}}{L}$, where $l_{pore} = \frac{a_0 L^2}{d}$. Furthermore, we choose to scale the time variable in the system by the characteristic time scale of diffusion $\tau := \frac{L^2}{d}$ of the fastest species (i.e. the monomers). This particular choice of time scale leads to two further dimensionless numbers:

- the *Thiele modulus*
$$\Lambda := \frac{L^2}{d} u_0 \beta_{11} \tag{3.21}$$
- the *Biot number*
$$Bi := a_0 \frac{L^2}{d} \frac{u_0}{v_0}. \tag{3.22}$$

According to our reference parameters, we estimate that $\Lambda = 42.91$ and $Bi =$ 7.6914e-08. The order of magnitude of the Thiele modulus Λ indicates that the characteristic reaction time is small compared to the characteristic time of monomers diffusion, the overall reaction-diffusion process being with this scaling in its fast reaction regime. The order of magnitude of the Biot number Bi points out the slow deposition regime. Essentially, since $\frac{L u_0}{v_0} = \mathcal{O}(1)$, we have $Bi = \mathcal{O}(\varepsilon)$. To remove a proportionality constant in the scaled boundary condition (3.25), we take $L := \frac{v_0}{u_0}$.

Finally, we obtain the following dimensionless system of governing equations:

$$\partial_t u_i + \nabla \cdot (-d_i \nabla u_i) = \Lambda R_i(u) \qquad \text{in } \Omega, \tag{3.23}$$
$$\partial_t v_i = Bi(a_i u_i - b_i v_i) \qquad \text{on } \Gamma, \tag{3.24}$$

with the boundary conditions

$$-d_i \nabla u_i \cdot n = \varepsilon(a_i u_i - b_i v_i) \qquad \text{on } \Gamma, \tag{3.25}$$
$$-d_i \nabla u_i \cdot n = 0 \qquad \text{on } \Gamma_N, \tag{3.26}$$
$$u_i(t,x) = \frac{u_D(t,x)}{u_0} \qquad \text{on } \Gamma_D, \tag{3.27}$$

and the initial conditions

$$u_i(0,x) = \frac{u_i^0(x)}{u_0} \qquad \text{for } x \in \Omega, \tag{3.28}$$

$$v_i(0,x) = \frac{v_i^0(x)}{v_0} \qquad \text{for } x \in \Gamma. \tag{3.29}$$

3.4 Derivation of the macroscopic model

In this section, we suppose that our porous medium has an internal structure that can be sufficiently well approximated by an array of periodically-distributed microstructures. For this situation, starting off from a partly dissipative model for the dynamics of large populations of interacting colloids at the pore level (i.e. within the microstructure), we derive upscaled equations governing the approximate macroscopically observable behavior. To do this, we employ the technique of periodic homogenization; see, for instance, [13, 81, 21]. In what follows, we apply the technique in an algorithmic way, giving complete and explicit calculations.

3.4.1 Colloids dynamics in structured media. The periodic homogenization procedure

The porous medium Ω^ε that we consider is modeled here as a composite periodic structure with $\varepsilon > 0$ as a small scale parameter, which relates the the pore length scale to the domain length scale. Ω^ε is depicted in Figure 3.1. We assume in this context that this scale parameter is of the same order of magnitude as ε introduced in (3.20). Note in Figure 3.1 the periodic array of cells approximating the porous media under consideration. Each element is a rescaled (by ε) and translated copy of the standard cell Y.

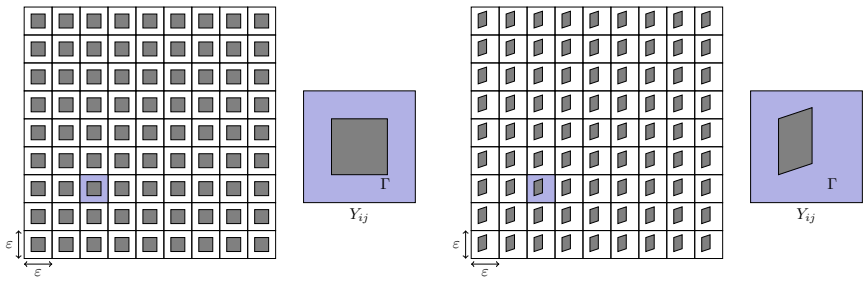

FIGURE 3.1: Microstructure of Ω^ε. Left: isotropic case; Right: anisotropic case. Here Y_{ij} is the periodic cell.

$(0,T)$	= time interval of interest
Ω	= bounded domain in $\mathbb{R}^n$
$\partial\Omega$	$= \Gamma_R \cup \Gamma_N$ piecewise smooth boundary of Ω, $\Gamma_R \cap \Gamma_N = \emptyset$
$\vec{e}_i$	= ith unit vector in $\mathbb{R}^n$ ($n = 2$ or $n = 3$)
Y	$= \{\sum_{i=1}^n \lambda_i \vec{e}_i : 0 < \lambda_i < 1\}$ unit cell in $\mathbb{R}^n$
Y_0	= open subset of Y that represents the solid grain
Y_1	$= Y \setminus \overline{Y}_0$
Γ	$= \partial Y_0$ piecewise smooth boundary of Y_0
X^k	$= X + \sum_{i=1}^n k_i \vec{e}_i$, where $k \in \mathbb{Z}^n$ and $X \subset Y$

TABLE 3.1: ε-independent objects.

Ω_0^ε	$= \cup\{\varepsilon Y_0^k : Y_0^k \subset \Omega^\varepsilon, k \in \mathbb{Z}^n\}$ array of pores
Ω^ε	$= \Omega \setminus \overline{\Omega}_0^\varepsilon$ matrix skeleton
Γ^ε	$= \partial\Omega_0^\varepsilon$ pore boundaries

TABLE 3.2: ε-dependent objects.

Note that Figure 3.1 we use the term "isotropic" loosely. What we mean is that the medium is symmetric in the Cartesian x and y directions.

As customary in periodic homogenization applications, we introduce the fast variable $y := x/\varepsilon$ and let all the unknowns be represented by the following expansions:

$$\begin{cases} u^\varepsilon(x) & := u_0(x,y) + \varepsilon u_1(x,y) + \varepsilon^2 u_2(x,y) + \mathcal{O}(\varepsilon^3), \\ v^\varepsilon(x) & := v_0(x,y) + \varepsilon v_1(x,y) + \varepsilon^2 v_2(x,y) + \mathcal{O}(\varepsilon^3). \end{cases} \tag{3.30}$$

The asymptotic expansions (3.30) can be justified by means of the concept of two-scale convergence by Nguetseng and Allaire; see Chapter 4 for the mathematical analysis of a more complex case including also thermal effects, and [55] for a closely related scenario.

Now, taking into account the chain rule $\nabla := \nabla_x + \frac{1}{\varepsilon}\nabla_y$, we get:

$$\nabla u_i^\varepsilon = \varepsilon^{-1}\nabla_y u_{i,0}^\varepsilon + \varepsilon^0(\nabla_x u_{i,0}^\varepsilon + \nabla_y u_{i,1}^\varepsilon) + \varepsilon^1(\nabla_x u_{i,1}^\varepsilon + \nabla_y u_{i,2}^\varepsilon) + \mathcal{O}(\varepsilon^2).$$
$$\nabla v_i^\varepsilon = \varepsilon^{-1}\nabla_y v_{i,0}^\varepsilon + \varepsilon^0(\nabla_x v_{i,0}^\varepsilon + \nabla_y v_{i,1}^\varepsilon) + \varepsilon^1(\nabla_x v_{i,1}^\varepsilon + \nabla_y v_{i,2}^\varepsilon) + \mathcal{O}(\varepsilon^2).$$

This gives us the following diffusion term:

$$\begin{aligned}\nabla \cdot (d_i(y)\nabla u_i^\varepsilon) = &\varepsilon^{-2}\nabla_y \cdot (d_i(y)\nabla_y u_{i,0}^\varepsilon)\\ &+ \varepsilon^{-1}(d_i(y)\nabla_x \cdot \nabla_y u_{i,0}^\varepsilon + \nabla_y \cdot (d_i(y)\nabla_x u_{i,0}^\varepsilon) + \nabla_y \cdot (d_i(y)\nabla_y u_{i,1}^\varepsilon))\\ &+ \varepsilon^0(d_i(y)\Delta u_{i,0}^\varepsilon + d_i(y)\nabla_x \cdot \nabla_y u_{i,1}^\varepsilon\\ &\quad + \nabla_y \cdot (d_i(y)\nabla_x u_{i,1}^\varepsilon) + \nabla_y \cdot (d_i(y)\nabla_y u_{i,2}^\varepsilon)) + \mathcal{O}(\varepsilon^1).\end{aligned}$$

Collecting the terms with ε^{-2} gives:

$$\nabla_y \cdot (d_i(y)\nabla u_{i,0}^\varepsilon) = 0.$$

Recalling that this PDE with periodic boundary conditions has a solution unique up to a constant, we get $u_{i,0}^\varepsilon = u_{i,0}^\varepsilon(x)$. Consequently, we have $\nabla_y u_{i,0}^\varepsilon = 0$.

The terms with ε^{-1} can be arranged as

$$\nabla_y \cdot (d_i(y)\nabla_y u_{i,1}^\varepsilon) = -\nabla_y d_i(y) \cdot \nabla_x u_{i,0}^\varepsilon. \tag{3.31}$$

Let $w_j(y)$ solve the following *cell problem* endowed with periodic boundary conditions:

$$\nabla_y \cdot (d_i(y)\nabla w_j) = -(\nabla d_i(y))_j \qquad j \in \{1, \dots, d\}, y \in Y \tag{3.32}$$

Using (3.32), we can express the first order term in (3.30) as:

$$u_{i,1}^\varepsilon(x, y) = w(y) \cdot \nabla u_{i,0}^\varepsilon(x) + u_{i,1}^\varepsilon(x), \tag{3.33}$$

where the function $u_{i,1}^\varepsilon(x)$ does not depend on the variable y. Note that

$$\nabla_y u_{i,1}^\varepsilon(x, y) = \nabla w(y) \cdot \nabla u_{i,0}^\varepsilon(x). \tag{3.34}$$

The terms with ε^0 give:

$$\begin{aligned}\partial_t u_{i,0}^\varepsilon = &d_i(y)\Delta u_{i,0}^\varepsilon + d_i(y)\nabla w(y) : \nabla\nabla u_{i,0}^\varepsilon\\ &+ \nabla_y \cdot (d_i(y)\nabla_x u_{i,1}^\varepsilon + d_i(y)\nabla_y u_{i,2}^\varepsilon) + \Lambda R_i(u_0).\end{aligned}$$

Integrating over Y and noting that $|Y| = 1$ yields:

$$\partial_t u_{i,0}^\varepsilon = \bar{\mathbb{D}}_i : \nabla\nabla u_{i,0}^\varepsilon - \int_{\partial Y} d_i(y)(\nabla_x u_{i,1}^\varepsilon + \nabla_y u_{i,2}^\varepsilon) \cdot n d\sigma(y) + \Lambda R_i(u_0). \tag{3.35}$$

The upscaled diffusion tensors $\bar{\mathbb{D}}_i := [\bar{D}_{ijk}]$ reads:

$$\bar{D}_{ijk} = \int_Y d_i(y)(\delta_{jk} + \partial_{y_j} w_k(y))dy \quad i \in \{1, \dots, N\}; j, k \in \{1, \dots, d\}. \tag{3.36}$$

Because of the periodic boundary conditions, the active part of ∂Y is only Γ. Here we have:

$$\partial_t u_{i,0}^\varepsilon = \bar{\mathbb{D}}_i : \nabla\nabla u_{i,0}^\varepsilon - \int_\Gamma d_i(y)(\nabla_x u_{i,1}^\varepsilon + \nabla_y u_{i,2}^\varepsilon) \cdot n d\sigma(y) + \Lambda R_i(u_0). \tag{3.37}$$

The boundary term in (3.37) can be expressed recalling the corresponding deposition boundary condition:

$$- d_i \nabla u_i \cdot n = \varepsilon(a_i^\varepsilon u_i - b_i^\varepsilon v_i^\varepsilon) \tag{3.38}$$

Using the prescribed asymptotic expansions, (3.38) becomes:

$$\begin{aligned} &-d_i(y)(\varepsilon^{-1}\nabla_y u_{i,0}^\varepsilon + \varepsilon^0(\nabla_x u_{i,0}^\varepsilon + \nabla_y u_{i,1}^\varepsilon) + \varepsilon^1(\nabla_x u_{i,1}^\varepsilon + \nabla_y u_{i,2}^\varepsilon)) \cdot n \\ &\quad = a_i^\varepsilon(y)(\varepsilon^1 u_{i,0}^\varepsilon + \varepsilon^2 u_{i,1}^\varepsilon) - b_i^\varepsilon(y)(\varepsilon^1 v_0^\varepsilon + \varepsilon^2 v_1^\varepsilon) + \mathcal{O}(\varepsilon^2). \end{aligned}$$

Consequently, we obtain

$$-d_i(y)(\nabla_x u_{i,1}^\varepsilon + \nabla_y u_{i,2}^\varepsilon) \cdot n = a_i^\varepsilon(y) u_{i,0}^\varepsilon - b_i^\varepsilon(y) v_0^\varepsilon.$$

Finally, the upscaled equation for u_i^ε reads:

$$\partial_t u_i - \nabla \cdot (\bar{\mathbb{D}}_i \nabla u_i) + A_i u_i - B_i v_i = \Lambda R_i(\mathbf{u}). \tag{3.39}$$

Note that the microscopic surface exchange term turns as $\varepsilon \to 0$ into the macroscopic bulk term $A_i u_i - B_i v_i$. Furthermore, the upscaled equation for v_i is

$$\partial_t v_i = A_i u_i - B_i v_i, \tag{3.40}$$

where the effective constants A_i and B_i are defined by

$$A_i := Bi \int_\Gamma a_i(y)\, d\sigma(y) \tag{3.41}$$

and

$$B_i := Bi \int_\Gamma b_i(y)\, d\sigma(y). \tag{3.42}$$

Summarizing, the upscaled system describing the macroscopic dynamics of the colloids is:

$$\begin{aligned}
&\partial_t u_i - \nabla \cdot (\bar{\mathbb{D}}_i \nabla u_i) + A_i u_i - B_i v_i = \Lambda R_i(\mathbf{u}) && \text{in } \Omega, i \in \{1, \dots, N\} && (3.43)\\
&\partial_t v_i = A_i u_i - B_i v_i && \text{in } \Omega, i \in \{1, \dots, N\} && (3.44)\\
&-(\bar{\mathbb{D}}_i \nabla u_i) \cdot n = f_i && \text{on } \Gamma_R, i \in \{1, \dots, N\} && (3.45)\\
&u_i = u_{iD} && \text{on } \Gamma_D, i \in \{1, \dots, N\} && (3.46)\\
&u_i(\cdot, 0) = u_i^0 && \text{in } \Omega, i \in \{1, \dots, N\} && (3.47)\\
&v_i(\cdot, 0) = v_i^0 && \text{in } \Omega, i \in \{1, \dots, N\}. && (3.48)
\end{aligned}$$

3.4.2 Computation of the effective diffusion tensors $\bar{\mathbb{D}}_i = \bar{D}_{ijk}$

We rely on equation (3.36) to approximate the main effective transport coefficients – the effective diffusion tensors $\bar{D}_{ijk}$ responsible in this scenario for the

transport of the N species of colloids. See Table 3.3 for a calculation example (notice the symmetry of the tensors corresponding to the isotropic case).

Figure 3.2 and Figure 3.3 show the solutions to the cell problems (3.32) for the isotropic and anisotropic geometry case, respectively. The 2D solver for elliptic PDE with periodic boundary conditions needed for these periodic cell problems was implemented in C++ using `deal.II` Numerics library; see [5] for details on this platform.

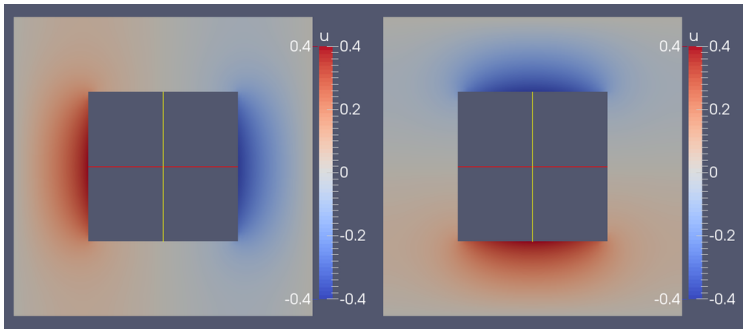

FIGURE 3.2: Solutions to the cell problems that correspond to isotropic periodic geometry (Figure 3.1, left). See Table 3.3 for the resulting effective diffusion tensor.

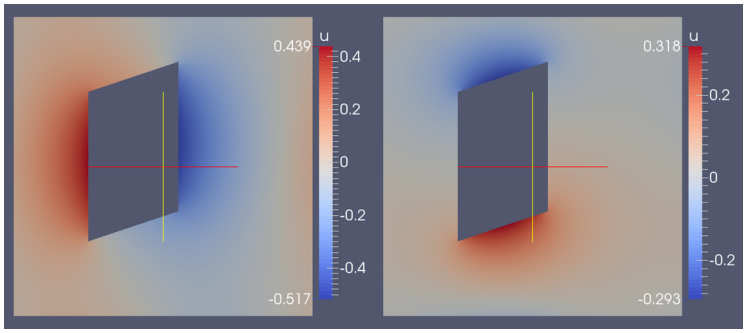

FIGURE 3.3: Solutions to the cell problems that correspond to anisotropic periodic geometry (Figure 3.1, right). See Table 3.3 for the resulting effective diffusion tensor.

Controlling the cell functions allows us also to approximate the tortuosity tensor in a direct manner, avoiding complex analytical calculations hard to justify theoretically or experimentally; compare e.g. with Ref. [49]. An example in this sense is shown in Figure 3.4. To obtain it, we use the relation

$$\bar{\mathbb{D}}_1 = d_1 \phi \bar{\mathbb{T}}^*,$$

Isotropic	Anisotropic
$\bar{\mathbb{D}}_1 = \begin{bmatrix} 0.75 & 0.171476 \\ 0.171476 & 0.75 \end{bmatrix}$	$\bar{\mathbb{D}}_1 = \begin{bmatrix} 0.817467 & 0.0786338 \\ 0.214942 & 0.817467 \end{bmatrix}$

TABLE 3.3: Examples of effective diffusion tensors corresponding to the first species (i.e. to the monomer population) for the two choices of microstructures shown in Figure 3.1.

where d_1 is a scalar diffusion coefficient, ϕ is the porosity, and $\bar{\mathbb{T}}^*$ is the tortuosity (see [10], e.g.) and the fact that for the microstructures shown in Figure 3.1 we know that the porosity for the isotropic case is 0.75, while the porosity for the anisotropic case amounts to 0.85. We refer the reader to [59] for more numerical examples of multiscale investigations of anisotropy effects on transport in periodically perforated media.

Isotropic	Anisotropic
$\bar{\mathbb{T}}^* = \begin{bmatrix} 1.0000 & 0.2286 \\ 0.2286 & 1.0000 \end{bmatrix}$	$\bar{\mathbb{T}}^* = \begin{bmatrix} 0.9617 & 0.0925 \\ 0.2529 & 0.9617 \end{bmatrix}$

TABLE 3.4: Examples of effective tortuosity tensors corresponding to the first species (i.e. the monomer population) for the two choices of microstructures shown in Figure 3.1.

As soon as the covering with microstructures lacks ergodicity and/or stationarity, such evaluations are often replaced by efforts to calculate accurate upper bounds on the prominent effective coefficients; see Ref. [86], for instance, for details in this direction.

3.4.3 Extensions to non-periodic microstructures

One can relax the periodicity assumption on the distribution of the microstructures. Instead of promoting the stochastic homogenization approach (cf. Ref. [127], e.g.) which is prohibitory expensive from the computational point of view, we indicate two computationally tractable cases: (1) the locally periodic arrays of microstructures (see [15, 34, 92]) and (2) the weakly stochastic case (see [76] and references cited therein). We will show elsewhere not only how our model formulation and asymptotics as $\varepsilon \to 0$ translate into the frameworks of these two non-periodic settings, but also the way the new effective transport coefficients can be approximated numerically.

3.5 Simulation studies

In this section, we study how aggregation affects deposition during the transport of colloids in porous media. Within this frame we work with a reference parameter regime pointing out to the *fast aggregation – slow deposition regime*, that is high Λ and low Bi.

We take the model from [61] as the starting point of this discussion and aim at recovering their results. We interpret all coefficients from [61] in terms of our effective coefficients obtained by the asymptotic homogenization performed in Section 3.4. As main task, we search for new effects coming into play due to colloids aggregation.

The model for the evolution of the single mobile colloid species $n(x,t)$ and the surface coverage of the porous matrix by the immobile colloids $\theta(x,t)$ (that corresponds to the amount of mass deposited) is as follows: Find the pair (n,θ) satisfying the balance equations

$$\partial_t n = -v_p \cdot \nabla n + D_h \Delta n - \frac{f}{\pi a_p^2}\partial_t \theta, \tag{3.49}$$

$$\partial_t \theta = \pi a_p^2 k n B(\theta), \tag{3.50}$$

with the switch boundary conditions

$$n(t,0) = \begin{cases} n_0 & t \in [0,t_0] \\ 0 & t > t_0 \end{cases}, \tag{3.51}$$

$$\frac{\partial n}{\partial \nu}(t,L) = 0, \tag{3.52}$$

and initial conditions

$$n(0,x) = 0, \tag{3.53}$$

$$\theta(0,x) = 0,\ x \in [0,L]. \tag{3.54}$$

Here v_p is the interstitial particle velocity of the suspended colloids, D_h is the hydrodynamic particle dispersion, a_p is the particle radius, while f is the specific surface area. t_0 is the switching off time in the boundary condition.

Given a column of cross-section surface S and height Z randomly packed with spherical collector beads of radius a_c and porosity (void volume fraction) ϕ typically of order of 0.4, f can be calculated (cf. [104]) as the ratio of the total surface area of all beads in the column to the void volume ϕZS. For spherical beads of uniform radius, the specific surface area f is

$$f(\phi) := \frac{3(1-\phi)}{\phi a_c}. \tag{3.55}$$

The dynamic blocking function $B(\theta)$ arising in (3.50) accounts for the transient rate of particle deposition. As the colloids accumulate on the surface of the

Interstitial particle velocity	$v_p = \frac{U}{\phi}(2 - (1 - \frac{a_p}{r_0})^2)$
Hydrodynamic dispersion coefficient	$D_h = \frac{D_\infty}{\tau} + \alpha_L v_p$
Particle radius	$a_p = 0.15\,[\mu m]$
Specific surface area	$f = \frac{3(1-\phi)}{\phi a_c}$
Collector grain radius	$a_c = 0.16\,[mm]$
Pore radius	$r_0 = (1.1969\varepsilon - 0.1557)a_c$
Darcy velocity	$U = 1.02 \times 10^{-4}\,[m/s]$
Porosity	$\phi = 0.392\,[-]$
Dispersivity parameter	$\alpha_L = 0.692\,[mm]$
Kinetic rate constant	$k = 0.25\eta U = 5 \times 10^{-7}\,[m/s]$
Characteristic length	$L = 0.101\,[m]$
Characteristic time	$t_0 = 5445\,[s]$
Initial concentration	$n_0 = 5.58 \times 10^8\,[cm^{-3}]$

TABLE 3.5: Reference parameters for simulation studies. The numerical values are taken from [61].

porous matrix, they exclude a part of the surface, limiting the amount of sites for further particle attachment.

We used the Finite Element Numerics toolbox DUNE [7] to implement a solver for the model. We employed the Newton method to deal with the nonlinearities in the aggregation term (counterpart of $R(\cdot)$ cf. Section 3.2.1) and in the blocking function term (here denoted by $B(\cdot)$). An implicit Euler iteration is used for time-stepping.

The first results of our simulation with the reference parameters indicated in Table 3.5 are shown in Figure 3.4. Essentially, a single-species system (3.49)-(3.54) is compared to a two-species system with a square pulse going from one side of the domain for a fixed amount of time in the first species only. The resulting breakthrough curves are plotted. It is of interest to compare the breakthrough curves for the total amount of mass going through, no matter if it is in the form of small or large particles. As we can observe, there is a perceptible difference between the two curves, being the mass for the two-species case coming in slower. This is due to larger particles having higher affinity for deposition.

Let us focus now our attention on a specific aspect of the deposition process, namely on the effect of the dynamic blocking functions. The context is as follows: The rate of colloidal deposition is known to go down as more particles attach themselves the the favorable deposition sites of the porous matrix; see, for instance, [79] and references cited therein.

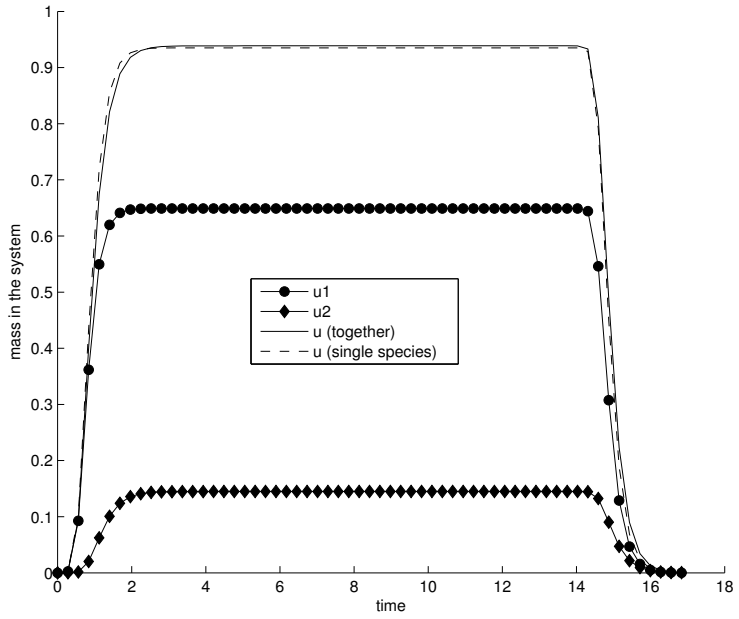

FIGURE 3.4: Simulation comparison for a single species system *versus* an aggregating system. The straight line is the breakthrough curve for the colloidal mass for the problem without aggregation. The dashed line is the breakthrough curve for the colloidal mass for the problem with aggregation. It is obtained by summing mass-wise the breakthrough curves for the monomers u_1 and dimers u_2.

One of the choices for the blocking function in (3.50) corresponds to Langmuir's molecular adsorption model [75]. It is an affine function in terms of θ, reaching the maximum of 1 when the fraction of the surface covered is zero. In other words, $B(\cdot)$ is defined as

$$B(\theta) := 1 - \beta\theta. \tag{3.56}$$

For the simulations, we used the value $\beta = 2.9$. This corresponds to the hard sphere jamming limit $\theta_\infty = 0.345$, which is specific to spherical collector geometry and the experimental conditions described in [60].

A simulation example of our balance equations (3.49)-(3.54) with the Langmuirian blocking function is shown in Figure 3.5.

Another choice is the RSA dynamic blocking function as developed in [112]. RSA stands for "random sequential adsorption". The RSA blocking choice is based on a third order expansion of excluded area effects and can be used for low and moderate surface coverage. Here $B(\theta)$ is defined as:

$$B(\theta) := 1 - 4\theta_\infty\beta\theta + 3.308(\theta_\infty\beta\theta)^2 + 1.4069(\theta_\infty\beta\theta)^3. \tag{3.57}$$

Here, θ_∞ is the hard sphere jamming limit. A simulation example of the balance equations (3.49)-(3.54) including the RSA blocking function is shown in Figure 3.6.

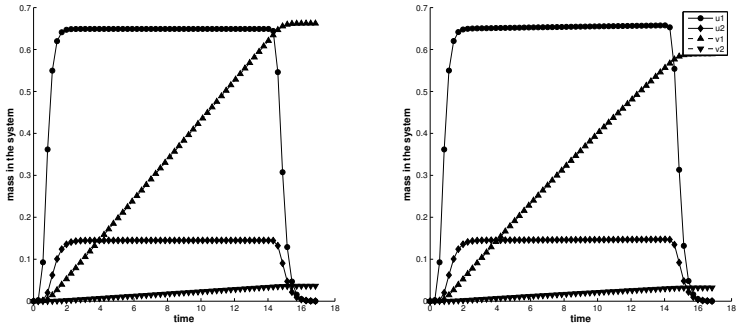

FIGURE 3.5: The effect of the Langmuirian dynamic blocking function on the deposition (right) *versus* no blocking function (left). u_1 and u_2 are the breakthrough curves, while v_1 and v_2 are the concentrations of the deposited species.

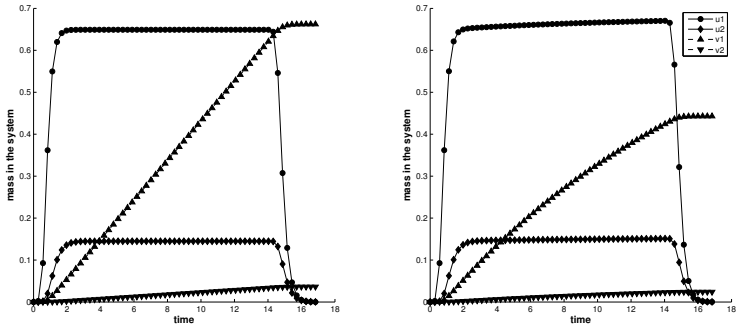

FIGURE 3.6: The effect of the RSA dynamic blocking function on the deposition (right) *versus* no blocking function (left). u_1 and u_2 are the breakthrough curves, while v_1 and v_2 are the concentrations of the deposited species.

3.6 Discussion

This chapter sheds light on transport, aggregation, fragmentation and deposition of colloidal particles in heterogeneous media. We succeeded to recover basic results obtained with standard models for (single class, single species) colloidal transport. Furthermore, our model includes information about the multiscale structure of the porous medium and demonstrates new effects attributed to flocculation, such as the occurrence of an overall decrease in the species mobility

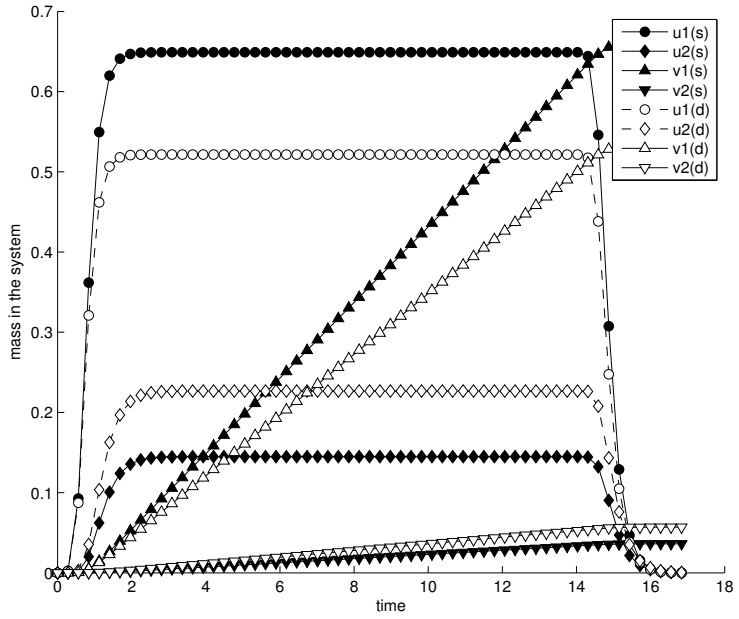

FIGURE 3.7: The effect of aggregation rates on the breakthrough curves. In the first case, the default rate of aggregation is used, in the second - it is doubled. A change of aggregation rate can be achieved by varying the concentration of salt in the suspension, according to the DLVO theory. Note the strong effect of aggregation on deposition.

due to a higher affinity for deposition of the large size classes of colloidal species; see Figure 3.7 for this effect. The simulations show that our model depends continuously on the initial data, the boundary data and the model parameters.

Extensions of this work can go in multiple directions:

(i) Cf. [79], the extent of colloidal transport in groundwater is largely determined by the rate at which colloids deposit on stationary grain surfaces. The assumption of stationarity can be potentially relaxed, thus aiming to incorporate the interplay between biofilms growth and deposition, hence obtaining a better understanding of the clogging/blocking of the pores; see e.g. [99, 107].

(ii) If repulsive forces between colloids are absent due to suitable chemical conditions, then the deposition rate tends to increase as colloids accumulate on the grain surface (see Figure 3.1). Based on [79], this enhancement of deposition kinetics is attributed to the retained particles and is generally referred to as ripening. Active repulsive forces seem to lead to a decline in the deposition kinetics. These effects could be investigated by our model, provided suitable modifications of the fluxes responsible for the transport

of colloidal species are taken into account [52].

(iii) The role of the electrolyte concentration (typically a salt, e.g. KCl) and the effect of the interplay between the electrostatic and van der Waals interactions on deposition kinetics can be studied by further developing the model. A few basic ideas on how to proceed in this case are collected, for instance, in [106].

(iv) Non-periodic distributions of microstructures are relevant for practical applications. We leave as further work the extension of our solver towards the MsFEM approach, where cell problems are solved for each grid element, parametrized by the localized properties of the medium. We refer the reader to Section 3.4.3 for comments in this direction.

Chapter 4

Mathematical Analysis and Homogenization of the Thermo-Diffusion Problem for Colloidal Populations

4.1 Introduction

We aim at understanding processes driven by coupled fluxes through media with microstructures. In this Chapter, we study a particular type of coupling: we look at the interplay between diffusion fluxes of a fixed number of colloidal populations and a heat flux, the effects included here are incorporating an approximation of the Dufour ad Soret effects (cf. Section 4.2.3, see also [46]. The type of system of evolution equations that we encounter in Section 4.2.4 resembles very much cross-diffusion and chemotaxis-like systems; see e.g. [124, 41]. The structure of the chosen equations is useful in investigating transport, interaction, and deposition of a large numbers of hot multiple-sized particles in porous media.

Practical applications of our approach would include predicting the response of refractory concrete to high-temperatures exposure in steel furnaces, propagation of combustion waves due to explosions in tunnels, drug delivery in biological tissues, etc.; see for instance [11, 12, 111, 116, 44, 43]. Within this framework, our focus lies exclusively on two distinct theoretical aspects:

(i) the mathematical understanding of the microscopic problem (i.e. the well-posedness of the starting system);

(ii) the averaging of the thermo-diffusion system over arrays of periodically-distributed microstructures (the so-called, *homogenization asymptotics limit*; see, for instance, [13, 86] and references cited therein).

The complexity of the microscopic system makes numerical simulations on the macro scale very expensive. That is the reason that the aspect (ii) is of concern here. Obviously, the study does not close with these questions. Many other issues

like derivation of corrector estimates, design of efficient convergent numerical multiscale schemes, multiscale parameter identification etc. need also to be treated. Possible generalizations could point out to coupling heat transfer with Nernst-Planck-Stokes systems (extending [106]) or with semiconductor equations [83]. The Chapteris structured in the following manner. We present the basic notation and explain the multiscale geometry as well as some of the relevant physical processes in Section 4.2. Section 4.3 contains the proof of the solvability of the microstructure model. Finally, the homogenization procedure is performed in Section 4.4. The strong formulation of the upscaled thermo-diffusion model with Smoluchowski interactions is emphasized in Section 4.4.3.

4.2 Notations and assumptions

4.2.1 Model description and geometry

The geometry of the problem is depicted in Figure 4.1, given a scale factor $\varepsilon > 0$. The standard cell is shown in Figure 4.2.

$(0,T)$	= time interval of interest
Ω	= bounded domain in $\mathbb{R}^n$
$\partial\Omega$	= piecewise smooth boundary of Ω
$\vec{e}_i$	= ith unit vector in $\mathbb{R}^n$
Y	= $\{\sum_{i=1}^n \lambda_i \vec{e}_i : 0 < \lambda_i < 1\}$ unit cell in $\mathbb{R}^n$
Y_0	= open subset of Y that represents the solid grain
Y_1	= $Y \setminus \overline{Y}_0$
Γ	= ∂Y_0 piecewise smooth boundary of Y_0
X^k	= $X + \sum_{i=1}^n k_i \vec{e}_i$, where $k = (k_1, \ldots, k_n) \in \mathbb{Z}^n$ and $X \subset Y$
Ω_0^ε	= $\cup\{(\varepsilon Y_0)^k : (Y_0)^k \subset \Omega^\varepsilon, k \in \mathbb{Z}^n\}$ pore skeleton
Ω^ε	= $\Omega \setminus \overline{\Omega}_0^\varepsilon$ pore space
Γ^ε	= $\partial\Omega_0^\varepsilon$ boundary of the pore skeleton

The cells regions without the grain εY_1^k are filled with water and we denote their union by Ω^ε. Colloidal species are dissolved in the pore water. They react between themselves and participate in diffusion and convective transport. The colloidal matter cannot penetrate the grain boundary Γ^ε, but it deposits there reducing the amount of mass floating inside Ω^ε. Here $\partial\Omega^\varepsilon = \partial\Omega \cup \Gamma^\varepsilon$, where $\Gamma^\varepsilon = \Gamma_N^\varepsilon \cup \Gamma_R^\varepsilon$ and $\Gamma_N^\varepsilon \cap \Gamma_R^\varepsilon = \emptyset$. The boundary Γ_N^ε is insulated to the heat flow, while Γ_R^ε admits flux.

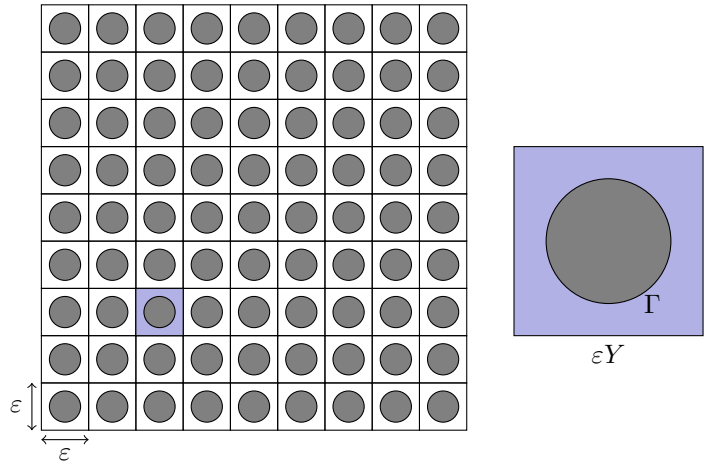

FIGURE 4.1: Porous medium geometry $\Omega = \Omega_0^\varepsilon \cup \Omega^\varepsilon$, where the pore skeleton Ω_0^ε is marked with gray color and the pore space Ω^ε is white.

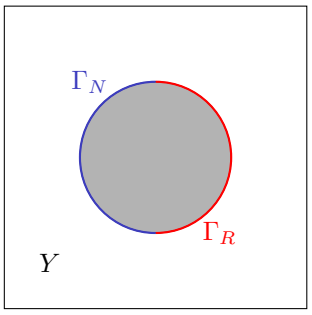

FIGURE 4.2: The unit cell geometry. The colloidal species u_i and temperature θ^ε are defined in Y, while the deposited species v_i^ε are defined on $\Gamma = \Gamma_R \cup \Gamma_N$. The boundary conditions for θ^ε differ on Γ_R and Γ_N, while the boundary conditions for u_i are uniform on Γ.

The unknowns are:

- θ^ε – the temperature in Ω^ε.
- u_i – the concentration of the species that contains i monomers in Ω^ε.
- v_i^ε – the mass of the deposited species on Γ^ε.

Furthermore, for a given $\delta > 0$ we introduce the mollifier:

$$J_\delta(s) := \begin{cases} Ce^{1/(|s|^2-\delta^2)} & \text{if } |s| < \delta, \\ 0 & \text{if } |s| \geq \delta, \end{cases} \tag{4.1}$$

where the constant $C > 0$ is selected such that

$$\int_{\mathbb{R}^d} J_\delta = 1,$$

see [32] for details.

Using J_δ from (4.1), define the mollified gradient:

$$\nabla^\delta f := \nabla \left[\int_{B(x,\delta)} J_\delta(x-y) f(y) dy \right]. \tag{4.2}$$

The following statement holds for all $f \in L^\infty(\Omega^\varepsilon)$, $g \in L^p(\Omega^\varepsilon)^d$ and $1 \leq p \leq \infty$:

$$\|\nabla^\delta f \cdot g\|_{L^p(\Omega^\varepsilon)} \leq c^\delta \|f\|_{L^\infty(\Omega^\varepsilon)} \|g\|_{L^p(\Omega^\varepsilon)^d}. \tag{4.3}$$

$$\|\nabla^\delta f\|_{L^p(\Omega^\varepsilon)} \leq c^\delta \|f\|_{L^2(\Omega^\varepsilon)} \tag{4.4}$$

In the equations below all norms are $L^2(\Omega^\varepsilon)$ unless specified otherwise, with c^δ independent of the choice of ε.

4.2.2 Smoluchowski population balance equations

We want to model the transport of aggregating colloidal particles under the influence of thermal gradients. We use the Smoluchowski population balance equation, originally proposed in [115], to account for colloidal aggregation:

$$R_i(s) := \frac{1}{2} \sum_{k+j=i} \beta_{kj} s_k s_j - \sum_{j=1}^{N} \beta_{ij} s_i s_j, \qquad i \in \{1, \ldots, N\};\ N > 2. \tag{4.5}$$

Equation (4.5) is explained in detail in Chapter 2. Here s_i is the concentration of the colloidal species that consists of i monomers, N is the number of species, i.e. the maximal aggregate size that we consider, $R_i(s)$ is the rate of change of s_i, and $\beta_{ij} > 0$ are the coagulation coefficients, which tell us the rate aggregation between particles of size i and j [31]. Colloidal aggregation rates are described in more detail in [68].

4.2.3 Soret and Dufour effects

The system we have in mind is inspired by the model proposed by Shigesada, Kawasaki and Teramoto [113] in 1979 when they have studied the segregation of

competing species. For the case of two interacting species u and v, the diffusion term looks like:

$$\partial_t u = \Delta(d_1 u + \alpha uv), \tag{4.6}$$

where the second term in the flux is due to cross-diffusion. The second term can be expressed as:

$$\Delta(uv) = u\Delta v + v\Delta u + 2\nabla u \cdot \nabla v. \tag{4.7}$$

As a first step in our approach, we consider only the last term of (4.7), i.e. $\nabla u \cdot \nabla v$, as the driving force of cross-diffusion and we postpone the study of terms $u\Delta v$ and $v\Delta u$ until later.

From mathematical point of view, still it is not easy to treat the term $\nabla u \cdot \nabla v$. Hence, in the paper we approximate this term by $\nabla^\delta u \cdot \nabla v$ for $\delta > 0$.

4.2.4 Setting of the model equations

We consider the following balance equations for the temperature and colloid concentrations:

(P^ε)

$$\partial_t \theta^\varepsilon + \nabla \cdot (-\kappa^\varepsilon \nabla \theta^\varepsilon) - \tau^\varepsilon \sum_{i=1}^{N} \nabla^\delta u_i \cdot \nabla \theta^\varepsilon = 0, \quad \text{in } (0,T) \times \Omega^\varepsilon, \tag{4.8}$$

$$\partial_t u_i^\varepsilon + \nabla \cdot (-d_i \nabla u_i^\varepsilon) - \delta_i^\varepsilon \nabla^\delta \theta^\varepsilon \cdot \nabla u_i^\varepsilon = R_i(u), \quad \text{in } (0,T) \times \Omega^\varepsilon, \tag{4.9}$$

with boundary conditions:

$$-\kappa^\varepsilon \nabla \theta^\varepsilon \cdot n = 0, \quad \text{on } (0,T) \times \Gamma_N^\varepsilon, \tag{4.10}$$

$$-\kappa^\varepsilon \nabla \theta^\varepsilon \cdot n = \varepsilon g_0 \theta^\varepsilon, \quad \text{on } (0,T) \times \Gamma_R^\varepsilon, \tag{4.11}$$

$$-\kappa^\varepsilon \nabla \theta^\varepsilon \cdot n = 0, \quad \text{on } \partial\Omega, \tag{4.12}$$

$$-d_i \nabla u_i^\varepsilon \cdot n = 0, \quad \text{on } \partial\Omega, \tag{4.13}$$

and a boundary condition for colloidal deposition:

$$-d_i \nabla u_i^\varepsilon \cdot n = \varepsilon(a_i^\varepsilon u_i - b_i^\varepsilon v_i^\varepsilon), \quad \text{on } (0,T) \times \Gamma^\varepsilon, \tag{4.14}$$

$$\partial_t v_i^\varepsilon = a_i^\varepsilon u_i - b_i^\varepsilon v_i^\varepsilon, \quad \text{on } (0,T) \times \Gamma^\varepsilon. \tag{4.15}$$

As initial conditions, we take for $i \in \{1, \ldots, N\}$:

$$\theta^\varepsilon(0,x) = \theta^{\varepsilon,0}(x), \quad \text{in } \Omega^\varepsilon, \tag{4.16}$$

$$u_i^\varepsilon(0,x) = u_i^{\varepsilon,0}(x), \quad \text{in } \Omega^\varepsilon, \tag{4.17}$$

$$v_i^\varepsilon(0,x) = v_i^{\varepsilon,0}(x), \quad \text{on } \Gamma^\varepsilon. \tag{4.18}$$

We refer to (4.8)- (4.18) as (P^ε) – our reference microscopic model. Note that the Soret and Dufour coefficients determine the structure of the particular

κ^ε	heat conduction coefficient
d_i	diffusion coefficient
τ^ε	Soret coefficient
δ^ε	Dufour coefficient
g_i	Robin boundary coefficient, $i \in \{0, \dots, N\}$
a_i^ε	Deposition coefficient 1, $i \in \{1, \dots, N\}$
b_i^ε	Deposition coefficient 2, $i \in \{1, \dots, N\}$

cross-diffusion system (see [46], [113] [4], [11], [96], [124]). The coefficients a_i^ε and b_i^ε describe the deposition interaction between u_i and v_i^ε. Consequently, each u_i has a different affinity to sediment as well as a different mass.

All functions defined in Ω^ε and on Γ^ε are taken to be ε-periodic, i.e. $\kappa^\varepsilon(x) = \kappa(x/\varepsilon)$ and so on.

Note the use of the mollified gradient in the cross diffusion terms in (4.8) and (4.9). This is a choice that we have to make at this point in order to obtain the necessary estimates for our equations. From a physical point of view, smoothed gradients causing advection can be interpreted as there being no turbulence.

4.2.5 Assumptions on data

(A_1) κ^ε, τ^ε, and d_i, $g_i, a_i^\varepsilon, b_i^\varepsilon$ are positive constants for $i \in \{1, \dots, N\}$ and $\epsilon > 0$. Moreover, $\kappa_0 \le \kappa^\varepsilon \le \kappa_*$, $\tau^\epsilon \le \tau_*$, $d_0 \le d_i^\epsilon \le d_*$, $\delta_i^\epsilon \le \delta_*$, $a_0 \le a_i^\epsilon \le a_*$ and $b_i^\epsilon \le b_*$ for $i \in \{1, \dots, N\}$ and $\epsilon > 0$, where $\kappa_0, \kappa_*, d_0, d_*, \delta_*, a_0, a_*$ and b_* are positive constants.

(A_2) $\theta^{\varepsilon,0} \in L^\infty_+(\Omega^\varepsilon) \cap H^1(\Omega^\epsilon)$, $u_i^0 \in L^\infty_+(\Omega^\varepsilon) \cap H^1(\Omega^\epsilon)$, $v_i^{\varepsilon,0} \in L^\infty_+(\Gamma^\varepsilon)$ for $i \in \{1, \dots, N\}$ and $\epsilon > 0$. Moreover, $||\theta^{\varepsilon,0}||_{H^2(\Omega^\epsilon)} \le C_0$, $||u_i^0||_{H^2(\Omega^\epsilon)} \le C_0$, and $||v_i^{\varepsilon,0}||_{L^\infty(\Gamma^\epsilon)} \le C_0$ for $i \in \{1, \dots, N\}$ and $\epsilon > 0$. Here C_0 is a positive constant independent of ε.

4.3 Global solvability of problem (P^ε)

Definition 1. *The triplet $(\theta^\varepsilon, u_i, v_i^\varepsilon)$ is a solution to problem (P^ε) if the following holds:*

$$\begin{aligned} &\theta^\varepsilon, u_i \in H^1(0,T; L^2(\Omega^\varepsilon)) \cap L^\infty(0,T; H^1(\Omega^\varepsilon)) \cap L^\infty((0,T) \times \Omega^\varepsilon), \\ &v_i^\varepsilon \in H^1(0,T; L^2(\Gamma^\varepsilon)) \cap L^\infty((0,T) \times \Gamma^\varepsilon), \end{aligned} \tag{4.19}$$

for all $\phi \in H^1(\Omega^\varepsilon)$:

$$\int_{\Omega^\varepsilon} \partial_t \theta^\varepsilon \phi + \int_{\Omega^\varepsilon} \kappa^\varepsilon \nabla \theta^\varepsilon \cdot \nabla \phi + g_0 \int_{\Gamma_R^\varepsilon} \theta^\varepsilon \phi = \tau^\varepsilon \sum_{i=1}^N \int_{\Omega^\varepsilon} \nabla^\delta u_i \cdot \nabla \theta^\varepsilon \phi, \tag{4.20}$$

for all $\psi_i \in H^1(\Omega^\varepsilon)$:

$$\begin{aligned}\int_{\Omega^\varepsilon} \partial_t u_i \psi_i + \int_{\Omega^\varepsilon} d_i \nabla u_i \cdot \nabla \psi_i + g_i \int_{\Gamma_R^\varepsilon} u_i \psi_i + \int_{\Gamma^\varepsilon} (a_i^\varepsilon u_i - b_i^\varepsilon v_i^\varepsilon)\psi_i \\ = \delta_i^\varepsilon \int_{\Omega^\varepsilon} \nabla^\delta \theta^\varepsilon \cdot \nabla u_i \psi_i + \int_{\Omega^\varepsilon} R_i(u)\psi_i,\end{aligned} \tag{4.21}$$

for all $\varphi_i \in L^2(\Gamma^\varepsilon)$:

$$\int_{\Gamma^\varepsilon} \partial_t v_i^\varepsilon \varphi_i = \int_{\Gamma^\varepsilon} (a_i^\varepsilon u_i - b_i^\varepsilon v_i^\varepsilon)\varphi_i. \tag{4.22}$$

together with (4.16), (4.17) and (4.18) for a fixed value of $\varepsilon > 0$.

Remark 4.3.1. *We note that each term appearing in Definition 1 is finite, since* $\nabla^\delta u_i$ *and* $\nabla^\delta \theta^\varepsilon$ *are bounded in* Ω^ε *due to (4.3).*

To prove the existence of solutions to problem (P^ε), we introduce the following auxiliary problems as iterations steps of the coupled system:

(P_1)

$$\begin{aligned}
&\partial_t \theta^\varepsilon + \nabla \cdot (-\kappa^\varepsilon \nabla \theta^\varepsilon) - \tau^\varepsilon \sum_{i=1}^N \nabla^\delta \bar{u}_i \cdot \nabla \theta^\varepsilon = 0, && \text{in } (0,T)\times\Omega^\varepsilon,\\
&-\kappa^\varepsilon \nabla \theta^\varepsilon \cdot n = 0, && \text{on } (0,T)\times\Gamma_N^\varepsilon,\\
&-\kappa^\varepsilon \nabla \theta^\varepsilon \cdot n = \varepsilon g_0 \theta^\varepsilon, && \text{on } (0,T)\times\Gamma_R^\varepsilon,\\
&-\kappa^\varepsilon \nabla \theta^\varepsilon \cdot n = 0, && \text{on } (0,T)\times\Gamma^\varepsilon,\\
&\theta^\varepsilon(0,x) = \theta^{\varepsilon,0}(x), && \text{in } \Omega^\varepsilon,
\end{aligned}$$

and

(P_2)

$$\begin{aligned}
&\partial_t u_i^\varepsilon + \nabla \cdot (-d_i \nabla u_i^\varepsilon) - \delta_i^\varepsilon \nabla^\delta \bar{\theta} \cdot \nabla u_i^\varepsilon = R_i^M(u), && \text{in } (0,T)\times\Omega^\varepsilon,\\
&-d_i \nabla u_i^\varepsilon \cdot n = 0, && \text{on } (0,T)\times\Gamma_N^\varepsilon,\\
&-d_i \nabla u_i^\varepsilon \cdot n = \varepsilon g_i u_i, && \text{on } (0,T)\times\Gamma_R^\varepsilon,\\
&-d_i \nabla u_i^\varepsilon \cdot n = \varepsilon(a_i^\varepsilon u_i - b_i^\varepsilon v_i^\varepsilon), && \text{on } (0,T)\times\Gamma^\varepsilon,\\
&u_i^\varepsilon(0,x) = u_i^{\varepsilon,0}(x), && \text{in } \Omega^\varepsilon,\\
&\partial_t v_i^\varepsilon = a_i^\varepsilon u_i - b_i^\varepsilon v_i^\varepsilon, && \text{on } (0,T)\times\Gamma^\varepsilon,\\
&v_i^\varepsilon(0,x) = v_i^{\varepsilon,0}(x), && \text{on } \Gamma^\varepsilon.
\end{aligned}$$

Here

$$R_i^M(s) := R_i(\sigma_M(s_1), \sigma_M(s_2), \dots, \sigma_M(s_N)), \text{ for } s \in \mathbb{R}^N \tag{4.23}$$

denotes our choice of truncation of R_i, where

$$\sigma_M(r) := \begin{cases} 0, & r < 0 \\ r, & r \in [0, M] \\ M, & r > M, \end{cases} \tag{4.24}$$

where $M > 0$ is a fixed threshold. Note that if M is large enough, the essential bounds obtained later in this paper will remain below M. This means that the existence result is obtained also for the uncut rates.

In the following, assuming (A_1)-(A_2), we show the existence, positivity and boundedness of solutions to (P_1) and (P_2).

When we denote the solutions as $\theta^\varepsilon = P_1(\bar{u})$ and $(u_i, v_i^\varepsilon) = P_2(\bar{\theta})$, we can define the solution operator $(\theta^\varepsilon, u_i, v_i^\varepsilon) = \mathbf{T}(\bar{\theta}, \bar{u}_i)$. We will show that the operator $\mathbf{T}$ is a contraction in the appropriate functional spaces and use the Banach fixed point theorem to prove the existence and uniqueness of solutions to (P^ε).

Notation 1. *Let* $K(T, M) := \{z \in L^2(0, T; L^2(\Omega^\varepsilon)) : |z| \leq M \text{ a.e. on } (0, T) \times \Omega^\varepsilon\}$.

Lemma 4.3.2. Existence of solutions to (P_1).
Let $\bar{u}_i \in K(T, M)$*, and assume that* (A_1)-(A_2) *hold.*
Then there exists $\theta^\varepsilon \in H^1(0, T; L^2(\Omega^\varepsilon)) \cap L^\infty(0, T; H^1(\Omega^\varepsilon))$ *that solves* (P_1) *in the sense:*

for all $\phi \in H^1(\Omega^\varepsilon)$ *and a.e. in* $[0, T]$*:*

$$\int_{\Omega^\varepsilon} \partial_t \theta^\varepsilon \phi + \int_{\Omega^\varepsilon} \kappa^\varepsilon \nabla \theta^\varepsilon \cdot \nabla \phi + g_0 \int_{\Gamma_R^\varepsilon} \theta^\varepsilon \phi = \tau^\varepsilon \sum_{i=1}^N \int_{\Omega^\varepsilon} \nabla^\delta \bar{u}_i \cdot \nabla \theta^\varepsilon \phi, \tag{4.25}$$

and

$$\theta^\varepsilon(0, x) = \theta^{\varepsilon,0}(x) \qquad \text{a.e. in } \Omega^\varepsilon. \tag{4.26}$$

Proof. Let $\{\xi_i\}$ be a Schauder basis of $H^1(\Omega^\varepsilon)$. Then for each $n \in \mathbb{N}$ there exists

$$\theta_n^{\varepsilon,0}(x) := \sum_{j=1}^n \alpha_j^{0,n} \xi_j(x) \text{ such that } \theta_n^{\varepsilon,0} \to \theta^{\varepsilon,0} \text{ in } H^1(\Omega^\varepsilon) \text{ as } n \to \infty. \tag{4.27}$$

We denote by θ_n^ε the Galerkin approximation of θ^ε, that is:

$$\theta_n^\varepsilon(t, x) := \sum_{j=1}^n \alpha_j^n(t) \xi_j(x) \qquad \text{for all } (t, x) \in (0, T) \times \Omega^\varepsilon. \tag{4.28}$$

By definition, θ_n^ε must satisfy (4.25) for all $\phi \in \text{span}\{\xi_i\}_{i=1}^n$, i.e.:

$$\int\limits_{\Omega^\varepsilon} \partial_t \theta_n^\varepsilon \phi + \int\limits_{\Omega^\varepsilon} \kappa^\varepsilon \nabla \theta_n^\varepsilon \cdot \nabla \phi + g_0 \int\limits_{\Gamma_R^\varepsilon} \theta_n^\varepsilon \phi = \tau^\varepsilon \sum_{i=1}^N \int\limits_{\Omega^\varepsilon} \nabla^\delta \bar{u}_i \cdot \nabla \theta_n^\varepsilon \phi. \tag{4.29}$$

The coefficients $\alpha_i^n(t)$ can be found by testing (4.29) with $\phi := \xi_i$ and using (4.27) to solve the resulting ODE system:

$$\partial_t \alpha_i^n(t) + \sum_{j=1}^n (A_{ij} + B_{ij} - C_{ij}) \alpha_j^n(t) = 0, \qquad i \in \{1, \dots, n\}, \tag{4.30}$$

$$\alpha_i^n(0) = \alpha_i^{0,n}. \tag{4.31}$$

The coefficients in (4.30) and (4.31) are defined by the following expressions

$$A_{ij} := \int\limits_{\Omega^\varepsilon} \kappa^\varepsilon \nabla \xi_i \cdot \nabla \xi_j, \qquad i, j \in \{1, \dots, n\},$$

$$B_{ij} := g_0 \int\limits_{\Gamma_R^\varepsilon} \xi_i \xi_j, \qquad i, j \in \{1, \dots, n\},$$

$$C_{ij} := \tau^\varepsilon \sum_{k=1}^N \int\limits_{\Omega^\varepsilon} \nabla^\delta \bar{u}_k \cdot \nabla \xi_j \xi_i \qquad i, j \in \{1, \dots, n\}.$$

Since the system (4.30) is linear, there exists for each fixed $n \in \mathbb{N}$ a unique solution $\alpha_i^n \in C^1([0,T])$.

To prove uniform estimates for θ_n^ε with respect to n, we take in (4.29) $\phi = \theta_n^\varepsilon$. We obtain:

$$\frac{1}{2}\partial_t \|\theta_n^\varepsilon\|^2 + \kappa^{\varepsilon,0} \|\nabla \theta_n^\varepsilon\|^2 + g_0 \|\theta_n^\varepsilon\|^2_{L^2(\Gamma_R^\varepsilon)} \le \tau^\varepsilon \sum_{i=1}^N \int\limits_{\Omega^\varepsilon} |\nabla^\delta \bar{u}_i \cdot \nabla \theta_n^\varepsilon \theta_n^\varepsilon| := \tau^\varepsilon \sum_{i=1}^N A_i.$$

Using the Cauchy-Schwarz inequality and Young's inequality in the form $ab \le \eta a^2 + b^2/4\eta$, where $\eta > 0$, we get:

$$A_i \le \eta \|\nabla \theta_n^\varepsilon\|^2 + \frac{1}{4\eta} \|\nabla^\delta \bar{u}_i \theta_n^\varepsilon\|^2 \le \eta \|\nabla \theta_n^\varepsilon\|^2 + \frac{1}{4\eta} \|\nabla^\delta \bar{u}_i\|^2_{L^4(\Omega^\varepsilon)} \|\theta_n^\varepsilon\|^2_{L^4(\Omega^\varepsilon)}.$$

The mollifier property (4.3) yields $\|\nabla^\delta \bar{u}_i\|^2_{L^4(\Omega^\varepsilon)} \le c^\delta \|\bar{u}_i\|^2_\infty$. Using Gagliardo-Nirenberg inequality (see [98] e.g.), we get:

$$\|\theta_n^\varepsilon\|^2_{L^4(\Omega^\varepsilon)} \le c \|\theta_n^\varepsilon\|^{1/2} \|\nabla \theta_n^\varepsilon\|^{3/2}. \tag{4.32}$$

Applying Young's inequality, we obtain:

$$c \|\theta_n^\varepsilon\|^{1/2} \|\nabla \theta_n^\varepsilon\|^{3/2} \le \eta \|\nabla \theta_n^\varepsilon\|^2 + c_\eta \|\theta_n^\varepsilon\|^2. \tag{4.33}$$

Finally, we obtain the structure:

$$\frac{1}{2}\partial_t\|\theta_n^\varepsilon\|^2 + (\kappa^{\varepsilon,0} - 2N\eta)\|\nabla\theta_n^\varepsilon\|^2 + g_0\|\nabla\theta_n^\varepsilon\|^2_{L^2(\Gamma_R^\varepsilon)} \le c_\eta^\delta \sum_{i=1}^N \|\bar{u}_i\|^2\|\theta_n^\varepsilon\|^2.$$

Gronwall's lemma gives:

$$\|\theta_n^\varepsilon(t)\|^2 + \kappa_\varepsilon^{\varepsilon,0}\int_0^t \|\nabla\theta_n^\varepsilon(t)\|^2 < C \qquad \text{for } t \in (0,T),$$

where $C > 0$ is independent of n, since $\bar{u}_i$ are uniformly bounded. This ensures that

$$\theta_n^\varepsilon \in L^\infty(0,T;L^2(\Omega^\varepsilon)) \cap L^2(0,T;H^1(\Omega^\varepsilon)). \tag{4.34}$$

To show uniform estimates for $\partial_t\theta_n^\varepsilon$ with respect to n, we take $\phi = \partial_t\theta_n^\varepsilon$ in (4.29) (note that we can do this due to H^1 regularity of $\partial_t\theta_n^\varepsilon$, which we have in the finite-dimensional case, due to the properties of the Schauder basis) and use the Cauchy-Schwarz and Young's inequalities, as well as the mollifier property (4.3) to get:

$$\begin{aligned}\|\partial_t\theta_n^\varepsilon\|^2 + \frac{1}{2}\partial_t\|\kappa^\varepsilon\nabla\theta_n^\varepsilon\|^2 + \frac{g_0}{2}\partial_t\|\theta_n^\varepsilon\|^2_{L^2(\Gamma_R^\varepsilon)} &\le \tau^\varepsilon\sum_{i=1}^N\int_{\Omega^\varepsilon}|\nabla^\delta\bar{u}_i\cdot\nabla\theta_n^\varepsilon\partial_t\theta_n^\varepsilon| \\ &\le \left(c^\delta\tau^\varepsilon\sum_{i=1}^N\|\bar{u}_i\|_{L^\infty(\Omega^\varepsilon)}\right)(\eta\|\partial_t\theta_n^\varepsilon\|^2 + \frac{C_\eta}{\kappa^{\varepsilon,0}}\|\kappa^\varepsilon\nabla\theta_n^\varepsilon\|^2).\end{aligned}$$

Gronwall's lemma gives:

$$\|\kappa^\varepsilon\nabla\theta_n^\varepsilon\|^2 + \int_0^t\|\partial_t\theta_n^\varepsilon\|^2 < C \qquad \text{for all } t \in (0,T),$$

where $C > 0$ depends on δ, but is independent of n. Together with (4.34) this ensures that:

$$\theta_n^\varepsilon \in H^1(0,T;L^2(\Omega^\varepsilon)) \cap L^\infty(0,T;H^1(\Omega^\varepsilon)). \tag{4.35}$$

Hence, we can choose a subsequence $\theta_{n_i}^\varepsilon \rightharpoonup \theta^\varepsilon$ in $H^1(0,T;L^2(\Omega^\varepsilon))$ and $\theta_{n_i}^\varepsilon \overset{*}{\rightharpoonup} \theta^\varepsilon$ in $L^\infty(0,T;H^1(\Omega^\varepsilon))$ as $i \to \infty$.

Now, using

$$v_m(t,x) := \sum_{j=1}^m \beta_j^m(t)\xi_j(x) \tag{4.36}$$

as a test function in (4.29) and integrating with respect to time we get:

$$\begin{aligned}\int_0^T\int_{\Omega^\varepsilon}\partial_t\theta_{n_i}^\varepsilon v_m + \int_0^T\int_{\Omega^\varepsilon}\kappa^\varepsilon\nabla\theta_{n_i}^\varepsilon\cdot\nabla v_m + g_0\int_0^T\int_{\Gamma_R^\varepsilon}\theta_{n_i}^\varepsilon v_m \\ = \tau^\varepsilon\sum_{i=1}^N\int_0^T\int_{\Omega^\varepsilon}\nabla^\delta\bar{u}_i\cdot\nabla\theta_{n_i}^\varepsilon v_m.\end{aligned} \tag{4.37}$$

Using (4.35), we pass to the limit as $i \to \infty$ to obtain:

$$\int_0^T \int_{\Omega^\varepsilon} \partial_t \theta^\varepsilon v_m + \int_0^T \int_{\Omega^\varepsilon} \kappa^\varepsilon \nabla \theta^\varepsilon \cdot \nabla v_m + g_0 \int_0^T \int_{\Gamma_R^\varepsilon} \theta^\varepsilon v = \tau^\varepsilon \sum_{i=1}^N \int_0^T \int_{\Omega^\varepsilon} \nabla^\delta \bar{u}_i \cdot \nabla \theta^\varepsilon v_m. \tag{4.38}$$

Note that (4.38) holds for all $v \in L^2(0,T;H^1(\Omega^\varepsilon))$ since we can approximate v with v_m in $L^2(0,T;H^1(\Omega^\varepsilon))$, hence

$$\int_0^T \int_{\Omega^\varepsilon} \partial_t \theta^\varepsilon v + \int_0^T \int_{\Omega^\varepsilon} \kappa^\varepsilon \nabla \theta^\varepsilon \cdot \nabla v + g_0 \int_0^T \int_{\Gamma_R^\varepsilon} \theta^\varepsilon v = \tau^\varepsilon \sum_{i=1}^N \int_0^T \int_{\Omega^\varepsilon} \nabla^\delta \bar{u}_i \cdot \nabla \theta^\varepsilon v,$$

holds for all $v \in L^2(0,T;H^1(\Omega^\varepsilon))$.

Finally, we show the initial condition holds. Indeed, the Aubin-Lions lemma guarantees that $\theta^\varepsilon_{n_i} \to \theta^\varepsilon$ in $C((0,T);L^2(\Omega^\varepsilon))$. Then on account of $\theta^\varepsilon_{n_i}(0) \to \theta^{\varepsilon,0}$ in $L^2(\Omega^\varepsilon)$ as $i \to \infty$, we get $\theta^\varepsilon(0) = \theta^{\varepsilon,0}$. □

Lemma 4.3.3. Positivity and boundedness of solutions to (P_1).
Let $\bar{u}_i \in K(T,M)$, $M > 0$, and assume (A_1)-(A_2).
Then $0 \le \theta^\varepsilon \le \|\theta^{\varepsilon,0}\|_{L^\infty(\Omega^\varepsilon)}$ a.e. in $(0,T) \times \Omega^\varepsilon$.

Proof. Let $\theta^\varepsilon := \theta^{\varepsilon,+} - \theta^{\varepsilon,-}$, where $z^+ := \max(z,0)$ and $z^- := \max(-z,0)$. Testing (4.25) with $\phi := -\theta^{\varepsilon,-}$, and using (4.3) gives:

$$\frac{1}{2}\partial_t \|\theta^{\varepsilon,-}\|^2 + \kappa^{\varepsilon,0}\|\nabla \theta^{\varepsilon,-}\|^2 + g_0 \|\theta^{\varepsilon,-}\|^2_{L^2(\Gamma_R^\varepsilon)} \le c^\delta \tau^\varepsilon \sum_{i=1}^N \|\bar{u}_i\|_\infty \|\nabla \theta^{\varepsilon,-}\theta^{\varepsilon,-}\|_{L^1(\Omega^\varepsilon)}$$

$$\le \left(C^\delta_\varepsilon \tau^\varepsilon \sum_{i=1}^N \|\bar{u}_i\|_\infty \right) \|\theta^{\varepsilon,-}\|^2 + \varepsilon \|\nabla \theta^{\varepsilon,-}\|^2.$$

Choosing $\varepsilon < \kappa^{\varepsilon,0}$ and taking into account that $\theta^{\varepsilon,-}(0) = 0$, Gronwall's lemma gives $\|\theta^{\varepsilon,-}\|^2 \le 0$. This means $\theta^\varepsilon > 0$ a.e. in Ω for all $t \in (0,T)$.

Let $\phi = (\theta^\varepsilon - M_0)^+$ in (4.25) with $M_0 \ge \|\theta^\varepsilon(0)\|_{L^\infty(\Omega^\varepsilon)}$:

$$\frac{1}{2}\partial_t \|(\theta^\varepsilon - M_0)^+\|^2 + \kappa^{\varepsilon,0}\|\nabla(\theta^\varepsilon - M_0)^+\|^2 + g_0 \|(\theta^\varepsilon - M_0)^+\|^2_{L^2(\Gamma_R^\varepsilon)}$$

$$+ \int_{\Gamma_R^\varepsilon} M_0 (\theta^\varepsilon - M_0)^+ \le \tau^\varepsilon \sum_{i=1}^N \int_{\Omega^\varepsilon} \nabla^\delta \bar{u}_i \cdot \nabla (\theta^\varepsilon - M_0)^+ (\theta^\varepsilon - M_0)^+$$

$$\le \left(\tau^\varepsilon c^\delta \sum_{i=1}^N \|\bar{u}_i\|_\infty \right) \left(c_\varepsilon \|(\theta^\varepsilon - M_0)^+\|^2 + \varepsilon \|\nabla(\theta^\varepsilon - M_0)^+\|^2 \right).$$

Discarding the positive terms on the left side and then applying Gronwall's lemma leads to:

$$\|(\theta^\varepsilon - M_0)^+(t)\|^2 \le \|(\theta^\varepsilon - M_0)^+(0)\|^2 \exp\left(\tau^\varepsilon c^\delta c_\varepsilon \sum_{i=1}^N \|\bar{u}_i\|_\infty t \right).$$

Since $\|(\theta^\varepsilon - M_0)^+(0)\| = 0$, we obtain $(\theta^\varepsilon - M_0)^+(t) = 0$. Thus the proof of the lemma is completed. □

Lemma 4.3.4. Existence of solutions to (P_2).
Let $\bar\theta \in K(T, M), M > 0$ and (A_1)-(A_2) hold.
Then (P_2) has solutions $u_i \in H^1(0,T;L^2(\Omega^\varepsilon)) \cap L^\infty(0,T;H^1(\Omega))$ and $v_i^\varepsilon \in H^1(0,T;L^2(\Gamma^\varepsilon))$ in the following sense:

For all $\psi_i \in H^1(\Omega^\varepsilon)$, it holds:

$$\begin{aligned}\int_{\Omega^\varepsilon} \partial_t u_i \psi_i + \int_{\Omega^\varepsilon} d_i \nabla u_i \cdot \nabla \psi_i + g_i \int_{\Gamma_R^\varepsilon} u_i \psi_i + \int_{\Gamma^\varepsilon} (a_i^\varepsilon u_i - b_i^\varepsilon v_i^\varepsilon)\psi_i \\ = \delta_i^\varepsilon \int_{\Omega^\varepsilon} \nabla^\delta \bar\theta \cdot \nabla u_i \psi_i + \int_{\Omega^\varepsilon} R_i^M(u)\psi_i\end{aligned} \tag{4.39}$$

$$u_i(0,x) = u_i^0(x) \quad \text{a.e. in } \Omega^\varepsilon, \tag{4.40}$$

and for all $\varphi_i \in L^2(\Gamma^\varepsilon)$:

$$\int_{\Gamma^\varepsilon} \partial_t v_i^\varepsilon \varphi_i = \int_{\Gamma^\varepsilon} (a_i^\varepsilon u_i - b_i^\varepsilon v_i^\varepsilon)\varphi_i, \tag{4.41}$$

$$v_i^\varepsilon(0,x) = v_i^{\varepsilon,0}(x) \quad \text{a.e. on } \Gamma^\varepsilon. \tag{4.42}$$

Proof. Let $\{\xi_j\}$ – Schauder basis of $H^1(\Omega^\varepsilon)$. Then, for each $n \in \mathbb{N}$, there exists

$$u_{i,n}^0(x) := \sum_{j=1}^n \alpha_{i,j}^{0,n} \xi_j(x) \text{ such that } u_{i,n}^0 \to u_i^0 \text{ in } H^1(\Omega^\varepsilon) \text{ as } n \to \infty. \tag{4.43}$$

We denote by $u_{i,n}$ the Galerkin approximation of u_i, that is:

$$u_{i,n}(t,x) := \sum_{j=1}^n \alpha_{i,j}^n(t)\xi_j(x) \qquad \text{for all } (t,x) \in (0,T)\times\Omega^\varepsilon. \tag{4.44}$$

$u_{i,n}$ must satisfy (4.39), and hence,

$$\begin{aligned}\int_{\Omega^\varepsilon} \partial_t u_{i,n} \psi_i + \int_{\Omega^\varepsilon} d_i \nabla u_{i,n} \cdot \nabla \psi_i + g_i \int_{\Gamma_R^\varepsilon} u_{i,n}\psi_i + \int_{\Gamma^\varepsilon} (a_i^\varepsilon u_{i,n} - b_i^\varepsilon v_i^\varepsilon)\psi_i \\ = \delta_i^\varepsilon \int_{\Omega^\varepsilon} \nabla^\delta \bar\theta \cdot \nabla u_{i,n}\psi_i + \int_{\Omega^\varepsilon} R_i^M(u_n)\psi_i, \qquad \text{for all } \psi_i \in \operatorname{span}\{\xi_j\}_{j=1}^n.\end{aligned} \tag{4.45}$$

Accordingly, let $\{\eta_j\}$ – an orthonormal basis of $L^2(\Gamma^\varepsilon)$. Then for each $n \in \mathbb{N}$ there exists

$$v_{i,n}^{\varepsilon,0}(x) := \sum_{j=1}^n \beta_{i,j}^{0,n} \eta_j(x) \text{ such that } v_{i,n}^{\varepsilon,0} \to v_i^{\varepsilon,0} \text{ in } L^2(\Gamma^\varepsilon) \text{ as } n \to \infty. \tag{4.46}$$

We denote by $v^\varepsilon_{i,n}$ the Galerkin approximation of v^ε_i, that is:

$$v^\varepsilon_{i,n}(t,x) := \sum_{j=1}^{n} \beta^n_{i,j}(t)\eta_j(x), \qquad \text{for all } (t,x) \in (0,T)\times\Gamma^\varepsilon. \tag{4.47}$$

$v^\varepsilon_{i,n}$ must satisfy (4.41), and hence,

$$\int_{\Gamma^\varepsilon} \partial_t v^\varepsilon_{i,n}\varphi_i = \int_{\Gamma^\varepsilon} (a^\varepsilon_i u_{i,n} - b^\varepsilon_i v^\varepsilon_{i,n})\varphi_i, \qquad \text{for all } \varphi_i \in \operatorname{span}\{\eta_j\}_{j=1}^n. \tag{4.48}$$

$\alpha^n_{i,j}(t)$ and $\beta^n_{i,j}(t)$ can be found by substituting $u_{i,n}$ and $v^\varepsilon_{i,n}$ into (4.39) – (4.42) and using ξ_k and η_k for $k \in \{1,\dots,n\}$ as test functions:

$$\begin{aligned}
&\partial_t \alpha^n_{i,k}(t) + \sum_{j=1}^{n}(A_{ijk} + B_{ijk} + C_{ijk} - D_{ijk})\alpha^n_{i,j}(t) - \sum_{j=1}^{n} E_{ijk}\beta^n_{i,j}(t) \\
&\quad = \int_{\Omega^\varepsilon} \xi_k \sum_{a=1}^{i-1} \beta_{a,i-a}\sigma_M\left(\sum_{b=1}^{n}\alpha^n_{a,b}(t)\xi_b\right)\sigma_M\left(\sum_{c=1}^{n}\alpha^n_{i-a,c}(t)\xi_c\right) \\
&\quad - \int_{\Omega^\varepsilon} \xi_k \sum_{a=1}^{N} \beta_{a,i}\sigma_M\left(\sum_{b=1}^{n}\alpha^n_{i,b}(t)\xi_b\right)\sigma_M\left(\sum_{c=1}^{n}\alpha^n_{a,c}(t)\xi_c\right),
\end{aligned} \tag{4.49}$$

$$\alpha^n_{i,j}(0) = \alpha^{0,n}_{i,j}, \tag{4.50}$$

$$\partial_t \beta^n_{i,k}(t) = \sum_{j=1}^{n} G_{ijk}\alpha^n_{i,j}(t) - H_{ijk}\beta^n_{i,j}(t), \tag{4.51}$$

$$\beta^n_{i,j}(0) = \beta^{0,n}_{i,j}. \tag{4.52}$$

The coefficients arising in (4.49) are defined by:

$$\begin{aligned}
A_{ijk} &:= \int_{\Omega^\varepsilon} d_i \nabla\xi_j\cdot\nabla\xi_k, & B_{ijk} &:= g_i \int_{\Gamma^\varepsilon_R} \xi_j\xi_k, \\
C_{ijk} &:= a^\varepsilon_i \int_{\Gamma^\varepsilon} \xi_j\xi_k, & D_{ijk} &:= \delta^\varepsilon_i \int_{\Omega^\varepsilon} \nabla^\delta\bar\theta\cdot\nabla\xi_j\xi_k, \\
E_{ijk} &:= b^\varepsilon_i \int_{\Gamma^\varepsilon} \xi_k\eta_j, & G_{ijk} &:= a^\varepsilon_i \int_{\Gamma^\varepsilon} \xi_j\eta_k, \\
H_{ijk} &:= b^\varepsilon_i \int_{\Gamma^\varepsilon} \eta_j\eta_k.
\end{aligned}$$

The left-hand side of this system of ODEs is linear, while the right-hand side is globally Lipschitz. Thus there exists a unique solution $\alpha^n_{i,j}(t), \beta^n_{i,j}(t) \in H^1(0,T)$ to (4.49) (4.52) for $t \in (0,T)$.

To show uniform in n estimates for $u_{i,n}$ and $v^\varepsilon_{i,n}$, we take $\psi_i = u_{i,n}$ and $\varphi_i = v^\varepsilon_{i,n}$ in (4.45) and (4.48) respectively. We get the inequality:

$$\begin{aligned}
&\frac{1}{2}\partial_t\|u_{i,n}\|^2 + d_i^0\|\nabla u_{i,n}\|^2 + g_i\|u_{i,n}\|^2_{L^2(\Gamma^\varepsilon_R)} + a_i^\varepsilon\|u_{i,n}\|^2_{L^2(\Gamma^\varepsilon)} \\
&\quad\le b_i^\varepsilon\int_{\Gamma^\varepsilon}|v^\varepsilon_{i,n}u_{i,n}| + \tau^\varepsilon c^\delta\|\bar\theta\|_\infty\|\nabla u_{i,n}\|\|u_{i,n}\| + \int_{\Omega^\varepsilon}R_i^M(u_n)u_{i,n} \\
&\quad\le \varepsilon\|u_{i,n}\|^2_{L^2(\Gamma^\varepsilon)} + C^\varepsilon\|v^\varepsilon_{i,n}\|^2_{L^2(\Gamma^\varepsilon)} + \varepsilon\|\nabla u_{i,n}\|^2 \\
&\qquad + C^{\delta\varepsilon}\|\bar\theta\|_\infty\|u_{i,n}\|^2 + C^M\|u_{i,n}\| \\
&\frac{1}{2}\partial_t\|v^\varepsilon_{i,n}\|^2_{L^2(\Gamma^\varepsilon)} + b_i^\varepsilon\|v^\varepsilon_{i,n}\|^2_{L^2(\Gamma^\varepsilon)} \le \varepsilon\|u_{i,n}\|^2_{L^2(\Gamma^\varepsilon)} + C^\varepsilon\|v^\varepsilon_{i,n}\|^2_{L^2(\Gamma^\varepsilon)}.
\end{aligned}$$

After adding the two inequalities, Gronwall's lemma gives:

$$\|u_{i,n}\|^2 + d_i^0\int_0^t\|\nabla u_{i,n}\|^2 + \|v^\varepsilon_{i,n}\|^2_{L^2(\Gamma^\varepsilon)} < C \qquad \text{for all } t\in(0,T), \tag{4.53}$$

where $C>0$ depends on δ, M and T, but is independent of n and ε, which ensures:

$$u_{i,n}\in L^\infty(0,T;L^2(\Omega^\varepsilon))\cap L^2(0,T;H^1(\Omega^\varepsilon)), \tag{4.54}$$
$$v^\varepsilon_{i,n}\in L^\infty(0,T;L^2(\Gamma^\varepsilon)). \tag{4.55}$$

To show uniform estimates for $\partial_t u_{i,n}$ and $\partial_t v^\varepsilon_{i,n}$ with respect to n, we take $\psi_i = \partial_t u_{i,n}$ and $\varphi_i = \partial_t v^\varepsilon_{i,n}$ in (4.45) and (4.48) respectively, noticing that they are in H^1 due to being in a finite-dimensional space. We obtain:

$$\begin{aligned}
&\|\partial_t u_{i,n}\|^2 + \int_{\Omega^\varepsilon}\frac{d_i}{2}\partial_t(\nabla u_{i,n})^2 + \frac{g_i}{2}\partial_t\|u_{i,n}\|^2_{L^2(\Gamma^\varepsilon_R)} + \frac{a_i^\varepsilon}{2}\partial_t\|u_{i,n}\|^2_{L^2(\Gamma^\varepsilon)} \\
&\qquad = b_i^\varepsilon\int_{\Gamma^\varepsilon}\partial_t u_{i,n}v^\varepsilon_{i,n} + \delta_i^\varepsilon\int_{\Omega^\varepsilon}\nabla^\delta\bar\theta\cdot\nabla u_{i,n}\partial_t u_{i,n} + \int_{\Omega^\varepsilon}R_i^M(u_n)\partial_t u_{i,n}
\end{aligned} \tag{4.56}$$

$$\|\partial_t v^\varepsilon_{i,n}\|^2_{L^2(\Gamma^\varepsilon)} + \frac{b_i^\varepsilon}{2}\partial_t\|v^\varepsilon_{i,n}\|^2_{L^2(\Gamma^\varepsilon)} = a_i^\varepsilon\int_{\Gamma^\varepsilon}u_{i,n}\partial_t v^\varepsilon_{i,n}. \tag{4.57}$$

Multiplying (4.56) by a_i^ε and (4.57) by b_i^ε, then adding them, and finally inte-

grating the result over $(0,T)$, we get:

$$\begin{aligned}
&\int_0^T a_i^\varepsilon \|\partial_t u_{i,n}\|^2 + \int_0^T b_i^\varepsilon \|\partial_t v_{i,n}^\varepsilon\|^2 + \frac{a_i^\varepsilon d_i^0}{2}\|\nabla u_{i,n}(T)\|^2 + \frac{a_i^\varepsilon g_i}{2}\|u_{i,n}(T)\|^2_{L^2(\Gamma_R^\varepsilon)} \\
&\quad + \frac{a_i^{\varepsilon,2}}{2}\|u_{i,n}(T)\|^2_{L^2(\Gamma^\varepsilon)} + \frac{b_i^{\varepsilon,2}}{2}\|v_{i,n}^\varepsilon(T)\|^2_{L^2(\Gamma^\varepsilon)} \\
&\quad - a_i^\varepsilon b_i^\varepsilon \|u_{i,n}(T)\|_{L^2(\Gamma^\varepsilon)}\|v_{i,n}^\varepsilon(T)\|_{L^2(\Gamma^\varepsilon)} + a_i^\varepsilon b_i^\varepsilon \|u_{i,n}(0)\|_{L^2(\Gamma^\varepsilon)}\|v_{i,n}^\varepsilon(0)\|_{L^2(\Gamma^\varepsilon)} \\
&\quad \le \frac{a_i^\varepsilon d_i^0}{2}\|\nabla u_{i,n}(0)\|^2 + \frac{a_i^\varepsilon g_i}{2}\|u_{i,n}(0)\|^2_{L^2(\Gamma_R^\varepsilon)} + \frac{a_i^{\varepsilon,2}}{2}\|u_{i,n}(0)\|^2_{L^2(\Gamma^\varepsilon)} \\
&\qquad + \frac{b_i^{\varepsilon,2}}{2}\|v_{i,n}^\varepsilon(0)\|^2_{L^2(\Gamma^\varepsilon)} + \varepsilon\int_0^T a_i^\varepsilon\|\partial_t u_{i,n}\|^2 + a_i^\varepsilon\delta_i^\varepsilon c^\delta c^\varepsilon\|\bar\theta\|_\infty \int_0^T \|\nabla u_{i,n}\|^2 \\
&\qquad + C^M C^\varepsilon + \varepsilon\int_0^T a_i^\varepsilon\|\partial_t u_{i,n}\|^2.
\end{aligned}$$

Dropping the positive terms on the left, and denoting the initial condition terms on the right as C_0, we get:

$$\begin{aligned}
&\int_0^T a_i^\varepsilon(1-2\varepsilon)\|\partial_t u_{i,n}\|^2 + \int_0^T b_i^\varepsilon\|\partial_t v_{i,n}^\varepsilon\|^2 + \frac{a_i^\varepsilon d_i^0}{2}\|\nabla u_{i,n}(T)\|^2 \\
&\qquad \le C_0 + a_i^\varepsilon\delta_i^\varepsilon c^\delta c^\varepsilon\|\bar\theta\|_\infty\int_0^T\|\nabla u_{i,n}\|^2 + C^M C^\varepsilon. \qquad (4.58)
\end{aligned}$$

Gronwall's lemma gives:

$$\|\nabla u_{i,n}\|^2 + \int_0^T\|\partial_t u_{i,n}\|^2 + \int_0^T\|\partial_t v_{i,n}^\varepsilon\|^2 \le C,$$

where $C>0$ depends on δ, M and T, but is independent of n. Together with (4.54) this gives:

$$u_{i,n} \in H^1(0,T;L^2(\Omega^\varepsilon)) \cap L^\infty(0,T;H^1(\Omega^\varepsilon)), \qquad (4.59)$$

$$v_{i,n}^\varepsilon \in H^1(0,T;L^2(\Gamma^\varepsilon)). \qquad (4.60)$$

Hence, we can choose subsequences $u_{i,n_j} \rightharpoonup u_i$ in $H^1(0,T;L^2(\Omega^\varepsilon))$ and $u_{i,n_j}\to u_i$ in $C([0,T],L^2(\Omega^\varepsilon))$ and weakly* in $L^\infty(0,T;H^1(\Omega^\varepsilon))$ as $i\to\infty$ and $v_{i,n_j}^\varepsilon \rightharpoonup v_i^\varepsilon$ in $H^1(0,T;L^2(\Gamma^\varepsilon))$ as $j\to\infty$. Since R_i^M is Lipschitz continuous, the rest of the proof follows the same line of arguments as in Lemma 4.3.2. □

Lemma 4.3.5. Positivity and boundedness of solutions to (P_2). *Let $\bar{\theta} \in K(T, M)$, $M > 0$ and assume (A_1)-(A_2). Then $0 \leq u_i \leq M_i(T+1)$ a.e. in $(0,T) \times \Omega^\varepsilon$, $0 \leq v_i^\varepsilon \leq \bar{M}_i(T+1)$ a.e. on $(0,T) \times \Gamma^\varepsilon$, where $M_i > 0$ and $\bar{M}_i > 0$ are independent of M.*

Proof. Testing (4.39) with $\psi_i = -u_i^-$ and the definition of R_i^M gives:

$$\begin{aligned}\frac{1}{2}\partial_t\|u_i^-\|^2 + d_i^0\|\nabla u_i^-\|^2 + g_i\|u_i^-\|^2_{L^2(\Gamma_R^\varepsilon)} + a_i^\varepsilon\|u_i^-\|^2_{L^2(\Gamma^\varepsilon)} + b_i^\varepsilon \int\limits_{\Gamma^\varepsilon} v_i^\varepsilon u_i^- \\ \leq \delta_i^\varepsilon c^\delta \|\bar{\theta}\|_\infty \int_\Omega \nabla u_i^- u_i^- - \int\limits_{\Omega^\varepsilon} \sum_{j=1}^{i-1} \beta_{j,i-j} u_j^+ u_{i-j}^+ u_i^- \\ + \int\limits_{\Omega^\varepsilon} \sum_{j=1}^{N} \beta_{ij} u_i^+ u_j^+ u_i^- .\end{aligned}$$

The second term on the right is always negative, while the third is always zero. We can discard them and apply Cauchy-Schwarz and Young's inequalities to the first term on the right, as well as discard the positive terms on the left to obtain:

$$\frac{1}{2}\partial_t\|u_i^-\|^2 + (d_i^0 - \eta)\|\nabla u_i^-\|^2 \leq \delta_i^\varepsilon c^\delta \|\bar{\theta}\|_\infty c^\eta \|u_i^-\|^2 + b_i^\varepsilon \int\limits_{\Gamma^\varepsilon} v_i^{\varepsilon,-} u_i^- . \tag{4.61}$$

Testing (4.41) with $\varphi_i = -v_i^{\varepsilon,-}$ gives:

$$\frac{1}{2}\partial_t\|v_i^{\varepsilon,-}\|^2_{L^2(\Gamma^\varepsilon)} \leq b_i^\varepsilon \|v_i^{\varepsilon,-}\|^2_{L^2(\Gamma^\varepsilon)} + a_i^\varepsilon \int\limits_{\Gamma^\varepsilon} v_i^{\varepsilon,-} u_i^- . \tag{4.62}$$

We rely on Cauchy-Schwarz, Young's and trace inequalities to estimate the last term. We obtain:

$$\begin{aligned}\int\limits_{\Gamma^\varepsilon} v_i^{\varepsilon,-} u_i^- &\leq \|v_i^{\varepsilon,-}\|_{L^2(\Gamma^\varepsilon)} \|u_i^-\|_{L^2(\Gamma^\varepsilon)} \leq c^\eta \|v_i^{\varepsilon,-}\|^2_{L^2(\Gamma^\varepsilon)} + \eta\|u_i^-\|^2_{L^2(\Gamma^\varepsilon)} \\ &\leq c^\eta \|v_i^{\varepsilon,-}\|^2_{L^2(\Gamma^\varepsilon)} + \eta C(\|u_i^-\|^2 + \|\nabla u_i^-\|^2)\end{aligned}$$

Adding (4.61) and (4.62) and choosing $\eta + \eta C < d_i^0$ and taking into account that $u_i^-(0) \equiv 0$, Gronwall's lemma gives $\|u_i^-\|^2 + \|v_i^{\varepsilon,-}\|^2 \leq 0$, that is $u_i \geq 0$ a.e. in Ω^ε and $v_i^\varepsilon \geq 0$ a.e. in Γ^ε for all $t \in (0,T)$.

Let $i = 1$ and $\psi_1 := (u_1 - M_1)^+$ in (4.39) and $\varphi_1 := (v_1^\varepsilon - \bar{M}_1)^+$ in (4.41).

Apply (4.3) for the cross-diffusion term to get:

$$\begin{aligned}
&\frac{1}{2}\partial_t\|(u_1-M_1)^+\|^2+d_1^0\|\nabla(u_1-M_1)^+\|^2\\
&\quad+g_1\|(u_1-M_1)^+\|^2_{L^2(\Gamma_R^\varepsilon)}+g_1\int\limits_{\Gamma_R^\varepsilon}M_1(u_1-M_1)^+\\
&\quad+a_1^\varepsilon\|(u_1-M_1)^+\|^2_{L^2(\Gamma^\varepsilon)}+(a_1^\varepsilon M_1-b_1^\varepsilon\bar{M}_1)\int\limits_{\Gamma^\varepsilon}(u_1-M_1)^+\\
&\quad+b_1^\varepsilon\int\limits_{\Gamma^\varepsilon}(v_1^\varepsilon-\bar{M}_1)^-(u_1-M_1)^+\le b_1^\varepsilon\int\limits_{\Gamma^\varepsilon}(v_1^\varepsilon-\bar{M}_1)^+(u_1-M_1)^+\\
&\quad+\delta_1^\varepsilon c^\delta\|\bar{\theta}\|_\infty\|\nabla(u_1-M_1)^+(u_1-M_1)^+\|_{L^1(\Omega^\varepsilon)}+c^M\|(u_1-M_1)^+\|\\
&\frac{1}{2}\partial_t\|(v_1^\varepsilon-\bar{M}_1)^+\|^2_{L^2(\Gamma^\varepsilon)}+b_1^\varepsilon\|(v_1^\varepsilon-\bar{M}_1)^+\|^2_{L^2(\Gamma^\varepsilon)}+a_1^\varepsilon\int\limits_{\Gamma^\varepsilon}(u_1-M_1)^-(v_1^\varepsilon-\bar{M}_1)^+\\
&\quad\le a_1^\varepsilon\int\limits_{\Gamma^\varepsilon}(v_1^\varepsilon-\bar{M}_1)^+(u_1-M_1)^++(a_1^\varepsilon M_1-b_1^\varepsilon\bar{M}_1)\int\limits_{\Gamma^\varepsilon}(v_1^\varepsilon-\bar{M}_1)^+.
\end{aligned}$$

Now, we add the two inequalities, while dropping the positive terms on the left and using Cauchy-Schwarz and Young's inequalities on the right to obtain:

$$\begin{aligned}
&\frac{1}{2}\partial_t\|(u_1-M_1)^+\|^2+(d_1^0-\eta)\|\nabla(u_1-M_1)^+\|^2+a_1^\varepsilon\|(u_1-M_1)^+\|^2_{L^2(\Gamma^\varepsilon)}\\
&\quad+\frac{1}{2}\partial_t\|(v_1^\varepsilon-\bar{M}_1)^+\|^2_{L^2(\Gamma^\varepsilon)}\le(a_1^\varepsilon+b_1^\varepsilon)(\eta\|(u_1-M_1)^+\|^2_{L^2(\Gamma^\varepsilon)}\\
&\quad+c^\eta\|(v_1^\varepsilon-\bar{M}_1)^+\|_{L^2(\Gamma^\varepsilon)})+\delta_1^\varepsilon c^\eta c^\delta\|\bar{\theta}\|_\infty\|(u_1-M_1)^+\|^2\\
&\quad+\eta+c^\eta c^M\|(u_1-M_1)^+\|^2+\eta+c^\eta(a_1^\varepsilon M_1-b_1^\varepsilon\bar{M}_1)\|(v_1^\varepsilon-\bar{M}_1)^+\|^2_{L^2(\Gamma^\varepsilon)}.
\end{aligned}$$

We choose M_1 and $\bar{M}_1$ such that $a_1^\varepsilon M_1-b_1^\varepsilon\bar{M}_1=0$. Then Gronwall's lemma gives:

$$\begin{aligned}
&\|(u_1-M_1)^+(t)\|^2+\|(v_1^\varepsilon-\bar{M}_1)^+\|^2_{L^2(\Gamma^\varepsilon)}\\
&\quad\le(\|(u_1-M_1)^+(0)\|^2+\|(v_1^\varepsilon-\bar{M}_1)^+(0)\|^2_{L^2(\Gamma^\varepsilon)})\exp\left(C(\delta_i^\varepsilon,\bar{\theta},\delta,M)t\right).
\end{aligned}$$

Since we choose M_1 to satisfy $\|(u_1-M_1)^+(0)\|=0$, and $\bar{M}_1$ to satisfy $\|(v_1^\varepsilon-\bar{M}_1)^+(0)\|_{L^2(\Gamma^\varepsilon)}=0$, we get $u_1\in\ L^\infty_+((0,T)\times\Omega^\varepsilon)$ and $v_1^\varepsilon\in L^\infty_+((0,T)\times\Gamma^\varepsilon)$.

Let $i=2$ and $\psi_2:=(u_2-M_2(t+1))^+$ in (4.39) and $\varphi_2:=(v_2^\varepsilon-\bar{M}_2(t+1))^+$

in (4.41):

$$\begin{aligned}
&\frac{1}{2}\partial_t(\|(u_2 - M_2(t+1))^+\|^2 + \|(v_2^\varepsilon - \bar{M}_2(t+1))^+\|^2_{L^2(\Gamma^\varepsilon)}) \\
&\quad + \frac{d_2^0}{2}\|\nabla(u_2 - M_2(t+1))^+\|^2 \\
&\quad + a_2^\varepsilon\|(u_2 - M_2(t+1))^+\|^2_{L^2(\Gamma^\varepsilon)} + b_2^\varepsilon\|(v_2^\varepsilon - \bar{M}_2(t+1))^+\|^2_{L^2(\Gamma^\varepsilon)} \\
&\quad \le C\|(u_2 - M_2(t+1))^+\|^2 + \int\limits_{\Omega^\varepsilon} R_2^M(u)(u_2 - M_2(t+1))^+ \\
&\qquad - M_2\int\limits_{\Omega^\varepsilon}(u_2 - M_2(t+1))^+ - \bar{M}_2(v_2^\varepsilon - \bar{M}_2(t+1))^+.
\end{aligned}$$

Here, we note that

$$R_2^M(u) \le \frac{1}{2}\beta_{11}\sigma_M(u_1)^2 \le \frac{1}{2}\beta_{11}u_1^2 \le \frac{1}{2}\beta_{11}M_1^2.$$

Similarly, we have:

$$\begin{aligned}
&\frac{1}{2}\partial_t(\|(u_2 - M_2(t+1))^+\|^2 + \|(v_2^\varepsilon - \bar{M}_2(t+1))^+\|^2_{L^2(\Gamma^\varepsilon)}) \\
&\quad \le C\|(u_2 - M_2(t+1))^+\|^2 + (\frac{1}{2}\beta_{11}M_1^2 - M_2)\int\limits_{\Omega^\varepsilon}(u_2 - M_2(t+1))^+ \\
&\quad \le C\|(u_2 - M_2(t+1))^+\|^2.
\end{aligned}$$

By applying Gronwall's lemma with $\frac{1}{2}\beta_{11}M_1^2 \le M_2$, we see that $u_2 \le M_2(T+1)$ in $(0,T)\times\Omega^\varepsilon$ and $v_2^\varepsilon \le \bar{M}_2(T+1)$ on $(0,T)\times\Gamma^\varepsilon$. Recursively, we can obtain the same estimates for u_i and v_i^ε for $i \ge 3$. □

Lemma 4.3.6. The boundedness of the concentration gradient for (P_2).

Let $\bar{\theta} \in K(T, M_0)$ and assume (A_1)-(A_2) to hold. Then there exists a positive constant $C(M_0)$ such that $\|\nabla u_i(t)\| \le C(M_0)$ and $\int_0^T ||\partial_t u_i(t)||^2 dt \le C(M_0)$ for $t \in (0,T)$.

Proof. Let $\psi_i = \partial_t u_i$ in (4.39):

$$\begin{aligned}
&\|\partial_t u_i\|^2 + \frac{d_i^0}{2}\partial_t\|\nabla u_i\|^2 + \frac{g_i}{2}\partial_t\|u_i\|^2_{L^2(\Gamma_R^\varepsilon)} + \frac{a_i^\varepsilon}{2}\partial_t\|u_i\|^2_{L^2(\Gamma^\varepsilon)} \le \\
&\qquad \underbrace{b_i^\varepsilon\int\limits_{\Gamma^\varepsilon} v_i^\varepsilon\partial_t u_i}_{A} + \underbrace{|\delta_i^\varepsilon\int\limits_{\Omega^\varepsilon}\nabla^\delta\bar{\theta}\cdot\nabla u_i\partial_t u_i|}_{B} + \underbrace{|\int\limits_{\Omega^\varepsilon} R_i(u)\partial_t u_i|}_{C}.
\end{aligned}$$

We shall now estimate one by one the terms A, B, and C. Note first that

$$A = b_i^\varepsilon\partial_t\int\limits_{\Gamma^\varepsilon} v_i^\varepsilon u_i - b_i^\varepsilon\int\limits_{\Gamma^\varepsilon} u_i\partial_t v_i^\varepsilon \le b_i^\varepsilon\partial_t\int\limits_{\Gamma^\varepsilon} v_i^\varepsilon u_i + \frac{1}{2}\|\partial_t v_i^\varepsilon\|^2_{L^2(\Gamma^\varepsilon)} + \frac{1}{2}b_i^{\varepsilon,2}\|u_i\|^2_{L^2(\Gamma^\varepsilon)}.$$

Then we have

$$B \le \frac{1}{2}\|\partial_t u_i\|^2 + \frac{\delta^{\varepsilon,2}}{2}\int\limits_{\Omega^\varepsilon}(\nabla^\delta\bar\theta)^2(\nabla u_i)^2 \le \frac{1}{2}\|\partial_t u_i\|^2 + \frac{\delta^{\varepsilon,2}}{2}c^\delta\|\bar\theta\|_\infty^2\|\nabla u_i\|^2,$$

and

$$C \le C_{B,\eta} + \eta\|\partial_t u_i\|^2.$$

All this leads to, after integration from 0 to T:

$$\begin{aligned}(\frac{1}{2}-\eta)\int_0^T \|\partial_t u_i\|^2 + \frac{d_i^0}{2}\|\nabla u_i(T)\|^2 + \frac{g_i}{2}\|u_i(T)\|^2_{L^2(\Gamma^\varepsilon_R)} + \frac{a_i^\varepsilon}{2}\|u_i(T)\|^2_{L^2(\Gamma^\varepsilon)}\\ + b_i^\varepsilon\int\limits_{\Gamma^\varepsilon}\bar v(0)u_i(0) \le TC_{B,\eta} + \frac{\delta^{\varepsilon,2}}{2}c^\delta\|\bar\theta\|_\infty^2\int_0^T\|\nabla u_i\|^2\\ + \frac{d_i^0}{2}\|\nabla u_i(0)\|^2 + \frac{g_i}{2}\|u_i(0)\|^2_{L^2(\Gamma^\varepsilon_R)} + \frac{a_i^\varepsilon}{2}\|u_i(0)\|^2_{L^2(\Gamma^\varepsilon)}\\ \underbrace{+ b_i^\varepsilon\int\limits_{\Gamma^\varepsilon}\bar v(T)u_i(T)}_{D} + b_i^\varepsilon\int_0^T\int\limits_{\Gamma^\varepsilon}u_i\partial_t\bar v.\end{aligned}$$

Removing some positive terms on the left and using Cauchy-Schwarz and Young's inequalities to obtain an upper bound for D, we finally get:

$$\begin{aligned}(\frac{1}{2}-\eta)\int_0^T\|\partial_t u_i\|^2 + \frac{d_i^0}{2}\|\nabla u_i(T)\|^2 + (\frac{a_i^\varepsilon}{2}-\eta)\|u_i(T)\|^2_{L^2(\Gamma^\varepsilon)}\\ \le TC_{B,\eta} + \frac{\delta^{\varepsilon,2}}{2}c^\delta\|\bar\theta\|_\infty^2\int_0^T\|\nabla u_i\|^2 + C_0\\ + b_i^\varepsilon\|\bar v(T)\|^2_{L^2(\Gamma^\varepsilon)} + b_i^\varepsilon\|u_i\|_\infty\|\bar v\|_\infty,\end{aligned}$$

where C_0 depends on $\|u_i^0\|$. Using Gronwall's argument, we obtain the statement of the lemma. □

Lemma 4.3.7. The boundedness of the temperature gradient for (P_1).

Let $\bar u_i \in K(T, M_0)$ and assume (A_1)-(A_2) to hold. Then there exists a positive constant $C(M_0)$ such that $\|\nabla\theta^\varepsilon(t)\| \le C(M_0)$ and $\int_0^T \partial_t\theta^\varepsilon(t)||^2dt \le C(M_0)$ for $t \in (0,T)$.

Proof. Let $\phi_i = \partial_t\theta_i^\varepsilon$ in (4.25):

$$\|\partial_t\theta^\varepsilon\|^2 + \frac{\kappa_0^\varepsilon}{2}\partial_t\|\nabla\theta^\varepsilon\|^2 + \frac{g_0}{2}\|\theta^\varepsilon\|^2_{L^2(\Gamma^\varepsilon_R)} \le c^\delta MN(\eta\|\partial_t\theta^\varepsilon\|^2 + \frac{1}{4\eta}\|\nabla\theta^\varepsilon\|^2).$$

Applying Gronwall's lemma gives us the desired statement. □

Theorem 4.3.8. Existence and uniqueness of weak solutions (P^ε)
Let (A_1)-(A_2) hold. Then there exists a unique solution to (P^ε).

Proof. For any $M > 0$, $X_M := K(M,T) \times K(M,T)^N$ is a closed set of $X := L^2(0,T;L^1(\Omega^\varepsilon))^{N+1}$. Let $\bar\theta_1, \bar\theta_2, \bar u_{i,1}, \bar u_{i,2} \in K(M,T)$, for $i \in \{1,\dots,N\}$, and put $\bar\theta := \bar\theta_1 - \bar\theta_2$, $\bar u_i := \bar u_{i,1} - \bar u_{i,2}$, $(\theta_1^\varepsilon, u_{i,1}, v_{i,1}^\varepsilon) = \mathbf{T}(\bar\theta_1, \bar u_1)$ and $(\theta_2^\varepsilon, u_{i,2}, v_{i,2}^\varepsilon) = \mathbf{T}(\bar\theta_2, \bar u_2)$. Moreover, we define $\theta^\varepsilon = \theta_1^\varepsilon - \theta_2^\varepsilon$ and $u_i = u_{i,1} - u_{i,2}$ and $v_i^\varepsilon = v_{i,1}^\varepsilon - v_{i,2}^\varepsilon$.

By Lemma 4.3.3 and Lemma 4.3.5, $\mathbf{T} : X_M \to X_M$ for $M > \max(\|\theta^{\varepsilon,0}\|_{L^\infty(\Omega^\varepsilon)}, M_1(T+1), M_2(T+1), \dots, M_N(T+1),)$. Hence, we want to prove the existence of a positive constant $C < 1$ such that

$$\|\mathbf{T}(\bar\theta_1, \bar u_{i,1}) - \mathbf{T}(\bar\theta_2, \bar u_{i,2})\|_X \le C\|(\bar\theta_1, \bar u_{i,1}) - (\bar\theta_2, \bar u_{i,2})\|_X$$

for small $T > 0$. Substituting $\theta_1^\varepsilon, \theta_2^\varepsilon, u_{i,1}, u_{i,2}, v_1^\varepsilon, v_2^\varepsilon$ into the formulation:

$$\begin{aligned}
&\int_{\Omega^\varepsilon} \partial_t \theta_1^\varepsilon(\theta_1^\varepsilon - \theta_2^\varepsilon) + \int_{\Omega^\varepsilon} \kappa^\varepsilon \nabla\theta_1^\varepsilon \nabla(\theta_1^\varepsilon - \theta_2^\varepsilon) + g_0 \int_{\Gamma_R^\varepsilon} \theta_1^\varepsilon(\theta_1^\varepsilon - \theta_2^\varepsilon) \\
&\qquad = \tau^\varepsilon \sum_{i=1}^N \int_{\Omega^\varepsilon} \nabla^\delta \bar u_{i,1} \cdot \nabla\theta_1^\varepsilon(\theta_1^\varepsilon - \theta_2^\varepsilon), \\
&\int_{\Omega^\varepsilon} \partial_t \theta_2^\varepsilon(\theta_2^\varepsilon - \theta_1^\varepsilon) + \int_{\Omega^\varepsilon} \kappa^\varepsilon \nabla\theta_2^\varepsilon \nabla(\theta_2^\varepsilon - \theta_1^\varepsilon) + g_0 \int_{\Gamma_R^\varepsilon} \theta_2^\varepsilon(\theta_2^\varepsilon - \theta_1^\varepsilon) \\
&\qquad = \tau^\varepsilon \sum_{i=1}^N \int_{\Omega^\varepsilon} \nabla^\delta \bar u_{i,2} \cdot \nabla\theta_2^\varepsilon(\theta_2^\varepsilon - \theta_1^\varepsilon).
\end{aligned}$$

Adding the last two equations we obtain:

$$\begin{aligned}
&\frac{1}{2}\partial_t\|\theta^\varepsilon\|^2 + \kappa^{\varepsilon,0}\|\nabla\theta^\varepsilon\|^2 + g_0\|\theta^\varepsilon\|^2_{L^2(\Gamma_R^\varepsilon)} \\
&\qquad \le \tau^\varepsilon \sum_{i=1}^N \underbrace{\Big| \int_{\Omega^\varepsilon} (\nabla^\delta \bar u_{i,1} \cdot \nabla\theta_1^\varepsilon - \nabla^\delta \bar u_{i,2} \cdot \nabla\theta_2^\varepsilon)(\theta_1^\varepsilon - \theta_2^\varepsilon) \Big|}_{A}.
\end{aligned}$$

The term A can be expressed as:

$$\begin{aligned}
A &= \int_{\Omega^\varepsilon} (\nabla^\delta \bar u_{i,1} \cdot \nabla\theta_1^\varepsilon - \nabla^\delta \bar u_{i,2} \cdot \nabla\theta_1^\varepsilon)(\theta_1^\varepsilon - \theta_2^\varepsilon) \\
&\quad + \int_{\Omega^\varepsilon} (\nabla^\delta \bar u_{i,2} \cdot \nabla\theta_1^\varepsilon - \nabla^\delta \bar u_{i,2} \cdot \nabla\theta_2^\varepsilon)(\theta_1^\varepsilon - \theta_2^\varepsilon) \\
&= \underbrace{\int_{\Omega^\varepsilon} \nabla^\delta \bar u_i \cdot \nabla\theta_1^\varepsilon \theta^\varepsilon}_{B} + \underbrace{\int_{\Omega^\varepsilon} \nabla^\delta \bar u_{i,2} \cdot \nabla\theta^\varepsilon \theta^\varepsilon}_{C}.
\end{aligned}$$

With the help of Lemma 4.3.7, the terms B and C can be estimated as follows:

$$B \leq c^\delta M\|\bar{u}_i\|^2 + M\|\theta^\varepsilon\|^2$$
$$C \leq c^\delta \|\bar{u}_{i,2}\|_\infty(\eta\|\nabla\theta^\varepsilon\|^2 + \frac{1}{4\eta}\|\theta^\varepsilon\|^2).$$

Looking at the formulation for the concentrations, we have:

$$\begin{aligned}
&\int_{\Omega^\varepsilon} \partial_t u_{i,1}(u_{i,1}-u_{i,2}) + \int_{\Omega^\varepsilon} d_i\nabla u_{i,1}\cdot\nabla(u_{i,1}-u_{i,2}) + g_i\int_{\Gamma_N^\varepsilon} u_{i,1}(u_{i,1}-u_{i,2})\\
&\quad + a_i^\varepsilon\int_{\Gamma^\varepsilon} u_{i,1}(u_{i,1}-u_{i,2}) - b_i^\varepsilon\int_{\Gamma^\varepsilon} v_{i,1}^\varepsilon(u_{i,1}-u_{i,2})\\
&\quad = \delta^\varepsilon\int_{\Omega^\varepsilon}\nabla^\delta\bar{\theta}_1\cdot u_{i,1}(u_{i,1}-u_{i,2}) + \int_{\Omega^\varepsilon} R_i(u_1)(u_{i,1}-u_{i,2}),\\
&\int_{\Omega^\varepsilon} \partial_t u_{i,2}(u_{i,2}-u_{i,1}) + \int_{\Omega^\varepsilon} d_i\nabla u_{i,2}\cdot\nabla(u_{i,2}-u_{i,1}) + g_i\int_{\Gamma_N^\varepsilon} u_{i,2}(u_{i,2}-u_{i,1})\\
&\quad + a_i^\varepsilon\int_{\Gamma^\varepsilon} u_{i,2}(u_{i,2}-u_{i,1}) - b_i^\varepsilon\int_{\Gamma^\varepsilon} v_{i,2}^\varepsilon(u_{i,2}-u_{i,1})\\
&\quad = \delta^\varepsilon\int_{\Omega^\varepsilon}\nabla^\delta\bar{\theta}_2\cdot u_{i,2}(u_{i,2}-u_{i,1}) + \int_{\Omega^\varepsilon} R_i(u_2)(u_{i,2}-u_{i,1}).
\end{aligned}$$

We also test the deposition equation with v_i^ε to obtain:

$$\frac{1}{2}\|v_i^\varepsilon\|^2_{L^2(\Gamma^\varepsilon)} = a_i^\varepsilon\int_{\Gamma^\varepsilon} v_i^\varepsilon u_i - b_i^\varepsilon\|v_i^\varepsilon\|^2_{L^2(\Gamma^\varepsilon)}.$$

After adding the three above equations, we obtain:

$$\begin{aligned}
&\frac{1}{2}\partial_t\|u_i\|^2 + \frac{1}{2}\partial_t\|v_i^\varepsilon\|^2_{L^2(\Gamma^\varepsilon)} + d_i^0\|\nabla u_i\|^2 + g_i\|u_i\|^2_{L^2(\Gamma_R^\varepsilon)} + a_i^\varepsilon\|u_i\|^2_{L^2(\Gamma^\varepsilon)}\\
&\quad \leq (a_i^\varepsilon + b_i^\varepsilon)\int_{\Gamma^\varepsilon}|v_i^\varepsilon u_i| - b_i^\varepsilon\|v_i^\varepsilon\|^2_{L^2(\Gamma^\varepsilon)} + \int_{\Omega^\varepsilon}|(\nabla^\delta\bar{\theta}_1\cdot\nabla u_{i,1} - \nabla^\delta\bar{\theta}_2\cdot\nabla u_{i,2})u_i|\\
&\quad + \int_{\Omega^\varepsilon}|(R_i(u_1)-R_i(u_2))u_i|,
\end{aligned}$$

$$\frac{1}{2}\partial_t\|u_i\|^2+\frac{1}{2}\partial_t\|v_i^\varepsilon\|^2_{L^2(\Gamma^\varepsilon)}+d_i^0\|\nabla u_i\|^2+g_i\|u_i\|^2_{L^2(\Gamma_R^\varepsilon)}+(a_i^\varepsilon-\eta)\|u_i\|^2_{L^2(\Gamma^\varepsilon)}\leq$$
$$(\frac{(a_i^\varepsilon+b_i^\varepsilon)^2}{4\eta}-b_i^\varepsilon)\|v_i^\varepsilon\|^2_{L^2(\Gamma^\varepsilon)}+\underbrace{\int_{\Omega^\varepsilon}|\nabla^\delta\bar\theta_1\cdot\nabla u_i u_i|}_{A}$$
$$+\underbrace{\int_{\Omega^\varepsilon}|\nabla u_{i,2}\cdot\nabla^\delta\bar\theta u_i|}_{B}+\underbrace{\int_{\Omega^\varepsilon}|(R_i(u_1)-R_i(u_2))u_i|}_{C},$$

where the sub-expressions can be estimated as:

$$A\leq\eta\|\nabla u_i\|^2+\frac{1}{4\eta}c^\delta\|\bar\theta\|^2_\infty\|u_i\|^2,$$
$$B\leq c^\delta M\|\bar\theta\|^2+M\|u_i\|^2.$$

Note that with the boundedness of u_i we can treat R_i as Lipschitz:

$$C\leq C_L\|u_i\|^2.$$

Adding up the estimates for the temperature and concentrations:

$$\frac{1}{2}\|u_i\|^2+\frac{1}{2}\|v_i^\varepsilon\|^2+\frac{1}{2}\|\theta^\varepsilon\|^2+\hat{d}_i\|\nabla u_i\|^2+\hat{\kappa^\varepsilon}\|\nabla\theta^\varepsilon\|^2+\hat{g}_i\|u_i\|^2_{L^2(\Gamma_R^\varepsilon)}$$
$$+\hat{a_i^\varepsilon}\|u_i\|^2_{L^2(\Gamma^\varepsilon)}+\hat{g_0}\|\theta^\varepsilon\|^2_{L^2(\Gamma_R^\varepsilon)}\leq c_1\|u_i\|^2+c_2\|v_i^\varepsilon\|^2+c_3\|\theta^\varepsilon\|^2$$
$$+c^\delta M(\|\bar u_i\|^2+\|\bar\theta\|^2).$$

Gronwall's lemma gives the estimate:

$$\|\theta^\varepsilon(t)\|^2+\|u_i(t)\|^2\leq C\left(\|\bar\theta\|^2_{L^2(0,T;L^2(\Omega^\varepsilon))}+\|\bar u_i\|^2_{L^2(0,T;L^2(\Omega^\varepsilon))}\right).$$

Integrating over $(0,T)$, we have:

$$\int_0^T\|\theta^\varepsilon(t)\|^2+\|u_i(t)\|^2\leq CT\left(\|\bar\theta\|^2_{L^2(0,T;L^2(\Omega^\varepsilon))}+\|\bar u_i\|^2_{L^2(0,T;L^2(\Omega^\varepsilon))}\right).$$

Accordingly, $\mathbf{T}$ is a contraction mapping for T' such that $CT'<1$. Then the Banach fixed point theorem shows that (P^ε)admits a unique solution in the sense of Definition 1 on $[0,T']$. Next, we consider (P^ε)on $[T',T]$. Then we can solve uniquely this problem on $[T',2T']$. Recursively, we can construct a solution of (P^ε)on the whole interval $[0,T]$. □

4.4 Passing to $\varepsilon \to 0$ (the homogenization limit)

4.4.1 Preliminaries on periodic homogenization

Now that the well-posedness of our microscopic system is available, we can investigate what happens as the parameter ε vanishes. Recall that ε defines both the microscopic geometry and the periodicity in the model parameters.

Lemma 4.4.1. Additional *a priori* estimates.
Let (A_1)-(A_2) *hold. Then the following bounds hold uniformly in* ε*:*

$$\|\partial_t \nabla \theta^\varepsilon\|_{L^2(\Omega^\varepsilon)} \leq C, \tag{4.63}$$

$$\|\partial_t \nabla u_i\|_{L^2(\Omega^\varepsilon)} \leq C, \tag{4.64}$$

where $C > 0$ *is independent of* ε*.*

Proof. For simplicity, we decide to do first a few formal calculations. We differentiate (4.8) and (4.9) with respect to time and then test with $\phi \in H^1(\Omega^\varepsilon)$. This gives

$$\int_{\Omega^\varepsilon} \partial_t^2 \theta^\varepsilon \phi + \int_{\Omega^\varepsilon} \kappa^\varepsilon \partial_t \nabla \theta^\varepsilon \cdot \nabla \phi + g_0 \int_{\Gamma_R^\varepsilon} \partial_t \theta^\varepsilon \phi = \tau^\varepsilon \sum_{i=1}^N \int_{\Omega^\varepsilon} \partial_t (\nabla^\delta u_i \cdot \nabla \theta^\varepsilon) \phi. \tag{4.65}$$

Choosing $\phi = \partial_t \theta^\varepsilon$, we get:

$$\frac{1}{2}\partial_t \|\partial_t \theta^\varepsilon\|^2 + \kappa_0^\varepsilon \|\partial_t \nabla \theta^\varepsilon\|^2 + \varepsilon g_0 \|\partial_t \theta^\varepsilon\|^2_{L^2(\Gamma_R^\varepsilon)} \leq$$
$$\leq \delta^\varepsilon \sum_{i=1}^N \int_{\Omega^\varepsilon} (\nabla^\delta u_i \cdot \partial_t \nabla \theta^\varepsilon \partial_t \theta^\varepsilon + \partial_t \nabla^\delta u_i \cdot \nabla \theta^\varepsilon \partial_t \theta^\varepsilon). \tag{4.66}$$

Here we see that

$$\tau^\epsilon \sum_{i=1}^N \int_{\Omega^\varepsilon} (\nabla^\delta u_i \cdot \partial_t \nabla \theta^\varepsilon \partial_t \theta^\varepsilon) \leq \tau^\epsilon \sum_{i=1}^N \int_{\Omega^\varepsilon} ||\nabla^\delta u_i||_{L^\infty(\Omega^\epsilon)} ||\partial_t \nabla \theta^\varepsilon|| ||\partial_t \theta^\varepsilon|| \leq$$

$$\tau^\epsilon C_\delta \sum_{i=1}^N ||u_i|| ||\partial_t \nabla \theta^\varepsilon|| ||\partial_t \theta^\varepsilon|| \leq \frac{\kappa_0}{2} ||\partial_t \nabla \theta^\varepsilon||^2 + \frac{1}{2\kappa_0} (\tau^\epsilon C_\delta N^2) ||u_i||^2 ||\partial_t \theta^\varepsilon||^2,$$

and also

$$\tau^\epsilon \sum_{i=1}^N \int_{\Omega^\varepsilon} (\partial_t \nabla^\delta u_i \cdot \nabla \theta^\varepsilon \partial_t \theta^\varepsilon) = \tau^\epsilon \sum_{i=1}^N \int_{\Omega^\varepsilon} (\nabla^\delta \partial_t u_i \cdot \nabla \theta^\varepsilon \partial_t \theta^\varepsilon) \leq$$

$$\tau^{\epsilon}\sum_{i=1}^{N}\int_{\Omega^{\varepsilon}}||\nabla^{\delta}\partial_t u_i||_{L^{\infty}(\Omega^{\epsilon})}||\nabla\theta^{\varepsilon}||||\partial_t\theta^{\varepsilon}||\leq\frac{1}{2}\tau^{\epsilon}C_{\delta}C(M_0)\sum_{i=1}^{N}(||\partial_t u_i||^2+||\partial_t\theta^{\varepsilon}||^2).$$

Since $||\partial_t\theta^{\varepsilon}(0)||\leq||\nabla\cdot\kappa^{\epsilon}\nabla\theta^{\varepsilon}(0)||+\tau^{\epsilon}\sum_{i=1}^{N}||\nabla^{\delta}u_i(0)\cdot\nabla\theta(0)||$ and taking into account that we already have estimated $\|u_i\|_{L^{\infty}(\Omega^{\varepsilon})}$, $\|\partial_t u_i\|_{L^{\infty}(\Omega^{\varepsilon})}$ and $\|\nabla\theta_i^{\varepsilon}\|_{L^2(\Omega^{\varepsilon})}$ in Lemma 4.3.5 and Lemma 4.3.6, Gronwall's lemma gives us (4.63). We get (4.64) in the same fashion. □

Definition 2. *(Two-scale convergence [95],[1]). Let (u^{ε}) be a sequence of functions in $L^2(0,T;L^2(\Omega))$, where Ω is an open set in $\mathbb{R}^n$ and $\varepsilon>0$ tends to 0. (u^{ε}) two-scale converges to a unique function $u_0(t,x,y)\in L^2((0,T)\times\Omega\times Y)$ if and only if for all $\phi\in C_0^{\infty}((0,T)\times\Omega,C_{\#}^{\infty}(Y))$ we have:*

$$\lim_{\varepsilon\to 0}\int_0^T\int_{\Omega}u^{\varepsilon}\phi(t,x,\frac{x}{\varepsilon})dxdt=\frac{1}{|Y|}\int_0^T\int_{\Omega}\int_{Y}u_0(t,x,y)\phi(t,x,y)dydxdt. \tag{4.67}$$

We denote (4.67) by $u^{\varepsilon}\overset{2}{\rightharpoonup}u_0$.

The space $C_{\#}^{\infty}(Y)$ refers to the space of all Y-periodic C^{∞}-functions. The spaces $H_{\#}^1(Y)$ and $C_{\#}^{\infty}(\Gamma)$ have a similar meaning; the index # is always indicating that is about Y-periodic functions.

Theorem 4.4.2. *(Two-scale compactness on domains)*

(i) From each bounded sequence (u^{ε}) in $L^2(0,T;L^2(\Omega))$, a subsequence may be extracted which two-scale converges to $u_0(t,x,y)\in L^2((0,T)\times\Omega\times Y)$.

(ii) Let (u^{ε}) be a bounded sequence in $H^1(0,T;H^1(\Omega))$, then there exists $\tilde{u}\in L^2((0,T)\times H_{\#}^1(Y))$ such that up to a subsequence (u^{ε}) two-scale converges to $u_0\in L^2(0,T;L^2(\Omega))$ and $\nabla u^{\varepsilon}\overset{2}{\rightharpoonup}\nabla_x u_0+\nabla_y\tilde{u}$.

Proof. See e.g. [95],[1]. □

Definition 3. *(Two-scale convergence for ε-periodic hypersurfaces [94]). A sequence of functions $(u^{\varepsilon})\in L^2((0,T)\times\Gamma_{\varepsilon})$ is said to two-scale converge to a limit $u_0\in L^2((0,T)\times\Omega^{\varepsilon}\times\Gamma)$ if and only if for all $\phi\in C_0^{\infty}((0,T)\times\Omega^{\varepsilon};C_{\#}^{\infty}(\Gamma))$ we have*

$$\lim_{\varepsilon\to 0}\varepsilon\int_0^T\int_{\Gamma_{\varepsilon}}u^{\varepsilon}\phi(t,x,\frac{x}{\varepsilon})=\frac{1}{|Y|}\int_0^T\int_{\Omega}\int_{\Gamma}u_0(t,x,y)\phi(t,x,y)d\gamma_y dxdt. \tag{4.68}$$

Theorem 4.4.3. *(Two-scale compactness on surfaces)*

(i) From each bounded sequence $(u^{\varepsilon})\in L^2((0,T)\times\Gamma_{\varepsilon})$ one can extract a subsequence u^{ε} which two-scale converges to $u_0\in L^2((0,T)\times\Omega^{\varepsilon}\times\Gamma)$.

(ii) If a sequence (u^ε) is bounded in $L^\infty((0,T)\times\Gamma_\varepsilon)$, then u^ε two-scale converges to a $u_0 \in L^\infty((0,T)\times\Omega^\varepsilon\times\Gamma)$

Proof. See [94] for proof of (i), and [82] for proof of (ii). □

Lemma 4.4.4. *Let (A_1)-(A_2)hold. Denote by u_i and θ^ε the Bochner extensions*[1] *in the space $L^2(0,T;H^1(\Omega))$ of the corresponding functions originally belonging to $L^2(0,T;H^1(\Omega^\epsilon))$. Then the following statement holds:*

(i) $u_i \rightharpoonup u_i$ and $\theta^\varepsilon \rightharpoonup \theta$ in $L^2(0,T;H^1(\Omega))$,

(ii) $u_i \overset{*}{\rightharpoonup} u_i$ and $\theta^\varepsilon \overset{*}{\rightharpoonup} \theta$ in $L^\infty((0,T)\times\Omega)$,

(iii) $\partial_t u_i \rightharpoonup \partial_t u_i$ and $\partial_t\theta^\varepsilon \rightharpoonup \partial_t\theta$ in $L^2(0,T;L^2(\Omega))$,

(iv) $u_i \to u_i$ and $\theta^\varepsilon \to \theta$ strongly in $L^2(0,T;H^\beta(\Omega))$ for $\frac{1}{2} < \beta < 1$ and $\sqrt{\varepsilon}\|u_i - u_i\|_{L^2((0,T)\times\Gamma_\varepsilon)} \to 0$ as $\varepsilon \to 0$,

(v) $u_i \overset{2}{\rightharpoonup} u_i$, $\nabla u_i \overset{2}{\rightharpoonup} \nabla_x u_i + \nabla_y u_i^1$ where $u_i^1 \in L^2((0,T)\times\Omega; H^1_\#(Y))$,

(vi) $\theta^\varepsilon \overset{2}{\rightharpoonup} \theta$, $\nabla\theta^\varepsilon \overset{2}{\rightharpoonup} \nabla_x\theta + \nabla_y\theta^1$ where $\theta^1 \in L^2((0,T)\times\Omega; H^1_\#(Y))$,

(vii) $v_i^\varepsilon \overset{2}{\rightharpoonup} v_i \in L^\infty((0,T)\times\Omega\times\Gamma)$ and $\partial_t v_i^\varepsilon \overset{2}{\rightharpoonup} \partial_t v_i \in L^2((0,T)\times\Omega\times\Gamma)$.

Proof. We obtain (i) and (ii) as a direct consequence of the fact that u_i and θ^ε are uniformly bounded in $L^\infty(0,T;H^1(\Omega)) \cap L^\infty((0,T)\times\Omega)$. A similar argument gives (iii). We get (iv) using the compact embedding $H^\alpha(\Omega) \hookrightarrow H^\beta(\Omega)$ for $\beta \in (\frac{1}{2}, 1)$ and $0 < \beta < \alpha \leq 1$, since Ω has Lipschitz boundary. Note that (iv) implies the strong convergence of u_i up to the boundary.

Denote $W := \{w \in L^2(0,T;H^1(\Omega))$ and $\partial_t w \in L^2(0,T;L^2(\Omega))\}$. We have $u_i, \theta^\varepsilon \in W$. Using Lions-Aubin lemma [77] we see that W is compactly embedded in $L^2(0,T;H^\beta(\Omega))$ for $\beta \in [0.5, 1]$. We then use the trace inequality for perforated medium from [55], namely for all $\phi \in H^1(\Omega^\varepsilon)$ there exists a constant C independent of ε such that:

$$\varepsilon\|\phi\|_{L^2(\Gamma^\varepsilon)} \leq C(\|\phi\|^2_{L^2(\Omega^\varepsilon)} + \varepsilon^2\|\nabla\phi\|^2_{L^2(\Omega^\varepsilon)}). \tag{4.69}$$

Applying (4.69) to $u_i - u_i$, we get:

$$\begin{aligned}\sqrt{\varepsilon}\|u_i - u_i\|^2_{L^2((0,T)\times\Gamma^\varepsilon)} &\leq C\|u_i - u_i\|^2_{L^2(0,T;H^\beta(\Omega^\varepsilon))} \\ &\leq C\|u_i - u_i\|^2_{L^2(0,T;H^\beta(\Omega))},\end{aligned} \tag{4.70}$$

where $\|u_i - u_i\|^2_{L^2(0,T;H^\beta(\Omega))} \to 0$ as $\varepsilon \to 0$. As for the rest of the statements (v)-(vii), since u_i are bounded in $L^\infty(0,T;H^1(\Omega))$, up to a subsequence we have that $u_i \overset{2}{\rightharpoonup} u_i$ in $L^2(0,T;L^2(\Omega))$, and $\nabla u_i \overset{2}{\rightharpoonup} \nabla_x u_i + \nabla_y u_i^1$, where $u_i^1 \in L^2((0,T)\times\Omega; H^1_\#(Y))$. By Theorem 4.4.3, $v_i^\varepsilon \overset{2}{\rightharpoonup} v_i \in L^\infty((0,T)\times\Omega\times\Gamma^\varepsilon)$ and $\partial_t v_i^\varepsilon \overset{2}{\rightharpoonup} \partial_t v_i \in L^2((0,T)\times\Omega\times\Gamma^\varepsilon)$. □

[1]For our choice of microstructure, the interior extension from $H^1(\Omega^\epsilon)$ into $H^1(\Omega))$ exists and the corresponding extension constant is independent of the choice of ϵ; see the standard extension result reported in Lemma 5 from [55].

4.4.2 Two-scale homogenization procedure

Theorem 4.4.5. *Let* (A_1)-(A_2)*hold. Then the sequence of solutions* $(\theta^\varepsilon, u_i, v_i^\varepsilon)$ *to* (P^ε)*converges as* $\varepsilon \to 0$ *to* $\theta, u_i \in H^1(0,T;L^2(\Omega)) \cap L^2(0,T;H^1(\Omega))$ *and* $v_i \in H^1((0,T);L^2(\Omega\times\Gamma))$ *respectively that satisfy (4.74), (4.75) and (4.76).*

Proof. Testing $(P^\varepsilon)$with oscillating functions $\phi(t,x) = \alpha(t,x)+\varepsilon\beta(t,x,\frac{x}{\varepsilon})$, where $\alpha \in C^\infty((0,T)\times\Omega)$ and $\beta \in C^\infty((0,T)\times\Omega; C^\infty_\#(Y))$, we obtain:

$$\int\limits_{\Omega^\varepsilon} \partial_t\theta^\varepsilon(\alpha+\varepsilon\beta) + \int\limits_{\Omega^\varepsilon} \kappa^\varepsilon(\frac{x}{\varepsilon})\nabla\theta^\varepsilon(\nabla_x\alpha + \varepsilon\nabla_x\beta + \nabla_y\beta)$$
$$+ g_0\varepsilon\int\limits_{\Gamma^\varepsilon}\theta^\varepsilon(\alpha+\varepsilon\beta) = \sum_{i=1}^N \int\limits_{\Omega^\varepsilon} \tau^\varepsilon(\frac{x}{\varepsilon})\nabla^\delta u_i\cdot\nabla\theta^\varepsilon(\alpha+\varepsilon\beta), \tag{4.71}$$

$$\int\limits_{\Omega^\varepsilon} \partial_t u_i(\alpha+\varepsilon\beta) + \int\limits_{\Omega^\varepsilon} d_i(\frac{x}{\varepsilon})\nabla u_i(\nabla_x\alpha + \varepsilon\nabla_x\beta + \nabla_y\beta)$$
$$+ g_i\varepsilon\int\limits_{\Gamma^\varepsilon} u_i(\alpha+\varepsilon\beta) + \varepsilon\int\limits_{\Gamma^\varepsilon}(a_i^\varepsilon u_i - b_i^\varepsilon v_i^\varepsilon)(\alpha+\varepsilon\beta)$$
$$= \int\limits_{\Omega^\varepsilon}\delta_i^\varepsilon(y)\nabla^\delta\theta^\varepsilon\cdot\nabla u_i(\alpha+\varepsilon\beta) + \int\limits_{\Omega^\varepsilon} R_i(u)(\alpha+\varepsilon\beta), \tag{4.72}$$

$$\varepsilon\int\limits_{\Gamma^\varepsilon}\partial_t v_i^\varepsilon(\alpha+\varepsilon\beta) = \varepsilon\int\limits_{\Gamma^\varepsilon}(a_i^\varepsilon(\frac{x}{\varepsilon})u_i - b_i^\varepsilon(\frac{x}{\varepsilon})v_i^\varepsilon)(\alpha+\varepsilon\beta). \tag{4.73}$$

Using the concept of two-scale convergence for $\varepsilon\to 0$ in (4.71), (4.72) and (4.73) yields:

$$\int\limits_\Omega \partial_t\theta^0\alpha + \frac{1}{|Y|}\int\limits_\Omega\int\limits_Y \kappa(y)(\nabla\theta^0 + \nabla_y\theta^1)(\nabla_x\alpha(x) + \nabla_y\beta(x,y))$$
$$+ g_0\frac{|\Gamma|}{|Y|}\int\limits_\Omega\theta^0\alpha = \sum_{i=1}^N\frac{1}{|Y|}\int\limits_\Omega\int\limits_Y \tau(y)\nabla^\delta u_i^0\cdot(\nabla\theta^0+\nabla_y\theta^1)\alpha \tag{4.74}$$

$$\int\limits_\Omega \partial_t u_i^0\alpha + \frac{1}{|Y|}\int\limits_\Omega\int\limits_Y d_i(y)(\nabla u_i^0 + \nabla_y u_i^1)(\nabla_x\alpha + \nabla_y\beta)$$
$$+ g_i\frac{|\Gamma|}{|Y|}\int\limits_\Omega u_i^0\alpha + \frac{1}{|Y|}\int\limits_\Omega\int\limits_\Gamma(a_i(y)u_i - b_i(y)v_i)\alpha$$
$$= \frac{1}{|Y|}\int\limits_\Omega\int\limits_Y \delta_i(y)\nabla^\delta\theta^0\cdot(\nabla u_i^0 + \nabla_y u_i^1)\alpha + \int\limits_\Omega R_i(u^0)\alpha \tag{4.75}$$

$$\int\limits_\Omega \partial_t v_i^0\alpha = \frac{1}{|Y|}\int\limits_\Omega\int\limits_\Gamma(a_i(y)u_i^0 - b_i(y)v_i^0)\alpha. \tag{4.76}$$

Note that we have used strong convergence for passing to the limit in the aggregation term in (4.75). Now we just need to find θ^1 and u_i^1. To do this we choose $\alpha = 0$ in (4.74) and (4.75). This gives for all $\beta \in C^\infty((0,T)\times\Omega; C^\infty_\#(Y))$ a system of decoupled equations:

$$\int_\Omega \int_Y \kappa(y)(\nabla\theta^0 + \nabla_y\theta^1)\nabla_y\beta(x,y) = 0 \tag{4.77}$$

$$\int_\Omega \int_Y d_i(y)(\nabla u_i^0 + \nabla_y u_i^1)\nabla_y\beta(x,y) = 0 \tag{4.78}$$

Since θ^1 and u_i^1 depend linearly on θ^0 and u_i^0 respectively, they can be defined as:

$$\theta^1 := \sum_{j=1}^{3} \partial_{x_j}\theta^0\bar{\theta}^j, \tag{4.79}$$

$$u_i^1 := \sum_{j=1}^{3} \partial_{x_j}u_i^0\bar{u}_i^j, \tag{4.80}$$

where $\bar{\theta}^j$ and $\bar{u}_i^j$ solve the cell problems (4.81)-(4.82) and (4.83)-(4.84), respectively:

$$\begin{cases} -\nabla_y\cdot(\kappa(y)\nabla_y\bar{\theta}^j) = \sum_{k=1}^{3}\partial_{y_k}\kappa_{jk}(y) & \text{in } Y, \quad (4.81)\\ \bar{\theta}^j \text{ is periodic in } Y, & (4.82)\end{cases}$$

$$\begin{cases} -\nabla_y\cdot(d_i(y)\nabla_y\bar{u}_i^j) = \sum_{k=1}^{3}\partial_{y_k}d_i^{jk}(y) & \text{in } Y, \quad (4.83)\\ \bar{u}^j \text{ is periodic in } Y. & (4.84)\end{cases}$$

Now, choose $\beta = 0$ in (4.74) to obtain:

$$\int_\Omega \partial_t\theta^0\alpha + \frac{1}{|Y|}\int_\Omega\int_Y \kappa(y)(\nabla\theta^0 + \nabla_y(\sum_{j=1}^{3}\partial_{x_j}\theta^0\bar{\theta}^j)\nabla_x\alpha(x))$$
$$+ g_0\frac{|\Gamma|}{|Y|}\int_\Omega \theta^0\alpha = \sum_{i=1}^{N}\frac{1}{|Y|}\int_\Omega\int_Y \tau(y)\nabla^\delta u_i^0\cdot(\nabla\theta^0 + \nabla_y(\sum_{j=1}^{3}\partial_{x_j}\theta^0\bar{\theta}^j)\alpha. \tag{4.85}$$

Integrating (4.85) w.r.t. y leads to:

$$\int_\Omega \partial_t\theta^0\alpha + \int_\Omega \mathbb{K}\nabla\theta^0\nabla_x\alpha + g_0\frac{|\Gamma|}{|Y|}\int_\Omega\theta^0\alpha = \sum_{i=1}^{N}\int_\Omega \mathbb{T}\nabla^\delta u_i^0\cdot\nabla\theta^0\alpha, \tag{4.86}$$

where

$$\mathbb{K}_{ij} := \frac{1}{|Y|}\int\limits_{Y}(\kappa_{ij}(y) + \sum_{k=1}^{3}\kappa_{kj}\partial_{y_k}\bar{\theta}^i(y)), \tag{4.87}$$

and

$$\mathbb{T}_{ij} := \frac{1}{|Y|}\int\limits_{Y}(\tau_{ij}(y) + \sum_{k=1}^{3}\tau_{kj}\partial_{y_k}\bar{\theta}^i(y)). \tag{4.88}$$

We can similarly derive from (4.75) that:

$$\int\limits_{\Omega}\partial_t u_i^0\alpha + \int\limits_{\Omega}\mathbb{D}_i\nabla u_i^0\nabla_x\alpha + g_i\frac{|\Gamma|}{|Y|}\int\limits_{\Omega}u_i^0\alpha + \int\limits_{\Omega}(A_i u_i^0 - B_i v_i^0)\alpha = \int\limits_{\Omega}\mathbb{F}_i\nabla^\delta\theta^0\cdot\nabla u_i^0\alpha + \int\limits_{\Omega}R_i(u^0)\alpha, \tag{4.89}$$

$$\int\limits_{\Omega}\partial_t v_i^0\alpha = \int\limits_{\Omega}(A_i u_i^0 - B_i v_i^0)\alpha, \tag{4.90}$$

where

$$\mathbb{D}_{l,ij} := \frac{1}{|Y|}\int\limits_{Y}(d_{l,ij}(y) + \sum_{k=1}^{3}d_{l,kj}\partial_{y_k}\bar{u}_l^i(y)), \tag{4.91}$$

$$A_i := \frac{1}{|Y|}\int\limits_{\Gamma}a_i(y), \tag{4.92}$$

$$B_i := \frac{1}{|Y|}\int\limits_{\Gamma}b_i(y), \tag{4.93}$$

$$\mathbb{F}_{l,ij} := \frac{1}{|Y|}\int\limits_{Y}(\delta_{l,ij}(y) + \sum_{k=1}^{3}\delta_{l,kj}\partial_{y_k}\bar{u}_l^i(y)). \tag{4.94}$$

We refer to the system (4.86)- (4.94) as (P^0). Note that the initial conditions for (P^0) are the same as for (P^ε). □

4.4.3 Strong formulation of (P^0)

We summarize the strong formulation for (P^0) in the following Lemma:

Lemma 4.4.6. (Strong formulation). *Assume* (A_1)-(A_2) *to hold. Then as* $\varepsilon \to 0$*, the sequence of weak solutions of the microscopic problem* (P^ε) *converges*

to the weak solution of the following macroscopic problem:

$$\partial_t \theta + \nabla \cdot (-\mathbb{K}\nabla\theta) + g_0 \frac{|\Gamma|}{|Y|}\theta - \sum_{i=1}^{N} \mathbb{T}_i \nabla^\delta u_i \cdot \nabla\theta = 0 \qquad \text{in } (0,T)\times\Omega \tag{4.95}$$

$$\partial_t u_i + \nabla \cdot (-\mathbb{D}_i \nabla u_i) + g_i \frac{|\Gamma|}{|Y|} u_i + A_i u_i - B_i v_i = \mathbb{F}_i \nabla^\delta \theta \cdot \nabla u_i + R_i(u) \qquad \text{in } (0,T)\times\Omega \tag{4.96}$$

$$\partial_t v_i = A_i u_i - B_i v_i \tag{4.97}$$

with boundary conditions:

$$-\mathbb{K}\nabla\theta \cdot n = 0, \qquad \text{on } (0,T)\times\partial\Omega, \tag{4.98}$$

$$-\mathbb{D}_i \nabla u_i \cdot n = 0, \qquad \text{on } (0,T)\times\partial\Omega, \tag{4.99}$$

and initial conditions:

$$\theta(0,x) = \theta^0(x) \qquad \text{in } \Omega, \tag{4.100}$$

$$u_i(0,x) = u_i^0(x) \qquad \text{in } \Omega, \tag{4.101}$$

$$v_i(0,x) = v_i^0(x) \qquad \text{on } \Gamma. \tag{4.102}$$

Here $|\Gamma|/|Y|$, $\mathbb{K}$, $\mathbb{D}_i$, A_i, and B_i are the effective coefficients defined in (4.91)-(4.94).

Proof. This follows from Theorem 4.4.5. See also [82] and [36] for a similar application of the two-scale convergence method. □

Chapter 5

Numerical Solution of the Transport Problem

5.1 Introduction

This Chapter describes the discretization techniques that we have used in order to solve our problem numerically. The main challenges are the very large number of unknowns resulting from the Smoluchowski equations, as well as the very large number of degrees of freedom for each unknown, resulting from the complexity of the porous medium geometry. We deal with these challenges by leveraging homogenization techniques in both cases, thus greatly reducing the computational effort, while still providing relevant information on the macroscopic scale, which is of most interest usually. The introduction to our problem can be found in Chapter 2, which also describes the physical phenomena related to aggregation and fragmentation as well as gives an overview on parameters and coefficients related to the implementation.

In this thesis, we use two different concepts of averaging. On one hand, we use periodic homogenization methods to treat the multiscale nature of the porous medium (cf. Chapter 3 and Chapter 4). On the other hand, we drastically reduce the original number of colloidal species (unknowns) to a computationally tractable amount. This is shown in Section 5.2, where we present an overview of discretization techniques for the Smoluchowski population balance equation (PBE). They describe not only how we discretize the right hand side of our system, but essentially they also explain how we choose the variables that we solve for, since solving the full system can result in millions of variables in some cases.

In Section 5.3, we give an overview of the techniques used to discretize our reaction-diffusion system, including the Newton method and iterative splitting schemes.

In Section 5.4 we give details related to solving numerically the cell problems that were introduced in Chapter 3, which we need to compute in order to obtain the effective coefficients on the macroscopic scale.

In Section 5.5 we give an overview of the Numerics libraries used to implement our discretization along with their advantages and drawbacks that we faced along

the way.

5.2 Discretization of the population balance equation

5.2.1 Basic equations

We consider the discrete aggregation-breakage PBE

$$\begin{aligned}\frac{\partial n_k(t)}{\partial t} =& \frac{1}{2}\sum_{i+j=k}\beta(a_i,a_j)n_i n_j - \sum_{i=1}^{N}\beta(a_k,a_i)n_i n_k \\ & - b_k n_k + \sum_{i=k}^{N}\gamma_{ki} b_i n_i,\end{aligned}$$

as well as its continuous version

$$\begin{aligned}\frac{\partial n(v,t)}{\partial t} =& \frac{1}{2}\int_0^v \beta(v-u,u)n(v-u)n(u)du - \int_0^\infty \beta(u,v)n(u)n(v)du \\ & - b(v)n(v) + \int_v^\infty \gamma(v,u)b(u)n(u)du \end{aligned} \tag{5.1}$$

together with suitable initial conditions. The moments M_i of the number density function $n(v,t)$ are defined as

$$M_i = \int_0^\infty v^i n(v,t)dv, \qquad \text{for } i \in \mathbb{N}. \tag{5.2}$$

Substitute (5.2) into (5.1) to obtain:

$$\begin{aligned}\frac{dM_i}{dt} =& -\frac{1}{2}\int_0^\infty dv \int_0^\infty du \left[v^i + u^i - (v+u)^i\right]\beta(v,u)n(v)n(u) \\ & + \int_0^\infty \left[\int_0^u \left(\frac{v}{u}\right)^i \gamma(v,u) - 1\right] n(u)b(u)u^i du\, dv. \end{aligned} \tag{5.3}$$

Integrating the continuous equation (5.1) over $[v_i, v_{i+1}]$ gives:

$$\begin{aligned}\frac{dN_i(t)}{dt} =& \frac{1}{2}\int_{v_i}^{v_{i+1}} dv \int_0^v \beta(v-u,u)n(v-u)n(u)du - \int_{v_i}^{v_{i+1}} n(v)dv \int_v^\infty \beta(u,v)n(u)n(v)du \\ & + \int_{v_i}^{v_{i+1}} dv \int_v^\infty \gamma(v,u)b(u)n(u)du - \int_{v_i}^{v_{i+1}} b(v)n(v)dv, \end{aligned} \tag{5.4}$$

where the quantity $N_i(t)$ is defined by

$$N_i(t) := \int_{v_i}^{v_{i+1}} n(v,t)dv. \tag{5.5}$$

A complete set of equations can be obtained by representing the right-hand side of (5.4) in terms of N_i. This is precisely the term modeling the aggregation and fragmentation of the colloidal species.

There are two major approximate approaches to discretizing (5.4): the M-I and M-II methods.

The M-I approach applies the mean-value theorem on the collision frequency:

$$\int_{v_i}^{v_{i+1}} dv \int_{v_j}^{v_{j+1}} \beta(u,v)n(u,t)n(v,t)du = \beta_{ij}N_i(t)N_j(t), \tag{5.6}$$

$$\beta_{ij} := \beta(x_i, x_j),\ x_i \in [v_i, v_{i+1}], x_j \in [v_j, v_{j+1}]. \tag{5.7}$$

The M-II approach applies the mean value theorem on the density:

$$\int_{v_i}^{v_{i+1}} dv \int_{v_j}^{v_{j+1}} \beta(u,v)n(u,t)n(v,t)du =$$

$$\bar{n}_i(t)\bar{n}_j(t) \int_{v_i}^{v_{i+1}} dv \int_{v_j}^{v_{j+1}} \beta(u,v)du, \tag{5.8}$$

$$\bar{n}_i(t) := \frac{1}{v_{i+1} - v_i} \int_{v_i}^{v_{i+1}} n(v,t)dv. \tag{5.9}$$

5.2.2 Discretization approaches for the aggregation term

In the following subsections we give an overview of discretization approaches for the right hand side of (5.1). For a practical application of some of these approaches see e.g. [105].

5.2.2.1 Hidy and Brock approach

The reference [53] used the M-I approach with a linear grid to restore autonomy for PBEs with only aggregation. They considered particle population in a size range $[v_i, v_{i+1}]$ to be represented by size $x_i = ix_1$:

$$n(v,t) = \sum_{j=1}^{N} N_j \delta(v - x_j). \tag{5.10}$$

Substitute (5.10) in (5.4), use $A_{ij} = \beta_{ij} N_i(t) N_j(t)$ for shortness:

$$\frac{dN_i}{dt} = \frac{1}{2}\sum_{j=1}^{i-1} A_{j,i-j} - \sum_{j=1}^{N} A_{ij}. \tag{5.11}$$

The variation of the μth moment can be obtained by substituting (5.10) in (5.3):

$$\frac{dM_\mu}{dt} = -\frac{1}{2}\sum_{i=1}^{N}\sum_{j=1}^{N}(x_i^\mu + x_j^\mu - (x_i + x_j)^\mu)A_{ij}. \tag{5.12}$$

Alternatively, multiplying (5.11) by x_i^μ and summing up over all i gives:

$$\frac{d}{dt}\left(\sum_i N_i x_i^\mu)\right) = \frac{dM_\mu}{dt} = -\frac{1}{2}\sum_{i=1}^{N}\sum_{j=1}^{N}(x_i^\mu + x_j^\mu - (x_i + x_j)^\mu)A_{ij}. \tag{5.13}$$

(5.12) and (5.13) are exactly the same for all values of μ. This is called "internal consistency". Thus, the discretization technique based on uniform grid yields a set of equations which is internally consistent. The major disadvantage of this technique is that it requires a large number of size ranges to cover the entire size range with acceptable resolution.

5.2.2.2 Batterham approach

The reference [8] used the M-I approach with a geometric grid $v_{i+1} = 2v_i$ for pure aggregation PBE. Particles in $[v_i, v_{i+1}]$ are represented by x_i. The aggregation of these particles led to the formation of new particles lying on the boundaries of a size range. The authors divided such particles equally (mass) between the adjoining size ranges. The particles formed in a sub-size range, e.g. $[x_i, v_{i+1}]$ for the ith size range, were assigned to x_i such that the mass was conserved:

$$\begin{aligned}\frac{dN_i(t)}{dt} = {} & \frac{3}{8}A_{i-1,i-2} + \frac{3}{4}A_{i,i-1} + \\ & A_{i-1,i-1} + \sum_{j=1}^{i-2}(1 + 2^{j-i})A_{ij} - \sum_{j=1}^{N} A_{ij} - A_{ii}.\end{aligned} \tag{5.14}$$

These equations conserve total mass(internal consistency with regard to first moment), but fail to yield the correct discrete equation for total numbers or any other moment.

5.2.2.3 Hounslow approach

[57] used the M-I approach with same grid as [8], but assumed the particles to be uniformly distributed in a size range. They identified four types of interactions that can change the total population in a size range and derived expressions for

each one of them separately. The set of equations derived was internally consistent w.r.t. only M_0, but with a correction factor, independent of aggregation kernel, also w.r.t. M_1. Here, we have:

$$\frac{dN_i(t)}{dt} = \sum_{j=1}^{i-2} 2^{j-i+1} A_{i-1,j} + \frac{1}{2} A_{i-1,i-1} - \sum_{j=1}^{i-1} 2^{j-i} A_{ij} - \sum_{j=1}^{N} A_{ij}. \tag{5.15}$$

5.2.2.4 Fixed pivot approach

This method is due to [72]. Consider quantity of interest $F(t)$ of entire population obtainable from property $f(x)$ of a single particle of volume $x \in (0, \infty)$:

$$F(t) = \int_0^\infty f(x) n(x,t) dx. \tag{5.16}$$

To obtain the evolution of $F(t)$, one calculates the evolution of the number density $n(x,t)$, which can also be used to obtain any other integral property. Another approach is to directly address how changes in certain desired properties $F_1(t), F_2(t), ...$ are brought about by enforcing exact preservation of changes in properties $f_1(x), f_2(x), ...$ when particles break or aggregate. In other words, discrete equations are designed to produce the "correct" equation for the evolution of $F(t)$.

Consider the aggregation of two particles of sizes x_j and x_k. In general, aggregation can be defined as change in property $f(x)$ from $f(x_j) + f(x_k)$ to $f(x_j + x_k)$. For uniform grid ($x_i = ix_1$, the size of a new aggregate always exactly matches with one of x_i's. Thus, for this discretization, changes in any property $f(x)$ corresponding to aggregation of two particles are exactly preserved.

If the size of the new particle does not match with any of the representative sizes, then many possibilities exist with regard to its representation. The particle should be assigned to the nearby representative sizes such that the changes in properties $f_1(x), f_2(x), ...$ due to aggregation or breakage events are exactly preserved in equations for $N_i(t)$.

Example 1. *We need to predict the evolution of the second moment of the distribution. A particle of size $v \in (x_i, x_{i+1})$ is formed due to breakage or aggregation. Particle v should be represented through populations at sizes x_i and/or x_{i+1} in a way that the second moment should be exactly preserved. The reassigned particles should have second moment equal to v^2. Formation of $(v/x_i)^2$ particles of size x_i or $(v/x_{i+1})^2$ particles of size x_{i+1}, both satisfy the requirement. Clearly, at least one more property should be preserved to uniquely specify an aggregation or breakage event.*

This method, unlike several others, does not distinguish between intra- and inter-interval events:

- all events leading to formation of new particle are birth terms,

- all events leading to loss of a particle are death terms.

Thus, the intra-interval events that result in the birth as well as loss of particles from the same size range will be considered twice, but treated like inter-interval events eliminating the need for special treatment of intra-interval events. This substantially simplifies the method.

When a new particle has its size corresponding to a representative size, all properties associated with it are naturally preserved. In other case, we assign to particle to the adjoining representative volumes such that two pre-chosen properties of interest are exactly preserved.

The formation of a particle of size $v \in [x_i, x_{i+1}]$, due to break up or aggregation, is represented by assigning fractions $a(v, x_i)$ and $b(v, x_{i+1})$ to particle populations at x_i and x_{i+1}, respectively. For the conservation of two general properties $f_1(v)$ and $f_2(v)$, these fractions must satisfy the following equations:

$$\begin{cases} a(v, x_i) f_1(x_i) + b(v, x_{i+1}) f_1(x_{i+1}) = f_1(v), \\ a(v, x_i) f_2(x_i) + b(v, x_{i+1}) f_2(x_{i+1}) = f_2(v). \end{cases}$$

Note that these equations can be generalized for the preservation of four properties by assigning a particle of size v to populations at x_{i-1},x_i,x_{i+1},x_{i+2}.

5.2.3 Approximation details

In what follows, we describe in detail the approximations for the terms on the right hand side of (5.4).

5.2.3.1 Approximation of the breakage mechanism

Dealing with the birth term. Using $B(v, u) := \gamma(v, u) b(u) n(u, t)$ for shortness, the birth term given by:

$$R_{b+} = \int_{v_i}^{v_{i+1}} dv \int_{v}^{\infty} B(v, u) du \tag{5.17}$$

is modified to

$$R_{b+} = \int_{x_i}^{x_{i+1}} a(v, x_i) dv \int_{v}^{\infty} B(v, u) du + \int_{x_{i-1}}^{x_i} b(v, x_i) dv \int_{v}^{\infty} B(v, u) du. \tag{5.18}$$

Since the particle population is assumed to be concentrated at representative sizes x_i,

$$n(v, t) = \sum_{i=1}^{N} N_i(t) \delta(v - x_i). \tag{5.19}$$

Substituting (5.19) into (5.17):

$$R_{b+} = \sum_{k\geq i} b_k N_k(t) \int_{x_i}^{x_{i+1}} a(v, x_i)\gamma(v, x_k)dv + \sum_{k\geq i} b_k N_k(t) \int_{x_{i-1}}^{x_i} b(v, x_i)\gamma(v, x_k)dv. \tag{5.20}$$

Substitute solutions of (5.17) into (5.20) to get:

$$R_{b+} = \sum_{k=i}^{N} \psi_{i,k} b_k N_k(t). \tag{5.21}$$

In (5.21) $\psi_{i,k}$ is interpreted as the contribution to population at ith representative size due to the breakage of particle of size x_k:

$$\psi_{i,k} := \frac{B_{i,k}^{(\xi)} x_{i+1}^{\eta} - B_{i,k}^{(\eta)} x_{i+1}^{\xi}}{x_i^{\xi} x_{i+1}^{\eta} - x_i^{\eta} x_{i+1}^{\xi}} + \frac{B_{i-1,k}^{(\xi)} x_{i-1}^{\eta} - B_{i-1,k}^{(\eta)} x_{i-1}^{\xi}}{x_i^{\xi} x_{i-1}^{\eta} - x_i^{\eta} x_{i-1}^{\xi}}, \tag{5.22}$$

$$B_{i,k}^{(\xi)} := \int_{x_i}^{x_{i+1}} v^{\xi}\gamma(v, x_k)dv. \tag{5.23}$$

The exact preservation of numbers and mass, for instance, is achieved by setting $\xi = 0, \eta = 1$. In this case:

$$\psi_{i,k} := \int_{x_i}^{x_{i+1}} \frac{x_{i+1} - v}{x_{i+1} - x_i}\gamma(v, x_k)dv + \int_{x_{i-1}}^{x_i} \frac{v - x_{i-1}}{x_i - x_{i-1}}\gamma(v, x_k)dv. \tag{5.24}$$

The first and second integral terms reduce to zero for $i = k$ and $i = 1$, respectively. The integral terms appearing in (5.23) or (5.24) can be evaluated analytically for a large class of $\gamma(u, v)$ functions. Otherwise they can be computed numerically at negligible computational cost.

Dealing with the death term. Substituting (5.19) into death term(last term in (5.4)) given by:

$$R_{b-} = \int_{v_i}^{v_{i+1}} b(v)n(v, t)dv,$$

we obtain

$$R_{b-} = b_i N_i(t). \tag{5.25}$$

5.2.3.2 Approximation of the aggregation mechanism

Dealing with the birth term. Using $A(u,v) = \beta(u,v)n(u,t)n(v,t)$ for shortness, the birth term is given by:

$$R_{a+} = \frac{1}{2}\int_{v_i}^{v_{i+1}} dv \int_0^v A(v-u,u)du. \tag{5.26}$$

The population at representative volume x_i gets a fractional particle for every particle born in $(x_{i-1}, x_i) \cup (x_i, x_{i+1})$:

- $a(v, x_i)$ particles are assigned to x_i for particles born in (x_i, x_{i+1}),
- $b(v, x_i)$ particles are assigned to x_i for particles born in (x_{i-1}, x_i).

Here, we have:

$$R_{a+} = \frac{1}{2}\int_{x_i}^{x_{i+1}} a(v,x_i)dv \int_0^v A(v-u,u)du + \frac{1}{2}\int_{x_{i-1}}^{x_i} b(v,x_i)dv \int_0^v A(v-u,u)du. \tag{5.27}$$

Substitute $n(v,t)$ from (5.19):

$$R_{a+} = \sum_{\substack{k=1 \\ x_{i-1}\le(x_j+x_k)\le x_{i+1}}}^{N}\sum_{j=k}^{N} (1-\frac{1}{2}\delta_{jk})\phi_i^{jk}A_{jk}, \text{ where} \tag{5.28}$$

$$\phi_i^{jk} = \begin{cases} \frac{v^\xi x_{i+1}^\eta - v^\eta x_{i+1}^\xi}{x_i^\xi x_{i+1}^\eta - x_i^\eta x_{i+1}^\xi}, & x_i \le (v = x_j + x_k) \le x_{i+1} \\ \frac{v^\xi x_{i-1}^\eta - v^\eta x_{i-1}^\xi}{x_i^\xi x_{i-1}^\eta - x_i^\eta x_{i-1}^\xi}, & x_{i-1} \le (v = x_j + x_k) \le x_i. \end{cases} \tag{5.29}$$

For preservation of mass and numbers, ϕ_i^{jk} is given by a simple expression:

$$\phi_i^{jk} = \begin{cases} \frac{x_{i+1}-v}{x_{i+1}-x_i}, & x_i \le (v = x_j + x_k) \le x_{i+1} \\ \frac{v-x_{i-1}}{x_i-x_{i-1}}, & x_{i-1} \le (v = x_j + x_k) \le x_i. \end{cases} \tag{5.30}$$

Note that (5.28) applies for a general grid. Possible combinations of classes j and k satisfying the constraint $x_{i-1} \le (x_j + x_k) \le x_{i+1}$ are determined at the time of grid generation, which eliminates the need for checking the same inequalities repeatedly as the computation proceeds.

Dealing with the death term. Substituting (5.19) into death term(second term in (5.4)) given by

$$R_{a-} = \int_{v_i}^{v_{i+1}} \int_0^\infty A(u,v)du. \tag{5.31}$$

we obtain

$$R_{a-} = \sum_{k=1}^{N} A_{ik}. \tag{5.32}$$

5.2.3.3 Discretized equation for aggregation-breakage interactions

Summarizing, the discretized equations approximating the coupled aggregation-breakage problem are:

$$\frac{dN_i(t)}{dt} = \sum_{\substack{k=1}}^{N}\sum_{\substack{j=k \\ x_{i-1}\leq(x_j+x_k)\leq x_{i+1}}}^{N} (1-\frac{1}{2}\delta_{jk})\phi_i^{jk}A_{jk} - \sum_{k=1}^{N} A_{ik} + \sum_{k=i}^{N}\psi_{i,k}b_kN_k(t) - b_iN_i(t),$$

where

$$\phi_i^{jk} := \begin{cases} \frac{x_{i+1}-v}{x_{i+1}-x_i}, & x_i \leq (v = x_j + x_k) \leq x_{i+1} \\ \frac{v-x_{i-1}}{x_i-x_{i-1}}, & x_{i-1} \leq (v = x_j + x_k) \leq x_i \end{cases},$$

$$\psi_{i,k} := \frac{B_{i,k}^{(\xi)}x_{i+1}^{\eta} - B_{i,k}^{(\eta)}x_{i+1}^{\xi}}{x_i^{\xi}x_{i+1}^{\eta} - x_i^{\eta}x_{i+1}^{\xi}} + \frac{B_{i-1,k}^{(\xi)}x_{i-1}^{\eta} - B_{i-1,k}^{(\eta)}x_{i-1}^{\xi}}{x_i^{\xi}x_{i-1}^{\eta} - x_i^{\eta}x_{i-1}^{\xi}},$$

$$B_{i,k}^{(\xi)} := \int_{x_i}^{x_{i+1}} v^{\xi}\gamma(v, x_k)dv.$$

The parameters of the method are ξ and η. They determine which of the two moments of the distribution are needed to be preserved.

The present technique permits variations in the grid, allowing for an easy testing of the convergence and accuracy of the numerical solutions.

5.3 Time and space discretization of the diffusion-advection-reaction equation

This section presents a fully discrete numerical scheme that approximates the solution of the diffusion-reaction-deposition problem, where the Soret and Dufour coupling terms are taken into consideration.

5.3.1 Linearization schemes

Now we describe the Newton scheme and an iterative splitting scheme used to discretize our problem, which we recall here:

Find $\mathbf{u} = (\theta, u_1, \ldots, u_N, v_1, \ldots, v_N)$ satisfying:

$$\partial_t \theta + \nabla \cdot (-\kappa \nabla \theta) - \tau \sum_{i=1}^{N} \nabla^\delta u_i \cdot \nabla \theta = 0 \qquad \text{in } (0,T) \times \Omega \tag{5.33}$$

$$\partial_t u_i + \nabla \cdot (-d_i \nabla u_i) - \delta \nabla^\delta \theta \cdot \nabla u = R_i(u) \qquad \text{in } (0,T) \times \Omega, \tag{5.34}$$

$$\partial_t v_i = a_i v_i - b_i v_i \qquad \text{on } (0,T) \times \Gamma, \tag{5.35}$$

with the boundary conditions

$$-\kappa \nabla \theta \cdot n = 0 \qquad \text{on } (0,T) \times \Gamma_N, \tag{5.36}$$

$$\theta = \theta_D \qquad \text{on } (0,T) \times \Gamma_D, \tag{5.37}$$

$$-d_i \nabla u_i \cdot n = a_i u_i - b_i v_i \qquad \text{on } (0,T) \times \Gamma, \tag{5.38}$$

$$-d_i \nabla u_i \cdot n = 0 \qquad \text{on } (0,T) \times \Gamma_N, \tag{5.39}$$

$$u_i = u_{iD} \qquad \text{on } (0,T) \times \Gamma_D, \tag{5.40}$$

and the initial conditions

$$\theta(0,x) = \theta^0(x) \qquad \text{for } x \in \Omega, \tag{5.41}$$

$$u_i(0,x) = u_i^0(x) \qquad \text{for } x \in \Omega, \tag{5.42}$$

$$v_i(0,x) = v_i^0(x) \qquad \text{for } x \in \Gamma. \tag{5.43}$$

Recall also the definition of the weak solutions to (5.33)-(5.43):

Definition 4. *A vector* $\mathbf{u} = (\theta, u_1, \ldots, u_N, v_1, \ldots, v_N)$ *of functions is a weak solution of (5.33)-(5.43) if* $\theta, u_i \in L^2(0,T; H^1(\Omega))$ *and* $v_i \in L^2(0,T; L^2(\Omega))$ *for* $i \in \{1, \ldots, N\}$ *and the following identities hold:*

for all $\phi \in H^1(\Omega)$*:*

$$\int_{\Omega^\varepsilon} \partial_t \theta \phi + \int_{\Omega^\varepsilon} \kappa \nabla \theta \cdot \nabla \phi = \tau \sum_{i=1}^{N} \int_{\Omega^\varepsilon} \nabla^\delta u_i \cdot \nabla \theta \phi, \tag{5.44}$$

and for all $\psi_i \in H^1(\Omega)$*:*

$$\begin{aligned} \int_{\Omega^\varepsilon} \partial_t u_i \psi_i + \int_{\Omega^\varepsilon} \nabla d_i u_i \cdot \nabla \psi_i + \int_{\Gamma^\varepsilon} (a_i^\varepsilon u_i - b_i^\varepsilon v_i) \psi_i \\ = \delta_i \int_{\Omega^\varepsilon} \nabla^\delta \theta \cdot \nabla u_i \psi_i + R_i(u_i) \psi_i, \end{aligned} \tag{5.45}$$

and for all $\varphi_i \in L^2(\Omega)$*:*

$$\int_{\Gamma^\varepsilon} \partial_t v_i \varphi_i = \int_{\Gamma^\varepsilon} (a_i^\varepsilon u_i - b_i^\varepsilon v_i) \varphi_i, \tag{5.46}$$

together with (5.41)-(5.43).

Recall that in Chapter 4 we have proven existence, uniqueness, positivity and boundedness of solutions to (5.33)-(5.43) under the assumptions:

1. $0 < \kappa^0 \leq \kappa \leq \kappa^1$, $0 < d^0 \leq d_i \leq d^1$, $\delta_i < \delta^1$, $a^{\varepsilon,0} \leq a_i^{\varepsilon} \leq a^{\varepsilon,1}$, and $b_i^{\varepsilon} \leq b^{\varepsilon,1}$ for $i \in \{1, \ldots, N\}$ where κ^0, κ^1, d^0, d^1, δ^1, $a^{\varepsilon,0}$, $a^{\varepsilon,1}$ and $b^{\varepsilon,1}$ are positive constants.

2. $\theta^0 \in L_+^{\infty}(\Omega) \cap H^2(\Omega)$, $u_i \in L^{\infty}(\Omega) \cap H^2(\Omega)$, and $v_i^0 \in L^{\infty}(\Gamma)$ for $i \in \{1, \ldots, N\}$.

We split our time interval $[0, T]$ into a finite number of closed subintervals $[t_0 := 0, t_1]$, $[t_1, t_2], \ldots,$ $[t_{N-1}, t_N := T]$. The subintervals need not be equidistant, so we denote their lengths as $\tau_j = t_j - t_{j-1}$. Further, denote $u_i^j(x) := u_i(t_j, x)$, and $v_i^j(x) := v_i(t_j, x)$, and $\theta^j(x) := \theta(t_j, x)$.

We now use the following approximations to the time derivatives

$$\partial_t \theta(t_j, x) \approx \frac{\theta^j(x) - \theta^{j-1}(x)}{\tau_j}, \tag{5.47}$$

$$\partial_t u_i(t_j, x) \approx \frac{u_i^j(x) - u_i^{j-1}(x)}{\tau_j}, \tag{5.48}$$

$$\partial_t v_i(t_j, x) \approx \frac{v_i^j(x) - v_i^{j-1}(x)}{\tau_j}. \tag{5.49}$$

Using Rothe's method (see e.g. [103], [63]), we substitute (5.47)-(5.49) into (5.33)-(5.43) and obtain the following time-discrete nonlinear system.

Find $(\theta^j, u_1^j, \ldots, u_N^j, v_1^j, \ldots, v_N^j)$ satisfying

$$\begin{aligned}
&\frac{\theta^j - \theta^{j-1}}{\tau_j} + \nabla \cdot (-\kappa \nabla(\alpha\theta^j + (1-\alpha)\theta^{j-1})) - \\
&\quad \tau \sum_{i=1}^{N} \nabla^{\delta}(\alpha u_i^j + (1-\alpha)u_i^{j-1}) \cdot \nabla(\alpha\theta^j + (1-\alpha)\theta^{j-1}) = 0 \quad \text{in } \Omega
\end{aligned} \tag{5.50}$$

$$\begin{aligned}
&\frac{u_i^j - u_i^{j-1}}{\tau_j} + \nabla \cdot (-d_i \nabla(\alpha u_i^j + (1-\alpha)u_i^{j-1})) - \\
&\quad \delta \nabla^{\delta}(\alpha\theta^j + (1-\alpha)\theta^{j-1}) \cdot \nabla(\alpha u_i^j + (1-\alpha)u_i^{j-1}) \\
&\quad = R_i(\alpha u^j + (1-\alpha)u^{j-1}) \quad \text{in } \Omega,
\end{aligned} \tag{5.51}$$

$$\frac{v_i^j - v_i^{j-1}}{\tau_j} = a_i(\alpha u_i^j + (1-\alpha)u_i^{j-1}) - b_i(\alpha v_i^j + (1-\alpha)v_j^{j-1}) \quad \text{on } \Gamma, \tag{5.52}$$

with the boundary conditions

$$-\kappa\nabla\theta^j \cdot n = 0 \qquad \text{on } \Gamma_N, \quad (5.53)$$

$$\theta^j = \theta_D \qquad \text{on } \Gamma_D, \quad (5.54)$$

$$-d_i\nabla u_i^j \cdot n = a_i u_i^j - b_i v_i^j \qquad \text{on } \Gamma, \quad (5.55)$$

$$-d_i\nabla u_i^j \cdot n = 0 \qquad \text{on } \Gamma_N, \quad (5.56)$$

$$u_i^j = u_{iD}^j \qquad \text{on } \Gamma_D, \quad (5.57)$$

where θ^0, u_i^0 and v_i^0 are the given by the initial conditions. Note that we have introduced a parameter α here. The choose of $\alpha = 0$ corresponds to the explicit Euler method, while $\alpha = 1$ corresponds to the implicit Euler method. Both methods are first order accurate. Another choice of $\alpha = 0.5$ leads to the Crank-Nicholson method which is second order accurate and implicit.

Now that the time variable has been discretized, the next step is to discretize the spatial variable using the Finite Element method (see e.g. [16]). We multiply (5.50)-(5.52) with a test function and integrate over Ω and Γ respectively, integrating by parts where necessary. We obtain:

$$\begin{aligned}(\theta^j,\phi) - (\theta^{j-1},\phi) + \tau_j[\alpha(\kappa\nabla\theta^j,\nabla\phi) + (1-\alpha)(\kappa\nabla\theta^{j-1},\nabla\phi) - \\ \tau\sum_{i=1}^{N}(\nabla^\delta(\alpha u_i^j + (1-\alpha)u_i^{j-1})\cdot\nabla(\alpha\theta^j + (1-\alpha)\theta^{j-1},\phi))] = 0 \qquad (5.58)\end{aligned}$$

$$\begin{aligned}(u_i^j,\psi) - (u_i^{j-1},\psi) + \tau_j[\alpha(d_i\nabla u_i^j,\nabla\psi) + (1-\alpha)(d_i\nabla u_i^{j-1},\nabla\psi) + \\ \alpha(a_i u_i^j - b_i v_i^j,\psi)_\Gamma + (1-\alpha)(a_i u_i^{j-1} - b_i v_i^{j-1},\psi)_\Gamma \\ -\delta(\nabla^\delta(\alpha\theta^j + (1-\alpha)\theta^{j-1})\cdot\nabla(\alpha u_i^j + (1-\alpha)u_i^{j-1}),\psi)] = (R(u^j),\psi) \qquad (5.59)\end{aligned}$$

$$(v_i^j,\varphi) - (v_i^{j-1},\varphi) = \tau_j[\alpha(a_i u_i^j - b_i v_i^j,\varphi)_\Gamma + (1-\alpha)(a_i u_i^{j-1} - b_i v_i^{j-1},\varphi)_\Gamma]. \qquad (5.60)$$

We discretize the space variable by making a triangulation T^h of Ω and approximating $u_i^j(x) \approx \sum_k U_i^{j,k}\phi_i^{h,k}(x)$, where $\phi_i^{h,k}$ are the shape functions, polynomials on each triangle of T^h, that approximate the space $H^1(\Omega)$, and $U_i^{j,k}$ are the unknown nodal values of the solution.

Accordingly $\theta^j(x) \approx \sum_k T^{j,k}\psi^{h,k}(x)$ and $v_i^j(x) \approx \sum_k V_i^{j,k}\varphi_i^{h,k}(x)$, where $\psi^{h,k}(x)$ and $\varphi_i^{h,k}(x)$ are the appropriate shape functions.

We then substitute these expansions into (5.58)-(5.60), taking the test func-

tions to be $\phi_i^{h,k}$, $\psi^{h,k}$, $\varphi_i^{h,k}$, and $\alpha = 1$ for the implicit Euler method:

$$F_1(T^j, U_i^j, V_i^j) := M^\theta T^j - M^\theta T^{j-1} + \tau_j (A^\theta T^j - \sum_i U_i^{j,T} S T^j) = 0, \quad (5.61)$$

$$F_2^i(T^j, U_i^j, V_i^j) := M^u U_i^j - M^u U_i^{j-1} + \tau_j (A^u U_i^j - \sum_i U_i^{j,T} D T^j - R_i(U^j)) = 0, \quad (5.62)$$

$$F_3^i(T^j, U_i^j, V_i^j) := M^v V_i^j - M^v V_i^{j-1} + \tau_j (-C_i U_i^j + B_i V_i^j) = 0. \quad (5.63)$$

5.3.2 An iterative Newton scheme

Based on Newton's method, we compute the n^{th} approximate solution from the $n-1^{st}$, using a damping parameter β to ensure a better global convergence. Here we denote $\mathbf{U}^j := [T^j, U_i^j, V_i^j]$, and $F := [F_1, F_2^1, \ldots, F_2^N, F_3^1, \ldots, F_3^N]$:

$$\nabla F(\mathbf{U}^j) \Delta \mathbf{U}^j = -F(\mathbf{U}^j), \quad (5.64)$$

$$\mathbf{U}^{j+1} = \mathbf{U}^j + \beta \Delta \mathbf{U}^j. \quad (5.65)$$

Thus, we start with $\mathbf{U}^0$, which we interpolate from the initial conditions (5.41)-(5.43), and advance each step according to (5.65), solving a linear system to find ΔU^n. Below we give the matrix of this linear system, that depends on the solution of the previous step $\mathbf{U}^j$:

$$\nabla F(\mathbf{U}^j) = \begin{bmatrix} M^\theta + \tau_j (A^\theta - U_i^{j,T} S) & -\tau_j S T^j & 0 \\ -\tau_j U_i^{j,T} D & M^u + \tau_j (A_i^u - D T^j - \nabla R(U^j)) & 0 \\ 0 & \tau_j C_i & M^v + \tau_j B_i \end{bmatrix}$$

Here are the definitions of the matrices used in the definition of $\nabla F(\mathbf{U}^j)$:

$$M^{\theta}_{jk} := \int_{\Omega^\varepsilon} \psi^{j,h}\psi^{k,h}, \tag{5.66}$$

$$M^{u}_{i,jk} := \int_{\Omega^\varepsilon} \phi_i^{j,h}\phi_i^{k,h}, \tag{5.67}$$

$$A^{\theta}_{jk} := \int_{\Omega^\varepsilon} \kappa\nabla\psi^{j,h}\cdot\nabla\psi^{k,h}, \tag{5.68}$$

$$A^{u}_{i,jk} := \int_{\Omega^\varepsilon} d_i\nabla\phi_i^{j,h}\cdot\nabla\phi_i^{k,h}, \tag{5.69}$$

$$M^{v}_{i,jk} := \int_{\Gamma^\varepsilon} \varphi_i^{j,h}\varphi_i^{k,h}, \tag{5.70}$$

$$S_{ijk} := \int_{\Omega^\varepsilon} \tau\nabla\phi^{i,h}\cdot\nabla\psi^{j,h}\phi^{k,h}, \tag{5.71}$$

$$D_{ijk} := \int_{\Omega^\varepsilon} \delta_i\nabla\phi^{i,h}\cdot\psi^{j,h}\phi^{k,h}, \tag{5.72}$$

$$C_{ijk} := \int_{\Gamma^\varepsilon} a_i^{\varepsilon}\phi_j\varphi_k, \tag{5.73}$$

$$B_{ijk} := \int_{\Gamma^\varepsilon} b_i^{\varepsilon}\phi_j\varphi_k. \tag{5.74}$$

For each time step, we make the iterations (5.64)-(5.65) until the residual becomes smaller than the given tolerance. The Newton iterations converge quadratically when given a proper initial value [66].

5.3.3 An iterative splitting scheme

The matrix from the Newton scheme includes entries for all degrees of freedom in the system and can quickly become very large. This can be mitigated by an operator splitting scheme, that decouples the equations (5.33)-(5.35) and solves them sequentially, until the iterations converge to the fixed point.

We solve first the temperature equation, using the mobile concentrations from the last time step, then use the obtained temperature values and the immobile concentrations from the previous time step to solve for the new mobile concentrations, and finally use the new mobile concentrations to solve for the new immobile concentrations.

Consider a fixed-point operator $F := F_3 \circ F_2 \circ F_1$, where $F : (\theta^j, u_i^j, v_i^j) \to (\theta^j, u_i^j, v_i^j)$, and

- $F_1 : (\theta^j, u_i^j, v_i^j) \to (\theta^j, u_i^j, v_i^j)$ such that θ^j is the weak solution of (5.44).

- $F_2 : (\theta^j, u_i^j, v_i^j) \to (\theta^j, u_i^j, v_i^j)$ such that u_i^j are the weak solutions of (5.45).
- $F_3 : (\theta^j, u_i^j, v_i^j) \to (\theta^j, u_i^j, v_i^j)$ such that v_i^j are the weak solutions of (5.46).

Here's the algorithm to obtain the solution for the time step $\mathbf{U}^{j+1}$ from $\mathbf{U}^j$, we start with $\mathbf{U}^{j+1,0} = \mathbf{U}^j$ and

Algorithm 1. *(Iterative splitting scheme)*

1. *Find* $\mathbf{U}_1 = F_1(\mathbf{U}^{j+1,k})$
2. *Find* $\mathbf{U}_2 = F_2(\mathbf{U}_1)$
3. *Find* $\mathbf{U}^{j+1,k+1} = F_3(\mathbf{U}_2)$

We continue the iterations until $\|\mathbf{U}^{j+1,k+1} - \mathbf{U}^{j+1,k}\| < \varepsilon$, where ε is a given tolerance. These iterations are expected to converge linearly.

5.4 Discretization of cell problems and periodic boundary conditions

Periodic boundary conditions are usually used when a solution on a larger domain that repeats in one or more directions can be substituted with a solution on a representative piece of this domain as in Figure 5.1. The computation is then periodically extended to the other cells.

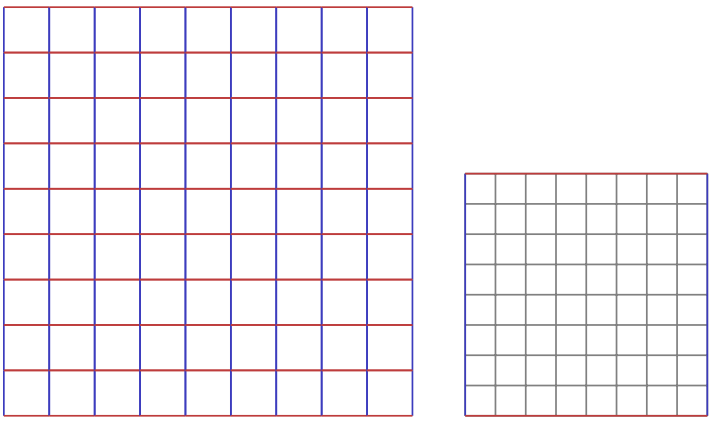

FIGURE 5.1: Illustration of the periodic domain (left) and a triangulation of the periodic cell (right). Boundaries of the same color must match.

Assuming the periodic cell in Figure 5.1 to be $[0,1] \times [0,1]$, the periodic boundary condition will look like:

$$u(0,y) = u(1,y) \qquad \text{for } x \in [0,1]$$
$$u(x,0) = u(x,1) \qquad \text{for } y \in [0,1]$$

To simplify the implementation of the periodic boundary conditions, assume that the mesh is uniformly refined, at least on the boundary. Then, after the FEM discretization there's an equal amount of nodes on the top and bottom, left and right boundaries respectively. And there is a correspondence between each respective node: for each degree of freedom on the boundary, i, there exists a degree of freedom on the opposite side of the boundary $p(i)$. Except for the corners, p reverses itself, i.e. $p(p(i)) = i$. So if we're representing our solution as $u_h(x) = \sum U_i \phi_i^h(x)$, we have to constrain:

$$U_i = U_{p(i)} \qquad \text{for all } i \in \mathcal{B},$$

where $\mathcal{B}$ is the set of the degrees of freedom on the boundary.

The algorithms used to implement generalized constraints for FEM are detailed in [6].

5.5 Overview of the used Numerics libraries

5.5.1 DUNE

DUNE, the Distributed and Unified Numerics Environment (cf. [7]) is a modular toolbox for solving partial differential equations (PDEs) with grid-based methods. It supports the easy implementation of methods like Finite Elements (FE), Finite Volumes (FV), and also Finite Differences (FD). DUNE is free software licensed under the GPL (version 2).

DUNE is designed to provide a slim interface that allows efficient use of legacy and/or new libraries. It used modern C++ templating techniques to enable very different implementations of the same concept (i.e. grids, solvers, ...) to have a common interface at a very low overhead.

DUNE is based on the following main principles:

- Separation of data structures and algorithms by abstract interfaces.
- Efficient implementation of these interfaces using generic programming techniques. Static polymorphism allows the compiler to do more optimizations, in particular function inlining, which in turn allows the interface to have very small functions (implemented by one or few machine instructions) without a severe performance penalty. In essence the algorithms are parametrized with a particular data structure and the interface is removed at compile time. Thus the resulting code is as efficient as if it would have been written for the special case.

- Reuse of existing finite element packages with a large body of functionality. In particular the finite element codes UG, ALBERTA, and ALUGrid have been adapted to the DUNE framework. Thus, parallel and adaptive meshes with multiple element types and refinement rules are available. All these packages can be linked together in one executable.

In our experience of using DUNE, the advantages listed above have some disadvantages to offset the advantages that they provide in some situations:

- The abstract interfaces being very loosely coupled through the use of templates can be seen as an advantage for adding new features and optimizations, has the drawback of being less inspectable and discoverable in the application usage.
- The efficiency of implementation that leverages templates greatly increases the compilation time. Most of the code needs to be re-compiled even with a very small change. But this is mainly a drawback of the current definition of the template aspects of C++, as well as the current implementation of the compilers. The compiler output in case of an error is quite overwhelming, being megabytes worth of text with many places to inspect the possible location of the error.
- The reuse of existing packages is good, although it comes at a price of a lengthy configuration to ensure that all the pieces of the library know about each other and can be used together.

DUNE provides many grid formats, of which we used mainly ALUGrid and YaspGrid (for testing). Particular grids can be created using third party tools and saved in gmsh format, which DUNE can read. The most of the widely used shape functions for the FEM are implemented, such as Lagrangian shape functions of arbitrary order, Monomial shape functions of arbitrary order for Discontinuous Galerkin methods, and Raviart-Thomas shape functions of the lowest order. DUNE contains ISTL (the Iterative Solver Template Library), which provides nice abstractions for the block matrices that result from our system. The solutions can be outputted in VTK format, and standard tools such as Paraview can be used to visualize the output. DUNE provides three discretization to choose from: dune-FEM, dune-fufem, and dune-PDELab, of which we chose dune-PDELab, since it was best suited for solving our problem. The main advantage of dune-PDELab is their implementation of product spaces for systems of equations, as well as the straightforward implementation for transient problems. We have used DUNE to produce the numerical results in Chapter 2 and in Chapter 3.

5.5.2 deal.II

deal.II (cf. [5]) is the successor to the Differential Equations Analysis Library. It is a C++ program library targeted at the computational solution of partial

differential equations using adaptive finite elements. It uses state-of-the-art programming techniques to offer a modern interface to the complex data structures and algorithms required.

The main aim of deal.II is to enable rapid development of modern finite element codes, using among other aspects adaptive meshes and a wide array of tools classes often used in finite element program. The library takes care of the details of grid handling and refinement, handling of degrees of freedom, input of meshes and output of results in graphics formats etc. Support for several space dimensions at once is included in a way such that programs can be written independent of the space dimension without unreasonable penalties on run-time and memory consumption.

We added deal.II to the implementation the discretization of our model in order to handle the periodic boundary conditions for the cell problems, which were difficult to implement in DUNE. deal.II is also much faster for prototyping, since it involves much less aggressive optimization than DUNE, i.e. usual polymorphism instead of static polymorphism. The extensive documentation and an open source license add a lot to the attractiveness of this library.

We have contributed to the documentation base of deal.II as well as to the source code [27].

We have used deal.II to produce the numerical results of Chapter 3, where it was instrumental in solving the related cell problems.

One disadvantage of deal.II over DUNE, is that it is only able to use rectangular elements for the triangulation, while DUNE can deal with a multitude of meshes, including mixed triangles and rectangles. This choice however greatly improves the clarity of the interfaces and allows for more optimization, since it is possible to prescribe many geometrical constants, such as number of faces per cell in each space dimension.

A big advantage of deal.II is its model of treating the constraints on the degrees of freedom, which was instrumental in implementing the periodic boundary conditions. After the assembly of the stiffness matrix, it is possible to constrain a degree of freedom to a linear combination of other degrees of freedom. As long as there are no cyclic dependencies, the library can handle these constraints. Another important advantage is the ease of implementation of various grid refinement strategies. Note that the grid adaptivity is a very attractive feature if one needs to resolve the relevant fluctuations in a multiscale model.

Chapter 6

Numerical Analysis of the Upscaled Thermo-Diffusion Problem

6.1 Introduction

We are interested in quantifying the effect of coupled macroscopic fluxes[1] on the aggregation, fragmentation and deposition of large populations of colloids traveling through a porous medium. To do so, we are using a well-posed partly-dissipative coupled system of quasilinear parabolic equations posed in a connected open set Ω with sufficiently smooth boundary. The particular structure of the system has been obtained via periodic homogenization techniques in [69] [see e.g. Ref. [55] for a methodological upscaling procedure of reactive flows through arrays of periodic microstructures]. For details, see Chapter 4.

The primary motivation of this part of the thesis is to develop and analyze appropriate numerical schemes to compute at macroscopic scales approximate solutions to our thermo-diffusion system with Smoluchowski interactions. Accounting for the interplay between heat, diffusion, attraction-repulsion, and deposition of the colloidal particles is of paramount importance for a number of applications including the dynamics of the colloidal suspension in natural or man-made products (e.g. milk, paints, toothpaste) [37], drug-delivery systems [3], hierarchical assembly of biological tissues [78], group formation in actively interacting populations [90], or heat shocks in porous materials [12]. Further details on colloids and their practical relevance are given in [31, 68], e.g.

The discretizations shown here have been successfully used in Chapter 3 (see also [70]) to capture the effect of multiscale aggregation and deposition mechanisms on the colloids dynamics traveling within a saturated porous medium in the absence of thermal effects. Now, we are preparing the stage to include the Soret and Dufour transport contributions – cross-effects between molecular diffusion and heat conduction; for more details on the macroscopic modeling of

[1] In this context, the fluxes are driven by a suitable combination of heat and diffusion gradients [46].

thermo-diffusion, we refer the reader to the monograph by De Groot and Mazur [46]. The *a priori* estimates are obtained in a similar fashion as for problems involving reactive flow in porous media (see, for instance, [71, 29] and references cited therein), however specifics of the cross transport, interaction terms, and of the non-dissipative (ode) structure play here an important role and need to be treated carefully. For the numerical analysis of case studies in cross diffusion, we refer the reader for instance to [42, 4] and [93]. Note that there is not yet a unified mathematical theory to deal with general cross-diffusion or thermo-diffusion systems. Due to the presence of the nonlinearly coupled transport terms, essential difficulties arise in controlling the temperature gradients (and the gradients in the concentrations of colloidal populations) especially in more space dimensions (see e.g. [11] for a nice discussion of a related PDE system posed in one space dimension), the problem sharing many common features with the Stefan-Maxwell system for multicomponent mixtures (compare Refs. [14, 62, 51] and the literature mentioned therein).

In this Chapter, we investigate the semidiscrete as well as the fully discrete *a priori* error analysis of the finite elements approximation of the weak solution to a thermo-diffusion reaction system posed in a macroscopic domain that allows for aggregation, dissolution as well as deposition of colloidal species. The main results are summarized in Theorem 6.4.7 and Theorem 6.5.5. The mathematical techniques used in the proofs include energy-like estimates and compactness arguments, exploiting the structure of both the interaction terms and nonlocal coupling. Once these *a priori* estimates are proven and, additionally, corrector estimates for the homogenization process explained in Chapter 4 become available, then the next natural analysis step is to prepare a functional framework for the design optimally convergent MsFEM schemes approximating, very much in the spirit of [56, 17], multiscale formulations of our thermo-diffusion system.

The Chapter has the following structure: Section 6.2 presents the setting of the model equations and briefly summarizes the meaning of the parameters and model components. We anticipate already at this point the main results. In Section 6.3, we list the main mathematical analysis aspects of our choice of thermo-diffusion system and briefly recall a collection of approximation theory results that are used in the sequel. Section 6.4 and Section 6.5 constitute the bulk of the Chapter. This is the place where we give the details of the proof of the semidiscrete and fully discrete *a priori* error control, i.e. the proofs for Theorem 6.4.7 and Theorem 6.5.5.

6.2 Formulation of the problem. Main results

Let I denote an open sub-interval within the time interval $(0, T]$, and let $x \in \Omega$ be the variable pointing out the space position. The unknowns of the system are the temperature field θ, the mobile colloidal populations u_i ($i \in \{1, \dots, N\}$), and the immobile (already deposited) colloidal populations v_i ($i \in \{1, \dots, N\}$). $N \in \mathbb{N}$ represents the amount of the monomers in the largest colloidal species

considered. All unknowns depend on both space and time variables $(x,t) \in \Omega \times I$.

Definition 5. *Given $\delta > 0$, we introduce the mollifier:*

$$J_\delta(s) := \begin{cases} Ce^{1/(|s|^2-\delta^2)} & \text{if } |s| < \delta, \\ 0 & \text{if } |s| \geq \delta, \end{cases} \tag{6.1}$$

where the constant $C > 0$ is selected such that

$$\int_{\mathbb{R}^d} J_\delta = 1,$$

see [32] for details.

Definition 6. *Using J_δ from (6.1), define the mollified gradient:*

$$\nabla^\delta f := \nabla \left[\int_{B(x,\delta)} J_\delta(x-y) f(y) dy \right], \tag{6.2}$$

where $B(x,\delta) \subset \mathbb{R}^d$ is a ball centered in $x \in \Omega$ with radius δ.

With the Definition 6.2 at hand, the following inequalities hold for all $f \in L^\infty(\Omega)$ and $g \in L^p(\Omega;\mathbb{R}^d)$ (with $1 \leq p \leq \infty$):

$$\|\nabla^\delta f \cdot g\|_{L^p(\Omega)} \leq C\|f\|_{L^\infty\Omega}\|g\|_{L^p(\Omega;\mathbb{R}^d)} \tag{6.3}$$

$$\|\nabla^\delta f\|_{p(\Omega)} \leq C\|f\|_{L^2(\Omega)}, \tag{6.4}$$

where the constant C depends on the choice of the parameter δ and structure of the mollifier J_δ.

For all $t \in I$, the setting of our thermo-diffusion equations is the following: Find the triplet (θ, u_i, v_i) satisfying

$$\partial_t\theta + \nabla \cdot (-\mathbb{K}\nabla\theta) - \sum_{i=1}^{N} \mathbb{T}_i \nabla^\delta u_i \cdot \nabla\theta = 0 \qquad \text{in } \Omega \tag{6.5}$$

$$\partial_t u_i + \nabla \cdot (-\mathbb{D}_i \nabla u_i) - \mathbb{F}_i \nabla^\delta\theta \cdot \nabla u_i + \tag{6.6}$$

$$+ A_i u_i - B_i v_i = R_i(u_i) \qquad \text{in } \Omega \tag{6.7}$$

$$\partial_t v_i = A_i u_i - B_i v_i \qquad \text{in } \Omega \tag{6.8}$$

$$-\mathbb{K}\nabla\theta \cdot n = 0 \qquad \text{on } \partial\Omega \tag{6.9}$$

$$u_i = 0 \qquad \text{on } \partial\Omega \tag{6.10}$$

$$\theta(0,\cdot) = \theta^0(\cdot) \qquad \text{in } \Omega, \tag{6.11}$$

$$u_i(0,\cdot) = u_i^0(\cdot) \qquad \text{in } \Omega, \tag{6.12}$$

$$v_i(0,\cdot) = v_i^0(\cdot). \qquad \text{in } \Omega. \tag{6.13}$$

Here for all $i \in \{1,\ldots,N\}$, the parameters K, D_i, F_i and T_i are effective transport coefficients for heat conduction, colloidal diffusion as well as Soret and

Dufour effects. Furthermore, A_i and B_i are effective deposition coefficients. θ^0 is the initial temperature profile, while u_i^0 and v_i^0 are the initial concentrations of colloids in mobile, and respectively, immobile state. General motivation on the ingredients of this system (particularly on Soret and Dufour effects) can be found in [46]. Note that as direct consequence of fixing the threshold N, the system coagulates colloidal species (groups) until size N only.

This particular structure of the system has been derived in [69] by means of periodic homogenization arguments (two-scale convergence), scaling up the involved physicochemical processes from the pore scale (microscopic level, representative elementary volume (REV)) to a macroscopically observable scale.

Remark 6.2.1. *Theorem (4.4.5) ensures the weak solvability of the system (6.5)–(6.13). Furthermore, under mild assumptions on the data and the parameters the weak solution is positive a.e. and satisfies a weak maximum principle. The basic properties of the weak solutions to (6.5)–(6.13) are given in Section 6.3.*

Denoting by $\theta^h(t)$ the continuous-in-time and semidiscrete-in-space approximation of $\theta(t)$ and by $\theta^{h,n}$ the corresponding fully discrete approximation, with similar notation for the other unknowns, we can formulate our main result: For all $t, t_n \in I$, the following *a priori* estimates hold:

$$\begin{aligned}\|\theta^h(t) - \theta(t)\| + \sum_{i=1}^{N} \|u_i^h(t) - u_i(t)\| + \sum_{i=1}^{N} \|v_i^h(t) - v_i(t)\| \\ \leq C_1\|\theta^{0,h} - \theta^0\| + C_2(\|u_i^{0,h} - u_i^0\| + \|v_i^{0,h} - v_i^0\|) + C_3h^2\end{aligned} \tag{6.14}$$

and

$$\begin{aligned}\|\theta^{h,n} - \theta^n\| + \sum_{i=1}^{N} \|u_i^{h,n} - u_i^n\| + \sum_{i=1}^{N} \|v_i^{h,n} - v_i^n\| \\ \leq C_4\|\theta^{h,0} - \theta^0\| + C_5\left(\sum_{i=1}^{N} \|u_i^{h,0} - u_i^0\| + \sum_{i=1}^{N} \|v_i^{h,0} - v_i^0\|\right) \\ + C_6(h^2 + \tau).\end{aligned} \tag{6.15}$$

The constants $C_1, \ldots, C_6$ depend on data, but are independent of the grid parameters h and τ. The hypotheses and the results under which (6.14) and (6.15) hold are stated in Theorem 6.4.7 and Theorem 6.5.5, respectively.

The following Sections focus exclusively on the proof of these inequalities.

6.3 Concept of weak solution. Technical preliminaries. Available results.

Our concept of weak solution is detailed as follows:

Definition 7. *The triplet (θ, u_i, v_i) is a solution to (6.5)-(6.13) if the following holds:*

$$\begin{aligned} &\theta, u_i \in H^1(0,T;L^2(\Omega)) \cap L^\infty(0,T;H^1(\Omega)),\\ &v_i \in H^1(0,T;L^2(\Omega)), \end{aligned} \tag{6.16}$$

and for all $t \in J$ and $\phi \in H^1(\Omega)$:

$$(\partial_t \theta, \phi) + (\mathbb{K}\nabla\theta, \nabla\phi) - \sum_{i=1}^{N} (\mathbb{T}_i \nabla^\delta u_i \cdot \nabla\theta, \phi) = 0, \tag{6.17}$$

$$\begin{aligned} &(\partial_t u_i, \phi) + (\mathbb{D}_i \nabla u_i, \nabla\phi) - (\mathbb{F}_i \nabla^\delta \theta \cdot \nabla u_i, \phi)\\ &\qquad + (A_i u_i - B_i v_i, \phi) = (R_i(u), \phi), \end{aligned} \tag{6.18}$$

$$(\partial_t v_i, \phi) = (A_i u_i - B_i v_i, \phi). \tag{6.19}$$

To be able to ensure the solvability of our thermo-diffusion problem, we assume that the following set of assumptions on the data (i.e. (A1)-(A2)) hold true:

(A_1) $\mathbb{T}_i$, $\mathbb{F}_i$, A_i, B_i are positive constants for $i \in \{1, \dots, N\}$, and there exist m and M such that: $0 < m \leq \mathbb{K} \leq M$ and $0 < m \leq \mathbb{D}_i \leq M$.

(A_2) $\theta^0 \in L^\infty_+(\Omega) \cap H^2(\Omega), u_i^0 \in L^\infty_+(\Omega) \cap H^2(\Omega), v_i^0 \in L^\infty_+(\Gamma)$ for $i \in \{1, \dots, N\}$.

Fix $h > 0$ sufficiently small and let T_h be a triangulation of Ω with

$$\max_{\tau \in \mathrm{T}_h} diam(\tau) \leq h.$$

Let S_h denote the finite dimensional space of continuous functions on Ω that reduce to linear functions in each of the triangles of T_h and vanish on $\partial\Omega$. Let $\{P_j\}_{j=1}^{N_h}$ be the interior vertices of T_h with $N_h \in \mathbb{N}$. A function in S_h is then uniquely determined by its values at the points P_j. Let Φ_j be the pyramid function in S_h which takes value 1 at P_j, but vanishes at the other vertices. Then $\{\Phi_j\}_{j=1}^{N_h}$ forms a basis for S_h. Consequently, every φ in S_h can be uniquely represented as

$$\varphi(x) = \sum_{j=1}^{N_h} \alpha_j \Phi_j(x), \quad \text{with } \alpha_j := \Phi(P_j), \text{for } j \in \{1, \dots, N_h\}, \tag{6.20}$$

see e.g. Ref. [66].

A smooth function σ defined on Ω which vanishes on $\partial\Omega$ can be approximated by its interpolant $I_h\sigma$ in S_h defined as:

$$I_h\sigma(x) := \sum_{j=1}^{N_h} \sigma(P_j)\Phi_j(x). \tag{6.21}$$

We denote below by $\|\cdot\|$ the norm of the space $L_2(\Omega)$ and by $\|\cdot\|_s$ that in the Sobolev space $H^s(\Omega) = W_2^s(\Omega)$ with $s \in \mathbb{R}$. If $s = 0$ we suppress the index.

We recall that for functions v lying in $H_0^1(\Omega)$, the objects $\|\nabla v\|$ and $\|v\|_1$ are equivalent norms. Let us also recall Friedrichs' lemma (see, for instance, [16, 23]): there exist constants $c_F > 0$ and $C_F > 0$ (depending on Ω, see Ref. [88] for explicit expressions for these constants) such that

$$c_F\|\sigma\|_1 \leq C_F\|\nabla\sigma\| \leq \|\sigma\|_1, \quad \text{for all } \sigma \in H_0^1(\Omega). \tag{6.22}$$

The following error estimates for the interpolant $I_h\sigma$ of σ [cf. (6.21)] are well-known (see, e.g., [16] or [23]), namely for all $\sigma \in H^2(\Omega) \cap H_0^1(\Omega)$ we have

$$\|I_h\sigma - \sigma\| \leq Ch^2\|\sigma\|_2 \tag{6.23}$$

$$\|\nabla(I_h\sigma - \sigma)\| \leq Ch\|\sigma\|_2. \tag{6.24}$$

Testing the equations (6.5)-(6.6) with $\varphi \in S_h$ leads to the following semi-discrete weak formulation of (6.5)-(6.13) as given in Definition 8.

Definition 8. *The triplet (θ^h, u_i^h, v_i^h) is a semidiscrete solution to (6.5)-(6.13) if the following identities hold true for all $t \in I$ and $\varphi \in S_h$:*

$$(\partial_t\theta^h, \varphi) + (\mathbb{K}\nabla\theta^h, \nabla\varphi) - \sum_{i=1}^{N}(\mathbb{T}_i\nabla^\delta u_i^h \cdot \nabla\theta^h, \varphi) = 0 \tag{6.25}$$

$$\begin{aligned}(\partial_t u_i^h, \varphi) + (\mathbb{D}_i\nabla u_i^h, \nabla\varphi) - (\mathbb{F}_i\nabla^\delta\theta^h \cdot \nabla u_i^h, \varphi)\\ + (A_i u_i^h - B_i v_i^h, \varphi) = (R_i(u^h), \varphi)\end{aligned} \tag{6.26}$$

$$(\partial_t v_i^h, \varphi) = (A_i u_i^h - B_i v_i^h, \varphi) \tag{6.27}$$

$$\theta^h(0) = \theta^{0,h} \tag{6.28}$$

$$u_i^h(0) = u_i^{0,h} \tag{6.29}$$

$$v_i^h(0) = v_i^{0,h}. \tag{6.30}$$

Here, $\theta^{0,h}$, $u_i^{0,h}$, and $v_i^{0,h}$ are suitable approximations of θ^0, u_i^0, and v_i^0 respectively in the finite dimensional space S_h.

Remark 6.3.1. *Note that v_i as solution to (6.8) can be expressed as:*

$$v_i(t) = \left(\int_0^t A_i u_i(s) e^{B_i s} ds\right) e^{-B_i t} + v_i^0 e^{-B_i t} \qquad \text{for all } t \in I. \tag{6.31}$$

We will make this substitution later and also use (6.31) to obtain an error estimate for v_i^h based on the error estimate for u_i^h. This path can be followed due to the linearity of the equation. If the right-hand side of the ordinary differential equations becomes nonlinear, then a one-sided Lipschitz structure is needed to allow for the Gronwall argument to work.

Remark 6.3.2. *The existence of solutions in the sense of Definition 7 is ensured by periodic homogenization arguments in [69], while the existence of solutions in the sense of Definition 8 follows by standard arguments. We omit to show the details of the existence proofs. Note that the existence of the respective solutions is nevertheless re-obtained here by straightforward compactness arguments. The proof of uniqueness of both kinds of solutions follows the lines of [69].*

We represent the approximate solutions to the system (6.5)–(6.13) by means of the standard Galerkin Ansatz as:

$$u_i^h(x,t) := \sum_{j=1}^{N_h} \alpha_{ij}(t)\Phi_j(x),$$
$$\theta^h(x,t) := \sum_{j=1}^{N_h} \beta_j(t)\Phi_j(x),$$
$$v_i^h(x,t) := \sum_{j=1}^{N_h} \gamma_{ij}(t)\Phi_j(x)$$

for all $(x,t) \in \Omega \times I$. Based on the Galerkin projections, the semidiscrete model equations read:

$$\sum_{j=1}^{N_h} \beta'_{ij}(t)(\Phi_j,\Phi_k) + \sum_{j=1}^{N_h} \beta_{ij}(\mathbb{K}_i\nabla\Phi_j,\nabla\Phi_k) - \sum_{i=1}^{N} \mathbb{T}_i \sum_{j=1}^{N_h}\sum_{l=1}^{N_h} \beta_{ij}(t)\alpha_{il}(t)(\nabla^\delta\Phi_l\cdot\nabla\Phi_j,\Phi_k) = 0 \tag{6.32}$$

$$\sum_{j=1}^{N_h} \alpha'_{ij}(t)(\Phi_j,\Phi_k) + \sum_{j=1}^{N_h} \alpha_{ij}(\mathbb{D}_i\nabla\Phi_j,\nabla\Phi_k) - \mathbb{F}_i \sum_{j=1}^{N_h}\sum_{l=1}^{N_h} \alpha_{ij}(t)\beta_l(t)(\nabla^\delta\Phi_l\cdot\nabla\Phi_j,\Phi_k) = (R_i(\sum_{j=1}^{N_h}\alpha_{ij}(t)\Phi_j),\Phi_k). \tag{6.33}$$

To abbreviate the writing of (6.32)-(6.33), we define:

$$\alpha_i := \alpha_i(t) = (\alpha_{i1}(t),\dots,\alpha_{i,N_h}(t))^T,$$
$$\beta := \beta(t) = (\beta_1(t),\dots,\beta_{N_h}(t))^T,$$
$$\gamma_i := \gamma_i(t) = (\gamma_{i1}(t),\dots,\gamma_{i,N_h}(t))^T,$$
$$G := (g_{jk}),\ g_{jk} := (\Phi_j,\Phi_k),$$
$$H_i^u := (h_{ijk}^u),\ h_{ijk}^u := (\mathbb{D}_i\nabla\Phi_j,\nabla\Phi_k),$$
$$H^\theta := (h_{jk}^\theta),\ h_{jk}^\theta := (\mathbb{K}\nabla\Phi_j,\nabla\Phi_k),$$
$$M := (m_{jkl}),\ m_{jkl} := (\nabla^\delta\Phi_l\cdot\Phi_j,\Phi_k).$$

Then (6.32)-(6.33) become:

$$\begin{cases} G\beta' + H^\theta\beta - \sum_{i=1}^N \mathbb{T}_i\alpha_i^T M\beta = 0 \\ G\alpha_i' + H_i^u\alpha_i - \mathbb{F}_i\beta^T M\alpha_i + G(A_i\alpha_i - B_i\gamma_i) \\ = (R_i(\sum_{j=1}^{N_h}\alpha\Phi_j), \Phi_k) \\ G\gamma_i' = A_iG\alpha_i - B_iG\gamma_i \\ \beta(0) = \beta^0 \\ \alpha_i(0) = \alpha_i^0 \\ \gamma_i(0) = \gamma_i^0. \end{cases} \tag{6.34}$$

Note that (6.34) is a nonlinear system of coupled ordinary differential equations. Based on (A_1)–(A_2), we see not only that H^θ and H_i^u are positive definite, but also that the right-hand side of the differential equations form a global Lipschitz continuous function, fact which ensures the well-posedness of the Cauchy problem (6.34) on I and eventually on its continuation on the whole interval $(0, T]$; we refer the reader to [2] for this kind of extension arguments for ordinary differential equations. Essentially, we get a unique solution vector

$$(\beta, \alpha_i, \gamma_i) \in C^1(\bar{I})^{N^h} \times C^1(\bar{I})^{NN^h} \times C^1(\bar{I})^{NN^h}$$

satisfying (6.34); see [91] for the proof of the global Lipschitz property of the right-hand side of a similar system of ordinary differential equations.

6.4 Semi-discrete error analysis

Our goal is to estimate the a priori error between the weak solutions of (6.25)–(6.30) and the weak solutions of (6.5)–(6.13). We proceed very much in the spirit of Thomeée [121]; cf., for instance, Chapter 13 and Chapter 14.

We write the error as a sum of two terms:

$$\theta^h - \theta = (\theta^h - \tilde{\theta}^h) + (\tilde{\theta}^h - \theta) = \psi + \rho. \tag{6.35}$$

In (6.35), $\tilde{\theta}^h$ is the elliptic projection in S_h of the exact solution θ, i.e. $\tilde{\theta}^h$ satisfies for all $t \geq 0$ the identity:

$$(\mathbb{K}\nabla(\tilde{\theta}^h(t) - \theta(t)), \nabla\varphi) - \sum_{i=1}^N (\mathbb{T}_i\nabla^\delta u_i \cdot \nabla(\tilde{\theta}^h(t) - \theta(t)), \varphi) = 0 \tag{6.36}$$

for all $\varphi \in S_h$.

Lemma 6.4.1. *Let $k \in C^1(\bar{\Omega})$, $b \in L^\infty(\Omega, \mathbb{R}^3)$, and $\nabla \cdot b \in L^\infty(\Omega)$. Suppose that $\gamma \in H_0^1(\Omega)$ is a weak solution to the elliptic boundary-value problem*

$$-\nabla \cdot (k\nabla\gamma + b\gamma) = \delta \quad \text{in } \Omega, \quad \gamma = 0 \quad \text{on } \partial\Omega. \tag{6.37}$$

Additionally, assume

$$\partial\Omega \in C^2. \tag{6.38}$$

Then we have

$$\|\gamma\|_2 \leq C\|\delta\|. \tag{6.39}$$

Proof. The proof of this result is a particular case of the proof of Theorem 4 given in [32, p. 317]. We omit to repeat the arguments here. □

Remark 6.4.2. *The condition (6.38) can be relaxed to* Ω *being a convex polygon, see [45, p. 147] (compare Theorem 3.2.1.2 and Theorem 3.2.1.3).*

Lemma 6.4.3. *Let* $k \in L^2(\Omega)$ *and* $b \in L^\infty(\Omega, \mathbb{R}^3)$*, and* $k(x) \geq m > 0$*, and* $m > \|b\|_\infty C_F$*, where* C_F *is the constant entering (6.22). Suppose that* $\gamma \in H_0^1(\Omega)$ *is a weak solution of the elliptic boundary-value problem*

$$-\nabla \cdot (k\nabla\gamma + b\gamma) = \delta \quad \text{in } \Omega, \quad \gamma = 0 \quad \text{on } \partial\Omega. \tag{6.40}$$

Then we have

$$\|\gamma\|_2 \leq C\|\delta\|. \tag{6.41}$$

Proof. We can directly verify that

$$\begin{aligned} m\|\gamma\|^2 &\leq (k\nabla\gamma, \nabla\gamma) = (\delta, \gamma) + (b \cdot \gamma, \nabla\gamma) \\ &\leq \|\delta\|\|\gamma\| + \|b\|_\infty \|\gamma\|\|\nabla\gamma\| \\ &\leq \|\delta\|\|\gamma\| + \|b\|_\infty C_F \|\nabla\gamma\|^2. \end{aligned}$$

Here, we used the Friedrichs inequality (6.22). Since $m > \|b\|_\infty C_F$, we have (6.41). □

Lemma 6.4.4. *Take* $k \in L^\infty(\Omega) \cap H^1(\Omega)$ *and* $b \in L^\infty(\Omega, \mathbb{R}^3) \cap H^1(\Omega, \mathbb{R}^3)$ *and assume that there exist* m *and* M *such that* $0 < m \leq k(x) \leq M$ *for all* $x \in \Omega$*. Let* $w \in H^2(\Omega) \cap H_0^1(\Omega)$ *satisfying*

$$(k\nabla(w_h - w), \nabla\varphi) - (b \cdot \nabla(w_h - w), \varphi) = 0 \qquad \text{for all } \varphi \in S_h. \tag{6.42}$$

Then the following estimates hold:

$$\|\nabla(w_h - w)\| \leq C_1 h \|w\|_2 \tag{6.43}$$

$$\|w_h - w\| \leq C_0 h^2 \|w\|_2. \tag{6.44}$$

Here, the constant C_1 *depends on* T_h*,* m*, and* M*. The constant* C_0 *depends additionally on the upper bound of* ∇k *and* b *in the corresponding* L^∞*-norm.*

Proof. We proceed very much in the spirit of Ciarlet estimates. By (A_1), we have that

$$\begin{aligned} m\|\nabla(w_h - w)\|^2 &\leq (k\nabla(w_h - w), \nabla(w_h - w)) = \\ &(k\nabla(w_h - w), \nabla(w_h - \varphi)) + (k\nabla(w_h - w), \nabla(\varphi - w)) = \\ &(b \cdot \nabla(w_h - w), w_h - \varphi) + (k\nabla(w_h - w), \nabla(\varphi - w)) \leq \\ &\|b\|_\infty \|\nabla(w_h - w)\| \|w_h - \varphi\| + M\|\nabla(w_h - w)\| \|\nabla(\varphi - w)\|. \end{aligned}$$

Take $\varphi := I_h w$ - the Clement interpolant of w. Then we have:

$$\begin{aligned} m\|\nabla(w_h - w)\| &\leq \|b\|_\infty(\|w_h - w\| + \|I_h w - w\|) \\ &+ M\|\nabla(I_h w - w)\| \leq C_1 h\|w\|_2, \end{aligned} \tag{6.45}$$

which yields

$$\begin{aligned} \|\nabla(w_h - w)\| &\leq (C_1 h + C_2\|b\|_\infty h^2)\|w\|_2 \\ &+ \frac{\|b\|_\infty}{m}\|w_h - w\|. \end{aligned} \tag{6.46}$$

It is worth noting that (6.46) leads to (6.43) when we show later that (at least)

$$\|w_h - w\| \leq Ch\|w\|_2.$$

Next, we show (6.44) using a duality argument. Let $\gamma \in H_0^1(\Omega)$ solve the problem

$$-\nabla \cdot (k\nabla\gamma - b\gamma) = \delta \quad \text{in } \Omega, \quad \gamma = 0 \quad \text{on } \partial\Omega.$$

Then

$$\begin{aligned} (w_h - w, \delta) &= (w_h - w, -\nabla \cdot (k\nabla\gamma - b\gamma)) \\ &= (k\nabla(w_h - w), \nabla\gamma) - (b \cdot \nabla(w_h - w), \gamma) \\ &= (k\nabla(w_h - w), \nabla(\gamma - \varphi)) - (b \cdot \nabla(w_h - w), \gamma - \varphi) \\ &+ (k\nabla(w_h - w), \nabla\varphi) - (b \cdot \nabla(w_h - w), \varphi). \end{aligned}$$

Let $\varphi := I_h\gamma$ and use (6.42):

$$\begin{aligned} (w_h - w, \delta) \leq M\|\nabla(w_h - w)\| \|\nabla(\gamma - I_h\gamma)\| \\ + \|b\|_\infty \|\nabla(w_h - w)\| \|\gamma - I_h\gamma\|. \end{aligned}$$

Using the standard approximation properties for $I_h\gamma$, we get:

$$(w_h - w, \delta) \leq (C_1 Mh + C_2\|b\|_\infty h^2)\|\gamma\|_2 \|\nabla(w_h - w)\|. \tag{6.47}$$

Using $\delta := w_h - w$ in (6.47), and either Lemma 6.4.1 or Lemma 6.4.3, we obtain:

$$\|w_h - w\| \leq (C_1 Mh + C_2\|b\|_\infty h^2) C_3 \|\nabla(w_h - w)\|. \tag{6.48}$$

Using (6.48) in (6.46) leads to:

$$\|\nabla(w_h - w)\| \leq C_1 h\|w\|_2 + C_2 h\|\nabla(w_h - w)\|. \tag{6.49}$$

After solving the recurrence in (6.49), (6.43) is proven, and hence (6.44) follows from (6.48). □

Lemma 6.4.5. *Let $\tilde{\theta}^h$ be defined by (6.36), and let $\rho := \tilde{\theta}^h - \theta$. Then the following estimates hold:*

$$\|\rho(t)\| + h\|\nabla\rho(t)\| \leq C(\theta)h^2 \qquad t \in I, \tag{6.50}$$

$$\|\rho_t(t)\| + h\|\nabla\rho_t(t)\| \leq C(\theta)h^2 \qquad t \in I. \tag{6.51}$$

Proof. Using Lemma 6.4.4, we have that $\|\nabla\rho\| \leq C_1 h\|\theta\|_2$ and $\rho \leq C_0 h^2\|\theta\|_2$, so (6.50) follows by adding these estimates.

To obtain (6.51), we differentiate (6.36) with respect to time to obtain:

$$(k\nabla\rho_t, \nabla\varphi) - (b_t \cdot \nabla\rho + b \cdot \nabla\rho_t, \varphi) = 0.$$

Assuming k uniformly bounded, which it is, since it doesn't depend on θ in our case:

$$\begin{aligned} m\|\nabla\rho_t\|^2 &\leq (k\nabla\rho_t, \nabla\rho_t) = (k\nabla\rho_t, \nabla(\tilde{\theta}_t^h - \varphi + \varphi - \theta_t)) \\ &= (k\nabla\rho_t, \nabla(\varphi - \theta_t)) + (k\nabla\rho_t, \nabla(\tilde{\theta}^h - \varphi)) \\ &= (k\nabla\rho_t, \nabla(\varphi - \theta_t)) + (b_t \cdot \nabla\rho + b \cdot \nabla\rho_t, \tilde{\theta}^h - \varphi). \end{aligned}$$

We have used (6.36) in the last equation since $(\tilde{\theta}^h - \varphi) \in S_h$. Thus we get that

$$m\|\nabla\rho_t\|^2 \leq M\|\nabla\rho_t\|\|\nabla(\varphi - \theta_t)\| + (C_1(b)\|\nabla\rho\| + C_2(b)\|\nabla\rho_t\|)\|\tilde{\theta}^h - \varphi\|.$$

Now, take $\varphi := I_h\theta_t$ to obtain:

$$\begin{aligned} m\|\nabla\rho_t\| &\leq M\|\nabla\rho_t\|Ch\|\theta_t\|_2 + (C_1(b)\|\nabla\rho\| + C_2(b)\|\nabla\rho_t\|)(\|\rho_t\| + Ch\|\theta_t\|_2) \\ &\leq \frac{m}{2}\|\nabla\rho_t\|^2 + Ch^2\|\theta_t\|_2^2 + Ch(\|\rho_t\| + Ch\|\theta_t\|_2) \\ &\quad + C_2(u)\|\nabla\rho_t\|\|\rho_t\| + C_2(u)Ch\|\nabla\rho_t\|\|\theta_t\|_2. \end{aligned}$$

Using Young's inequality a few times, it finally follows that:

$$\|\nabla\rho_t\|^2 \leq C_1 h^2 + C_2\|\rho_t\|^2, \tag{6.52}$$

where C_1 and C_2 are independent of h.

Now, we use the duality argument as in Lemma 6.4.4 to gain:

$$\begin{aligned} (\rho_t, \delta) &= (\rho_t, -\nabla \cdot (k\nabla\gamma - b\gamma)) = (k\nabla\rho_t, \nabla\gamma) - (b \cdot \nabla\rho_t, \gamma) \\ &= (k\nabla\rho_t, \nabla(\gamma - \varphi)) - (b \cdot \nabla\rho_t, \gamma - \varphi) + (k \cdot \nabla\rho_t, \nabla\varphi) - (b \cdot \nabla\rho_t, \varphi) \\ &= (k\nabla\rho_t, \nabla(\gamma - \varphi)) - (b \cdot \nabla\rho_t, \gamma - \varphi). \end{aligned}$$

Choosing $\varphi := I_h\gamma$ and $\delta := \rho_t$ yields

$$\begin{aligned}\|\rho_t\|^2 &\leq C_1\|\nabla\rho_t\|(Mh + \|b\|_\infty h^2)\|\gamma\|_2 \\ &\leq C_2\|\nabla\rho_t\|(Mh + \|b\|_\infty h^2)\|\delta\| \leq \\ &\leq C_2\|\nabla\rho_t\|(Mh + \|b\|_\infty h^2)\|\rho_t\|.\end{aligned}$$

We now see that

$$\|\rho_t\| \leq C(u,\theta)h\|\nabla\rho_t\|. \tag{6.53}$$

Combining (6.52) and (6.53) leads to convenient recurrence relations, thus proving the statement of the Lemma. □

Lemma 6.4.6. *Let $\tilde{\theta}^h$ be defined by (6.36). Then:*

$$\|\nabla\tilde{\theta}^h(t)\|_\infty \leq C(\theta) \qquad \text{for all } t \in I. \tag{6.54}$$

Proof. We rely now on the inverse estimate:

$$\|\nabla\varphi\|_\infty \leq Ch^{-1}\|\nabla\varphi\| \qquad \text{for all } \varphi \in S_h. \tag{6.55}$$

The statement (6.55) is trivial to prove for linear approximation functions, since in this case $\nabla\varphi$ is constant on each triangle. Using Lemma 6.4.5 and the known error estimate for $I_h\theta$, we have:

$$\begin{aligned}\|\nabla(\tilde{\theta}^h - I_h\theta)\|_\infty &\leq Ch^{-1}\|\nabla(\tilde{\theta}^h - I_h\theta)\| \\ &\leq Ch^{-1}(\|\nabla\rho\| + \|\nabla(I_h\theta - \theta)\|) \leq C(\theta).\end{aligned} \tag{6.56}$$

□

The main result on the *a priori* error control for the semi-discrete FEM approximation to our original system is given in the next Theorem.

Theorem 6.4.7. *Let (θ, u_i, v_i) solve (6.16)-(6.19) and (θ^h, u_i^h, v_i^h) solve (6.25)-(6.30), and let assumptions (A_1)-(A_2) hold. Then the following inequalities hold:*

$$\|\theta^h(t) - \theta(t)\| \leq C\|\theta^{0,h} - \theta^0\| + C(\theta)h^2 \qquad t \in I, \tag{6.57}$$

$$\|u_i^h(t) - u_i(t)\| \leq C\|u_i^{0,h} - u_i^0\| + C(u_i)h^2 \qquad t \in I, i \in \{1,\ldots,N\}. \tag{6.58}$$

Proof. With an error splitting as in (6.35), it is enough to show a suitable upper

bound for $\psi := \theta^h - \tilde{\theta}^h$. We proceed in the following manner:

$$\begin{aligned}
(\partial_t\psi,\varphi) + (\mathbb{K}\nabla\psi,\nabla\varphi) &= (\partial_t\theta^h,\varphi) + (\mathbb{K}\nabla\theta^h,\nabla\varphi) - \sum_{i=1}^{N}(\mathbb{T}_i\nabla^\delta u_i^h\cdot\theta^h,\varphi)\\
&+ \sum_{i=1}^{N}(\mathbb{T}_i\nabla^\delta u_i^h\cdot\theta^h,\varphi) - (\partial_t\tilde{\theta}^h,\varphi) - (\mathbb{K}\nabla\tilde{\theta}^h,\nabla\varphi)\\
&= -(\partial_t(\theta+\rho),\varphi) - (\mathbb{K}\nabla(\theta+\rho),\nabla\varphi) + \sum_{i=1}^{N}(\mathbb{T}_i\nabla^\delta u_i^h\cdot\theta^h,\varphi)\\
&= -(\partial_t\rho,\varphi) - (\mathbb{K}\nabla\rho,\nabla\varphi) + \sum_{i=1}^{N}(\mathbb{T}_i\nabla^\delta u_i\cdot\nabla\rho,\varphi)\\
&\quad + \sum_{i=1}^{N}(\mathbb{T}_i(\nabla^\delta u_i^h\cdot\nabla\theta^h - \nabla^\delta u_i\cdot\nabla\theta - \nabla^\delta u_i\cdot\nabla\rho),\varphi).
\end{aligned}$$

After eliminating the terms that vanish due to the definition of the elliptic projection, we obtain the following identity:

$$\begin{aligned}
&(\partial_t\psi,\varphi) + (\mathbb{K}\nabla\psi,\nabla\varphi)\\
&\quad = -(\partial_t\rho,\varphi) + \sum_{i=1}^{N}(\mathbb{T}_i(\nabla^\delta u_i^h\cdot\nabla\theta^h - \nabla^\delta u_i\cdot(\nabla\theta+\nabla\rho)),\varphi). \qquad (6.59)
\end{aligned}$$

We can deal with the second term on the right hand side of (6.59) as follows:

$$\begin{aligned}
&\nabla^\delta u_i^h\cdot\nabla\theta^h - \nabla^\delta u_i\cdot\nabla\theta - \nabla^\delta u_i\cdot\nabla\rho\\
&\quad = (\nabla^\delta u_i^h - \nabla^\delta u_i)\cdot\nabla\theta^h + \nabla^\delta u_i\cdot(\nabla\theta^h - \nabla\theta - \nabla\rho)\\
&\quad = (\nabla^\delta u_i^h - \nabla^\delta u_i)(\nabla\psi + \nabla\tilde{\theta}^h) + \nabla^\delta u_i\cdot\nabla\psi
\end{aligned}$$

Now using $\varphi := \psi$ as a test function and relying on the bound

$$\|\nabla\tilde{\theta}^h\|_\infty < C(\theta)$$

(available cf. Lemma 6.4.6), we obtain:

$$\begin{aligned}
&\frac{1}{2}\partial_t\|\psi\|^2 + m\|\nabla\psi\|^2 \le \frac{1}{2}\|\partial_t\rho\|^2 + \frac{1}{2}\|\psi\|^2\\
&\quad + \sum_{i=1}^{N}(C\|u_i^h - u_i\|^2 + \varepsilon\|\nabla\psi\|^2 + \varepsilon\|u_i\|_\infty(\|\nabla\rho\|^2 + \|\nabla\psi\|^2) + \|\psi\|^2).
\end{aligned}$$

Gronwall's inequality gives

$$\|\psi(t)\|^2 \le \|\psi(0)\|^2 + C\int_0^t(\|\partial_t\rho\|^2 + \|\nabla\rho\|^2 + \sum_{i=1}^{N}\|u_i^h - u_i\|^2).$$

The estimate

$$\|\psi(0)\| \leq \|\theta^{h,0} - \theta^0\| + \|\tilde{\theta}^h(0) - \theta^0\| \leq \|\theta^{h,0} - \theta^0\| + Ch^2\|\theta^0\|_2,$$

together with the estimate $\|u_i^h - u_i\| \leq C(u)h^2$ give the statement of the Theorem. □

6.5 Fully discrete error analysis

Let $\tau > 0$ to be a small enough time step and use $t_n := \tau n$ while denoting $\theta^n := \theta(t_n)$ and $u_i^n := u_i(t_n)$. The discrete in space approximations of θ^n and u_i^n are denoted as $\theta^{h,n}$ and $u_i^{h,n}$, respectively.

Definition 9. *The triplet $(\theta^{h,n}, u_i^{h,n}, v_i^{h,n})$ is a discrete solution to (6.5)-(6.13) if the following identities hold for all $n \in \{1, \ldots, N\}$ and $\varphi \in S_h$:*

$$\frac{1}{\tau}(\theta^{h,n+1} - \theta^{h,n}, \varphi) + (\mathbb{K}\nabla\theta^{h,n+1}, \nabla\varphi) - \sum_{i=1}^{N}(\mathbb{T}_i\nabla^\delta u_i^{h,n} \cdot \nabla\theta^{h,n+1}, \varphi) = 0, \tag{6.60}$$

$$\frac{1}{\tau}(u_i^{h,n+1} - u_i^{h,n}, \varphi) + (\mathbb{D}_i\nabla u_i^{h,n+1}, \nabla\varphi) - (\mathbb{F}_i\nabla^\delta\theta^{h,n} \cdot \nabla u_i^{h,n+1}, \varphi) + (A_i u_i^{h,n+1} - B_i v_i^{h,n+1}, \varphi) = (R_i(u^{h,n}), \varphi), \tag{6.61}$$

$$\frac{1}{\tau}(v_i^{h,n+1} - v_i^{h,n}, \varphi) = (A_i u_i^{h,n+1} - B_i v_i^{h,n+1}, \varphi), \tag{6.62}$$

$$\theta^{h,0} = \theta^{0,h}, \tag{6.63}$$

$$u_i^{h,0} = u_i^{0,h}, \tag{6.64}$$

$$v_i^{h,0} = v_i^{0,h}. \tag{6.65}$$

Here, $\theta^{0,h}$, $u_i^{0,h}$, and $v_i^{0,h}$ are the approximations of θ^0, u_i^0, and v_i^0 respectively in the finite dimensional space S_h.

Remark 6.5.1. *To treat (6.60) and (6.61), we use a semi-implicit discretization very much in the spirit of Ref. [74]. Note however that other options for the time discretization are possible.*

Lemma 6.5.2. (Consequence of Brouwer's fixed point theorem) *Given a mapping $G : S^h \to S^h$, such that:*

$$(G(\varphi), \varphi) > 0 \qquad \text{for } \|\varphi\| = q, \tag{6.66}$$

The equation $G(x) = 0$ has a solution $x \in B_q = \{\varphi \in S_h : \|\varphi\| \leq q\}$.

Proof. We follow along the lines of the proof of Theorem 13.1 from [121], see also [126, p. 52]. Assume that $G_h(\varphi) \neq 0$ in B_q. From this follows that the mapping $\Phi(\varphi) = \frac{-qG_h(\varphi)}{\|G_h(\varphi)\|} : B_q \to B_q$ is continuous. Therefore it has a fixed point $\psi \in B_q$ with $\|\psi\| = q$. But then

$$q^2 = \|\psi\|^2 = -\frac{(G(\psi), \psi)}{\|G(\psi)\|}. \tag{6.67}$$

Since the norm can't be negative, this contradicts the Lemma's assumption. □

Theorem 6.5.3. *Let assumptions* (A_1)-(A_2) *hold. Then there exists a solution* $(\theta^{h,n}, u_i^{h,n}, v_i^{h,n})$ *to (6.60)-(6.65).*

Proof. We will show the existence of solutions using the consequence of Brouwer's fixed point theorem in Lemma 6.5.2. Denoting $\varphi := (\varphi^\theta, \varphi_i^u, \varphi_i^v)$, we define the mapping $G_h : S_h \to S_h$ as:

$$\begin{aligned}(G_h(\varphi), \varphi) = &\underbrace{2(\varphi^\theta - \theta^{h,n}, \varphi^\theta)}_{I_1} + \underbrace{2\tau(\mathbb{K}\nabla\varphi^\theta, \nabla\varphi^\theta) - 2\tau\sum_{i=1}^{N}(\mathbb{T}_i\nabla^\delta u_i^{h,n} \cdot \nabla\varphi^\theta, \varphi^\theta)}_{I_2} \\ &+ \sum_{i=1}^{N}\Big[\underbrace{2(\varphi_i^u - u_i^{h,n}, \varphi_i^u)}_{I_1} + \underbrace{2\tau(\mathbb{D}_i\nabla\varphi_i^u, \nabla\varphi_i^u) - 2\tau(\mathbb{F}_i\nabla^\delta\theta^{h,n} \cdot \nabla\varphi_i^u, \varphi_i^u)}_{I_2} \\ &\quad + \underbrace{2\tau(A_i\varphi_i^u - B_i\varphi_i^v, \varphi_i^u) - 2\tau(A_i\varphi_i^u - B_i\varphi_i^v, \varphi_i^v)}_{I_3} - \underbrace{2\tau(R_i(u^{h,n}), \varphi_i^u)}_{I_4} \\ &\quad + \underbrace{2(\varphi_i^v - v^{h,n}, \varphi_i^v)}_{I_1}\Big]\end{aligned}$$

Since G_h was derived from (6.60)-(6.65), there exists a solution (θ^h, u_i^h, v_i^h) if $(G_h(\varphi), \varphi) = 0$ has a solution. We can use Lemma 6.5.2 for this. Essentially, we only need to show that there exists a $\varphi \in S_h$ such that $(G_h(\varphi), \varphi) > 0$. Below we give the estimates for the terms I_1, I_2, I_3, and I_4 that will give $(G_h(\varphi), \varphi) > 0$ when added together. The duplicate terms are omitted, since they can be treated

in the same way. We have:

$$
\begin{aligned}
I_1 &= 2(\varphi^\theta - \theta^{h,n}, \varphi^\theta) = 2\|\varphi^\theta\|^2 - \|\theta^{h,n}\|\|\varphi^\theta\| \geq \|\varphi^\theta\|^2 - \|\theta^{h,n}\|^2,\\
I_2 &= 2\tau(\mathbb{K}\nabla\varphi^\theta, \nabla\varphi^\theta) - 2\tau\sum_{i=1}^{N}(\mathbb{T}_i\nabla^\delta u_i^{h,n}\cdot\nabla\varphi^\theta, \varphi^\theta),\\
&\geq 2\tau(\mathbb{K}_0\|\nabla\varphi^\theta\|^2 - \mathbb{T}_{i,0}C^\delta\|u_i^{h,n}\|\|\nabla\varphi^\theta\|\|\varphi^\theta\|)\\
&\geq 2\tau((\mathbb{K}_0-\varepsilon)\|\nabla\varphi^\theta\|^2 - C^\varepsilon\|\varphi^\theta\|^2),\\
I_3 &= 2\tau(A_i\varphi_i^u - B_i\varphi_i^v, \varphi_i^u - \varphi_i^v)\\
&= 2\tau\Big[(A_i(\varphi_i^u-\varphi_i^v), \varphi_i^u-\varphi_i^v) - ((B_i-A_i)\varphi^v, \varphi^u) - ((A_i-B_i)\varphi^v, \varphi^v)\Big]\\
&\geq -2\tau\|A_i - B_i\|_\infty\left(\frac{1}{2}\|\varphi^u\|^2 + \frac{3}{2}\|\varphi^v\|^2\right),\\
I_4 &= -2\tau(R_i(u^{h,n}), \varphi_i^u) \geq \tau(2\|R_i(u^{h,n})\|^2 + \frac{1}{2}\|\varphi_i^u\|^2).
\end{aligned}
$$

Adding them together, provided $\tau > 0$ is small enough and $\|\varphi\| < \infty$ is large enough, we see that $(G_h(\varphi), \varphi) = I_1 + I_2 + I_3 + I_4 > 0$, which concludes the proof. □

Theorem 6.5.4. *Let assumptions* (A_1)*-*(A_2) *hold. Then there exists at most one solution* $(\theta^{h,n}, u_i^{h,n}, v_i^{h,n})$ *to (6.60)-(6.65).*

Proof. Let $x := (x^\theta, x_i^u, x_i^v)$ and $y := (y^\theta, y_i^u, y_i^v)$ be two solutions to (6.60)-(6.65) for a given $(\theta^{h,n}, u_i^{h,n}, v_i^{h,n})$. Substituting x and y into (6.60) and then subtracting leads to:

$$
\begin{aligned}
&(x^\theta - y^\theta, \varphi) + \tau(\mathbb{K}\nabla(x^\theta - y^\theta), \nabla\varphi)\\
&\qquad - \tau\sum_{i=1}^{N}(\mathbb{T}_i\nabla^\delta u_i^{h,n}\cdot\nabla(x^\theta - y^\theta), \varphi) = 0, \qquad \text{for all } \varphi \in S_h.
\end{aligned}
$$

Letting $\varphi := x^\theta - y^\theta$, we obtain

$$
\|x^\theta - y^\theta\|^2 + \tau\mathbb{K}_0\|\nabla(x^\theta - y^\theta)\|^2 \leq \tau(\sum_{i=1}^{N}\|\mathbb{T}_i\|_\infty C^\delta\|u_i^{h,n}\|)\|\nabla(x^\theta - y^\theta)\|\|x^\theta - y^\theta\|
$$

Now, using Young's inequality results in

$$
\|x^\theta - y^\theta\|^2 + \tau(\mathbb{K}_0 - \eta)\|\nabla(x^\theta - y^\theta)\|^2 \leq \tau C^\eta\|x^\theta - y^\theta\|^2
$$

We choose τ such that $\tau C^\eta < 1$, with $\eta < \mathbb{K}_0$, and hence we get $\|x^\theta - y^\theta\| = 0$.

The facts that $\|x_i^u - y_i^u\| = 0$ and $\|x_i^v - y_i^v\| = 0$ can be shown in a similar way. □

Theorem 6.5.5. *Let (θ, u_i, v_i) solve (6.16)-(6.19) and (θ^h, u_i^h, v_i^h) solve (6.60)-(6.65), and assumptions (A_1)-(A_2) hold. Then the following inequality holds:*

$$\begin{aligned}\|\theta^{h,n}-\theta^n\|+\sum_{i=1}^N\|u_i^{h,n}-u_i^n\|+\sum_{i=1}^N\|v_i^{h,n}-v_i^n\|\\ \le C_1\|\theta^{h,0}-\theta^0\|+C_2\sum_{i=1}^N\|u_i^{h,0}-u_i^0\|+C_3\sum_{i=1}^N\|v_i^{h,0}-v_i^0\|\\ +C_4(h^2+\tau).\end{aligned}\tag{6.68}$$

The constants $C_1,\dots,C_4$ entering (6.68) depend on controllable norms of θ, u_i, but are independent of h and τ.

Proof. Similar with the methodology of the proof of the semidiscrete *a priori* error estimates, we split the error terms into two parts:

$$\theta^{h,n}-\theta^n=\rho^{\theta,n}+\psi^{\theta,n}:=(\theta^{h,n}-R_h\theta^n)+(R_h\theta^n-\theta^n),\tag{6.69}$$

$$u_i^{h,n}-u_i^n=\rho^{u_i,n}+\psi^{u_i,n}:=(u_i^{h,n}-R_hu_i^n)+(R_hu_i^n-u_i^n),\tag{6.70}$$

where $R_h\theta$ and R_hu_i are the Ritz projections defined by:

$$(\mathbb{K}\nabla(R_h\theta-\theta),\nabla\varphi)=0,\qquad\forall\varphi\in S_h,\tag{6.71}$$

$$(\mathbb{D}_i\nabla(R_hu_i-u_i),\nabla\varphi)=0,\qquad\forall\varphi\in S_h, i\in\{1,\dots,N\}.\tag{6.72}$$

Here, $\psi^{\theta,n}$ and $\psi^{u_i,n}$ satisfy the following bounds:

$$\|\psi^{\theta,n}\|\le Ch^2\|\theta^n\|_2,\tag{6.73}$$

$$\|\psi^{u_i,n}\|\le Ch^2\|u_i^n\|_2,\tag{6.74}$$

so it remains to bound from above $\rho^{\theta,n}$ and $\rho^{u_i,n}$. We can write for $\rho^{\theta,n}$ the following identities:

$$\begin{aligned}\frac{1}{\tau}(\rho^{\theta,n+1}-\rho^{\theta,n},\varphi)+(\mathbb{K}\nabla\rho^{\theta,n+1},\nabla\varphi)&=\frac{1}{\tau}(\theta^{h,n+1}-\theta^{h,n},\varphi)+(\mathbb{K}\nabla\theta^{h,n+1},\nabla\varphi)\\ &-\sum_{i=1}^N(\mathbb{T}_i\nabla^\delta u_i^{h,n}\cdot\nabla\theta^{h,n+1},\varphi)+\sum_{i=1}^N(\mathbb{T}_i\nabla^\delta u_i^{h,n}\cdot\nabla\theta^{h,n+1},\varphi)\\ &-\frac{1}{\tau}(R_h\theta^{n+1}-R_h\theta^n,\varphi)-(\mathbb{K}\nabla R_h\theta^{n+1},\nabla\varphi)\\ &=\sum_{i=1}^N(\mathbb{T}_i\nabla^\delta u_i^{h,n}\cdot\nabla\theta^{h,n+1},\varphi)-\frac{1}{\tau}(R_h\theta^{n+1}-R_h\theta^n,\varphi)-(\mathbb{K}\nabla\theta^{n+1},\nabla\varphi)\\ &=\sum_{i=1}^N(\mathbb{T}_i\nabla^\delta u_i^{h,n}\cdot\nabla\theta^{h,n+1},\varphi)-\frac{1}{\tau}(R_h\theta^{n+1}-R_h\theta^n,\varphi)\\ &+(\partial_t\theta^{n+1},\varphi)-\sum_{i=1}^N(\mathbb{T}_i\nabla^\delta u_i^{n+1}\cdot\nabla\theta^{n+1},\varphi).\end{aligned}$$

After re-arranging the terms in the former expression, we obtain:

$$\begin{aligned}
&\frac{1}{\tau}(\rho^{\theta,n+1}-\rho^{\theta,n},\varphi)+(\mathbb{K}\nabla\rho^{\theta,n+1},\nabla\varphi)\\
&\quad=\underbrace{\sum_{i=1}^{N}(T_i(\nabla^\delta u_i^{h,n}\cdot\nabla\theta^{h,n+1}-\nabla^\delta u_i^{n+1}\cdot\nabla\theta^{n+1}),\varphi)}_{A}\\
&\qquad+\underbrace{(\partial_t\theta^{n+1}-\frac{1}{\tau}(\theta^{n+1}-\theta^n),\varphi)}_{B}-\underbrace{\frac{1}{\tau}(\psi^{\theta,n+1}-\psi^{\theta,n},\varphi)}_{C}.
\end{aligned}$$

Let us deal first with estimating the term C, then B, and finally, the term A.

To estimate the term C, we use our semidiscrete estimate for $\|\partial_t\psi\|$ stated in Lemma 6.4.5, we get:

$$\|\frac{1}{\tau}(\psi^{\theta,n+1}-\psi^{\theta,n})\|=\|\frac{1}{\tau}\int_{t^n}^{t^{n+1}}\partial_t\psi^\theta\|\leq C_C(\theta,u)h^2.$$

The term B can be estimated as follows:

$$B=(\frac{1}{\tau}\int_{t^n}^{t^{n+1}}(s-t^n)\partial_{tt}\theta(s)ds,\varphi)\leq\frac{\tau}{2}(\sup_{[t^n,t^{n+1}]}|\partial_{tt}\theta|)\|\varphi\|=C_B(\theta)\tau\|\varphi\|.$$

Finally, to tackle the term A, we proceed as follows:

$$\begin{aligned}
A&=(\nabla^\delta u_i^{h,n}\cdot\nabla\theta^{h,n+1}-\nabla^\delta u_i^{n+1}\cdot\nabla\theta^{n+1},\varphi)\\
&=(\nabla^\delta u_i^{h,n}\cdot(\nabla\theta^{h,n+1}-\nabla\theta^{n+1})+\nabla\theta^{n+1}\cdot(\nabla^\delta u_i^{h,n}-\nabla^\delta u_i^{n+1}),\varphi)\\
&\leq\varepsilon\|u_i^{h,n}\|_\infty(\|\nabla\rho^{n+1}\|^2+\|\nabla\psi^{n+1}\|^2)+C_\varepsilon\|\varphi\|^2\\
&\quad+\underbrace{(\nabla\theta^{n+1}\cdot(\nabla^\delta u_i^{h,n}-\nabla^\delta u_i^{n+1}),\varphi)}_{D}.
\end{aligned}$$

At its turn, the term D can be expressed as:

$$\begin{aligned}
D&=(\nabla\theta^{n+1}\cdot(\nabla^\delta u_i^{h,n}-\nabla^\delta u_i^n),\varphi)+(\nabla\theta^{n+1}\cdot(\nabla^\delta u_i^n-\nabla^\delta u_i^{n+1}),\varphi)\\
&\leq\|\nabla\theta^{n+1}\|_\infty(\varepsilon\|\nabla^\delta(u_i^{h,n}-u_i^n)\|^2+C_\varepsilon\|\varphi\|^2)+\underbrace{(\nabla\theta^{n+1}\cdot\int_{t^n}^{t^{n+1}}\partial_t\nabla^\delta u_i,\varphi)}_{E}.
\end{aligned}$$

Finally, the term E can be estimated as:

$$E\leq\|\nabla\theta^{n+1}\|_\infty\|\partial_t\nabla^\delta u_i\|_\infty\tau\|\varphi\|.$$

Adding together all the terms, and then substituting $\varphi := \rho^{\theta,n+1}$ we finally obtain:

$$\begin{aligned}\frac{1}{\tau}\|\rho^{\theta,n+1}\|^2 + m\|\nabla\rho^{\theta,n+1}\|^2 &\leq \frac{1}{\tau}\|\rho^{\theta,n}\|^2 + (C_B(\theta)\tau)^2 \\ &+ (C_C(\theta)h^2)^2 + \varepsilon\|u_i^{h,n}\|_\infty(\|\nabla\rho^{\theta,n+1}\|^2 + \|\nabla\psi^{n+1}\|^2) \\ &+ C_D\varepsilon\|\nabla^\delta(u_i^{h,n} - u_i^n)\|^2 + (C_E(u,\theta)\tau)^2 + C\|\rho^{\theta,n+1}\|^2 \\ &:= C\|\rho^{\theta,n+1}\|^2 + R_n, \end{aligned} \tag{6.75}$$

where the reminder R_n is defined by:

$$\begin{aligned}R_n := \frac{1}{\tau}\|\rho^{\theta,n}\|^2 + (C_B(\theta)\tau)^2 + (C_C(\theta)h^2)^2 + \varepsilon\|u_i^{h,n}\|_\infty(\|\nabla\rho^{\theta,n+1}\|^2 + \|\nabla\psi^{n+1}\|^2) \\ + C_D\varepsilon\|\nabla^\delta(u_i^{h,n} - u_i^n)\|^2 + (C_E(u,\theta)\tau)^2\end{aligned}$$

For R_n it holds:

$$R_n \leq C(\theta,u)(h^2+\tau)^2.$$

Note that we can derive a similar estimate for $\rho^{u_i,n+1}$, which we then add to (6.75).

To conclude, we denote

$$e^n := \|\rho^{\theta,n}\|^2 + \sum_{i=1}^{N}\|\rho^{u_i,n}\|^2,$$

to obtain the short structure

$$\frac{1}{\tau}e^{n+1} \leq \frac{1}{\tau}e^n + C(e^{n+1} + R_n).$$

From here it follows that:

$$(1 - C\tau)e^{n+1} \leq e^n + C\tau R_n.$$

For sufficiently small τ, we can instead write the expression

$$e^{n+1} \leq (1 + C\tau)e^n + C\tau R_n.$$

Iterating the later inequality, we obtain

$$e^{n+1} \leq (1 + C\tau)^{n+1}e^0 + C\tau\sum_{j=1}^{n} R_j.$$

Finally, this argument yields

$$e^{n+1} \leq C\|\theta^{h,0} - \theta^0\| + C\|u_i^{h,0} - u_i^0\| + C(\theta,u)(h^2+\tau),$$

which proves the Theorem 6.5.5. □

Chapter 7

Conclusions and Open Issues

7.1 Conclusions

In this thesis, we used multiscale reaction-diffusion systems with Smoluchowski production terms to describe the transport of colloids in porous media (consisting of arrays of periodically distributed microstructures). We focus here on the aggregation-fragmentation mechanism that enables us to differentiate between the populations of aggregates of different sizes, instead of just considering the whole of the colloidal mass as a single species. This modeling strategy allows us to assign different properties to each species that depend on the size of that species, such as the diffusion coefficient, the Soret and Dufour coefficients, as well as the deposition rates. Our study goes in a threefold direction:

(i) Modeling of the aggregation, fragmentation, deposition, and transport of colloids in porous media;

(ii) Multiscale mathematical analysis;

(iii) Multiscale simulation.

We developed a multiscale methodology that allowed us to proceed towards comparison with experiments. Our reaction-diffusion system contains information from two spatial scales (microscopic and macroscopic). We are interested primarily in the concentration profiles at the macroscopic scale. To obtain this information, we solve cell problems on the microscopic scale, incorporating the effects of the porous medium geometry into the effective coefficients of the macroscopic problem.

The models we discussed in the thesis incorporate the following important mechanisms:

- non-equilibrium exchange between populations of aggregates of different sizes;
- deposition of the colloids onto the porous matrix;
- advection of the colloids and heat due to Soret and Dufour effects (coupled flows).

We modeled the aggregation mechanism using the Smoluchowski population balance equations. This strategy leads to a coupled semilinear reaction-diffusion system in a spatially heterogeneous domain. The spatial heterogeneities as well as the population balance heterogeneities make the computational effort required to solve the full problem too expensive. To make our problem computationally tractable, we employ two different kinds of averaging techniques:

- Periodic homogenization allows to deal with the spatially oscillating coefficients;
- Lumping aggregates into size clusters allows us to treat a great range of sizes with relatively few species, while conserving chosen quantities, such as mass, consistently throughout the discretization method.

We dealt with the following mathematical issues:

1. Formal derivation of a transport model withing a periodic domain, including aggregation and deposition;
2. Well-posedness of the aggregation-deposition model in the presence of thermal fluxes (the thermo-diffusion problem);
3. Rigorous derivation of the upscaling of the thermo-diffusion problem;
4. Semi-discrete and fully-discrete *a priori* error estimates for the FEM discretization of the thermo-diffusion problem.

For our thermo-diffusion transport problem, we ensured the positivity and $L^\infty-$ bounds for the concentrations of mobile and immobile species, as well as for heat content and temperature. We then proved the global in time existence and uniqueness of positive and bounded solutions to this problem. In the proof we used the Galerkin approach for each sub-problem separately and then, thanks to the Banach fixed-point theorem, we did unite the sub-problems.

Efficient 2D/3D solvers were implemented in C++, extending the deal.II and DUNE numerics libraries to cope with the special structure of our model equations [27]. Newton method is used to handle the nonlinear terms in the system. Backward Euler and BDF methods are used for time discretization. Operator splitting is optionally used to decouple the transport part of the problem from the reaction part. In that case, the CVODE library from the SUNDIALS package is used to handle the resulting stiff system of ODEs.

The simulation results compare well with the breakthrough curves measured in [61] and [60]. Our model is quite complex, featuring more species and parameters than standard models for colloidal transport, so more detailed measurements are needed to fit and use the power all the available parameters and model components.

7.2 Open issues

There are a few modeling and mathematical issues that need further investigation.

7.2.1 Open issues at the modeling level

- The deposition of the colloids onto the boundary of the porous matrix typically leads to the growth of the matrix grains, and ultimately pores clogging. The foundation for this has been set up with our modeling of the aggregation terms, since it is the larger species of aggregates that will cause pore clogging and will feel its effects the most. The current mathematical analysis and upscaling techniques need then to be extended to include x-dependent microstructures (and hence x-dependent Bochner spaces) and averaging of non-periodic microstructures.

- The aggregation of colloids is heavily influenced by the chemical composition of the medium. The influence of the double layer repulsion and van der Waals attraction has been implemented as part of the code according to the DLVO theory. Some additional extensions such as steric interactions could be added, since they are not covered by the DLVO theory.

- The presence of colloids has an influence on the viscosity of the fluid that they are suspended in. It would be interesting to couple our system to the Navier-Stokes system, accounting for a colloids-dependent flow.

7.2.2 Open issues at the mathematical level

- It is hard to prove the well-posedness of the thermo-diffusion problem without using a mollifier. Nevertheless, it may be possible to achieve this in 1D.

- Corrector estimates for the upscaling of the thermo-diffusion problem need to be proven to be able to design convergent MsFEM schemes to capture efficiently the effects of the multiscale geometry.

- Rigorous mathematical analysis of the operator-splitting scheme applied to thermo-diffusion system is for the moment an open problem.

- Dealing in a consistent mathematical way with free-boundary formulations of spatial and temporal changes of the pore surfaces is currently out of reach. However, we believe that the approach by Lacey [73] and later by Nikolopoulos [97] would potentially be able to derive a macroscopic model that accounts for the porosity changes at the pore level.

List of Tables

List of Figures

Bibliography

[1] G. Allaire. "Homogenization and two-scale convergence". In: *SIAM Journal on Mathematical Analysis* 23.6 (1992), pp. 1482–1518.

[2] H. Amann. *Ordinary Differential Equations: An Introduction to Nonlinear Analysis*. De Gruyter Studies in Mathematics. de Gruyter, 1990.

[3] J. Andersson, J. Rosenholm, S. Areva, and M. Lindén. "Influences of material characteristics on ibuprofen drug loading and release profiles from ordered micro-and mesoporous silica matrices". In: *Chemistry of Materials* 16.21 (2004), pp. 4160–4167.

[4] B. Andreianov, M. Bendahmane, and R. Ruiz-Baier. "Analysis of a finite volume method for a cross-diffusion model in population dynamics". In: *Mathematical Models and Methods in Applied Sciences* 21.02 (2011), pp. 307–344.

[5] W. Bangerth, T. Heister, L. Heltai, G. Kanschat, M. Kronbichler, M. Maier, B. Turcksin, and T. D. Young. "The `deal.II` Library, Version 8.1". In: *arXiv preprint* `http://arxiv.org/abs/1312.2266v4` (2013).

[6] W. Bangerth and O. Kayser-Herold. "Data Structures and Requirements for hp Finite Element Software". In: *ACM Trans. Math. Softw.* 36.1 (2009), pp. 4/1–4/31.

[7] P. Bastian, M. Blatt, A. Dedner, C. Engwer, R. Klöfkorn, R. Kornhuber, M. Ohlberger, and O. Sander. "A generic grid interface for parallel and adaptive scientific computing. Part II: Implementation and tests in DUNE". In: *Computing* 82.2-3 (2008), pp. 121–138.

[8] R. Batterham, J. Hall, and G. Barton. "Pelletizing kinetics and simulation of full scale balling circuits". In: *Proceedings of the 3rd International Symposium on Agglomeration*. Vol. 136. 1981.

[9] R. Battino and H. L. Clever. "The solubility of gases in liquids". In: *Chemical Reviews* 66.4 (1966), pp. 395–463.

[10] J. Bear. *Dynamics of Fluids in Porous Media*. Dover, 1972.

[11] M. Beneš and R. Štefan. "Global weak solutions for coupled transport processes in concrete walls at high temperatures". In: *ZAMM – Zeitschrift für Angewandte Mathematik und Mechanik* 93.4 (2013), pp. 233–251.

[12] M. Beneš, R. Štefan, and J. Zeman. "Analysis of coupled transport phenomena in concrete at elevated temperatures". In: *Applied Mathematics and Computation* 219.13 (2013), pp. 7262–7274.

[13] A. Bensoussan, J.-L. Lions, and G. Papanicolaou. *Asymptotic Analysis for Periodic Structures*. Vol. 374. American Mathematical Soc., 2011.

[14] D. Bothe and W. Dreyer. *Continuum thermodynamics of chemically reacting mixtures*. Tech. rep. WIAS No. 1909. Berlin, Germany: Weierstraß-Institut, 2013.

[15] S. Boyaval. "Reduced-basis approach for homogenization beyond the periodic setting". In: *Multiscale Modeling and Simulation* 7.1 (2008), pp. 466–494.

[16] S. C. Brenner and R. Scott. *The Mathematical Theory of Finite Element Methods*. Vol. 15. Springer, 1994.

[17] C. L. Bris, F. Legoll, and A. Lozinski. "An MsFEM type approach for perforated domains". In: *arXiv preprint arXiv:1307.0876* (2013).

[18] C. C. Camejo, R. Gröpler, and G. Warnecke. "Existence and uniqueness of solutions to the coagulation equations with singular kernel". In: *arXiv preprint arXiv:1210.1500* (2012).

[19] T. Camp and P. Stein. "Velocity gradients and internal work in fluid motion". In: *Journal of the Boston Society of Civil Engineers* 85 (1943), pp. 219–37.

[20] A. Chavarria-Krauser and M. Ptashnyk. "Homogenization of long-range auxin transport in plant tissues". In: *Nonlinear Analysis: Real World Applications* 11.6 (2010), pp. 4524 –4532.

[21] G. A. Chechkin, A. L. Piatnitki, and A. S. Shamaev. *Homogenization: Methods and Applications*. Vol. 234. Translations of mathematical monographs. American Mathematical Society, 2007. ISBN: 9780821838730.

[22] O. Chepizhko, E. Altmann, and F. Peruani. "Collective motion in heterogeneous media". In: *Phys. Rev. Lett.* 2013 (2013), to appear.

[23] P. G. Ciarlet. *The Finite Element Method for Elliptic Problems*. Elsevier, 1978.

[24] D. Cioranescu and J. S. J. Paulin. *Homogenization of Reticulated Structures*. Springer, 1999.

[25] E. N. Cirillo and A. Muntean. "Dynamics of pedestrians in regions with no visibility: A lattice model without exclusion". In: *Physica A: Statistical Mechanics and its Applications* 392.17 (2013), pp. 3578–3588.

[26] P. Curşeu, O. Krehel, J. Evers, and A. Muntean. "Cognitive Distance, Absorptive Capacity and Group Rationality: A Simulation Study". In: *PloS One* (2014).

[27] *deal.II Authors*. `http://dealii.org/authors.html`.

[28] B. Derjaguin and L. Landau. "A theory of the stability of strongly charged lyophobic sols and the coalescence of strongly charged particles in electrolytic solution". In: *Acta Phys.-Chim. USSR* 14 (1941), pp. 633–662.

[29] C. Eck, B. Jadamba, and P. Knabner. "Error estimates for a finite element discretization of a phase field model for mixtures". In: *SIAM Journal on Numerical Analysis* 47.6 (2010), pp. 4429–4445.

[30] J. T. Edward. "Molecular volumes and the Stokes-Einstein equation". In: *Journal of Chemical Education* 47.4 (1970), p. 261.

[31] M. Elimelech, J. Gregory, X. Jia, and R. Williams. *Particle Deposition and Aggregation: Measurement, Modelling and Simulation*. Elsevier, 1998.

[32] L. Evans. *Partial Differential Equations*. Vol. 19. Graduate Studies in Mathematics. American Mathematical Society, 1998. ISBN: 0821807722.

[33] J. H. M. Evers and A. Muntean. "Modeling micro-macro pedestrian counterflow in heterogeneous domains". In: *Nonlinear Phenomena in Complex Systems* 14.1 (2011), pp. 27–37.

[34] T. Fatima, N. Arab, E. Zemskov, and A. Muntean. "Homogenization of a reaction–diffusion system modeling sulfate corrosion of concrete in locally periodic perforated domains". In: *Journal of Engineering Mathematics* 69.2-3 (2011), pp. 261–276.

[35] T. Fatima. "Multiscale Reaction-Diffusion Systems Describing Concrete Corrosion: Modeling and Analysis". PhD thesis. TU Eindhoven, 2013.

[36] T. Fatima and A. Muntean. "Sulfate attack in sewer pipes: derivation of a concrete corrosion model via two-scale convergence". In: *Nonlinear Analysis: Real World Applications* 15 (2014), pp. 326–344.

[37] D. Florea. "Mechanics and Dynamics in Colloidal Systems with Complex Interactions". PhD thesis. TU Eindhoven, 2014.

[38] F. Frank. "Numerical Studies of Models for Electrokinetic Flow and Charged Solute Transport in Periodic Porous Media". PhD thesis. University of Erlangen-Nuremberg, 2013.

[39] S. K. Friedlander. *Smoke, Dust and Haze: Fundamentals of Aerosol Behavior*. Vol. 198. Oxford University Press New York, 2000.

[40] N. Fuchs. "Über die Stabilität und Aufladung der Aerosole". In: *Zeitschrift für Physik A Hadrons and Nuclei* 89.11 (1934), pp. 736–743.

[41] T. Funaki, H. Izuhara, M. Mimura, and C. Urabe. "A link between microscopic and macroscopic models of self-organized aggregation." In: *Networks and Heterogeneous Media* 7.4 (2012), pp. 705–740.

[42] G. Galiano, M. L. Garzon, and A. Jüngel. "Analysis and numerical solution of a nonlinear cross-diffusion system arising in population dynamics". In: *Konstanzer Schriften in Mathematik und Informatik* 134 (2000).

[43] R. Golestanian. "Collective behavior of thermally active colloids". In: *Physical Review Letters* 108.3 (2012), p. 038303.

[44] Z.-X. Gong and A. S. Mujumdar. "Development of drying schedules for one-side-heating drying of refractory concrete slabs based on a finite element model". In: *Journal of the American Ceramic Society* 79.6 (1996), pp. 1649–1658.

[45] P. Grisvard. *Elliptic Problems in Nonsmooth Domains*. Vol. 69. SIAM, 2011.

[46] S. de Groot and P. Mazur. *Non-equilibrium Thermodynamics*. Series in physics. North-Holland Publishing Company - Amsterdam, 1962.

[47] S. Grosskinsky, C. Klingenberg, and K Oelschla¨ ger. "A rigorous derivation of Smoluchowski's equation in the moderate limit". In: *Stochastic analysis and applications* 22.1 (2004), pp. 113–141.

[48] M. Z. Guo, G. C. Papanicolaou, and S. R. S. Varadhan. "Nonlinear diffusion limit for a system with nearest neighbor interactions". In: *Comm. Math. Phys.* 118.1 (1988), pp. 31–59.

[49] P. Guo. "Dependency of tortuosity and permeability of porous media on directional distribution of pore voids". In: *Transport in porous media* 95.2 (2012), pp. 285–303.

[50] H. Hamaker. "The London - van der Waals attraction between spherical particles". In: *Physica* 4.10 (1937), pp. 1058–1072.

[51] M. Herberg, M. Meyries, J. Prüss, and M. Wilke. "Reaction-diffusion systems of Maxwell-Stefan type with reversible mass-action kinetics". In: *arXiv:1310.4723* (2013).

[52] M. Hertz and P. Knabner. *Including van der Waals forces in diffusion-convection equations - modeling, analysis, and numerical simulations*. Tech. rep. No. 373. Erlangen: Institute for Applied Mathematics, 2013.

[53] G. Hidy and J. Brock. *The Dynamics of Aerocolloidal Systems*. Vol. 1. Pergamon, 1970.

[54] U. Hornung. *Homogenization and Porous Media*. Springer, 1997.

[55] U. Hornung and W. Jäger. "Diffusion, convection, adsorption, and reaction of chemicals in porous media". In: *Journal of Differential Equations* 92.2 (1991), pp. 199–225.

[56] T. Hou, X. H. Wu, and Z. Cai. "Convergence of a multiscale finite element method for elliptic problems with rapidly oscillating coefficients". In: *Mathematics of Computation* 68.227 (1999), pp. 913–943.

[57] M. Hounslow, R. Ryall, and V. Marshall. "A discretized population balance for nucleation, growth, and aggregation". In: *AIChE Journal* 34.11 (1988), pp. 1821–1832.

[58] R. Hunter. "Foundations of Colloid Science". In: *Oxford New York* 2 (1989), pp. 31–32.

[59] E. Ijioma. "Homogenization approach to filtration combustion of reactive porous materials: modelling, simulation, analysis". PhD thesis. Tokyo, Japan: University of Meiji, 2014.

[60] P. R. Johnson and M. Elimelech. "Dynamics of colloid deposition in porous media: Blocking based on random sequential adsorption". In: *Langmuir* 11.3 (1995), pp. 801–812.

[61] P. R. Johnson, N. Sun, and M. Elimelech. "Colloid transport in geochemically heterogeneous porous media: Modeling and measurements". In: *Environ. Sci. Techn.* 30.11 (1996), pp. 3284–3293.

[62] A. Jüngel and I. Stelzer. "Existence analysis of Maxwell–Stefan systems for multicomponent mixtures". In: *SIAM Journal on Mathematical Analysis* 45.4 (2013), pp. 2421–2440.

[63] J. Kačur. *Method of Rothe in Evolution Equations*. Springer, 1986.

[64] P. Kapur. "Self-preserving size spectra of comminuted particles". In: *Chemical Engineering Science* 27.2 (1972), pp. 425–431.

[65] P. Knabner, K. Totsche, and I. Kögel-Knabner. "The modeling of reactive solute transport with sorption to mobile and immobile sorbents: 1. Experimental evidence and model development". In: *Water Resources Research* 32.6 (1996), pp. 1611–1622.

[66] P. Knabner and L. Angermann. *Numerical Methods for Elliptic and Parabolic Partial Differential Equations*. Springer, 2003.

[67] P. A. Korevaar, S. J. George, A. J. Markvoort, M. M. Smulders, P. A. Hilbers, A. P. Schenning, T. F. De Greef, and E. Meijer. "Pathway complexity in supramolecular polymerization". In: *Nature* 481.7382 (2012), pp. 492–496.

[68] O. Krehel, A. Muntean, and P. Knabner. *On modeling and simulation of flocculation in porous media*. In A.J. Valochi (Ed.), Proceedings of XIX International Conference on Water Resources. (pp. 1-8) CMWR. University of Illinois at Urbana-Champaign, 2012.

[69] O. Krehel, A. Muntean, and T. Aiki. *A thermo-diffusion system with Smoluchowski interactions: well-posedness and homogenization*. Tech. rep. No. 14-09. Eindhoven: CASA Report, 2014.

[70] O. Krehel, A. Muntean, and P. Knabner. *Multiscale modeling of colloidal dynamics in porous media including aggregation and deposition*. Tech. rep. No. 14-12. Eindhoven: CASA Report, 2014. arXiv: `1404.4207`.

[71] K. Kumar, I. Pop, and F. Radu. "Convergence analysis for a conformal discretization of a model for precipitation and dissolution in porous media". In: *Numerische Mathematik* (2013), pp. 1–35.

[72] S. Kumar and D. Ramkrishna. "On the solution of population balance equations by discretization–I. A fixed pivot technique". In: *Chemical Engineering Science* 51.8 (1996), pp. 1311–1332.

[73] A. Lacey and L. Herraiz. "Macroscopic models for melting derived from averaging microscopic Stefan problems I: simple geometries with kinetic undercooling or surface tension". In: *European Journal of Applied Mathematics* 11.02 (2000), pp. 153–169.

[74] O. Lakkis, A. Madzvamuse, and C. Venkataraman. "Implicit–explicit timestepping with finite element approximation of reaction–diffusion systems on evolving domains". In: *SIAM Journal on Numerical Analysis* 51.4 (2013), pp. 2309–2330.

[75] I. Langmuir. "The adsorption of gases on plane surfaces of glass, mica and platinum." In: *Journal of the American Chemical society* 40.9 (1918), pp. 1361–1403.

[76] C. Le Bris, F. Legoll, and F. Thomines. "Multiscale Finite Element approach for weakly random problems and related issues". In: *M2AN* (to appear) (2014).

[77] J. Lions. *Quelques méthodes de résolution des problèmes aux limites non linèaires*. Dunod, Paris, 1969.

[78] B. van Lith, S. Storm, and A. Muntean. "A continuum model for hierarchical fibril assembly". In: *Europhysics Letters* (2014).

[79] D. Liu, P. R. Johnson, and M. Elimelech. "Colloid deposition dynamics in flow-through porous media: Role of electrolyte concentration". In: *Environ. Sci. Techn.* 29.12 (1995), pp. 2963–2973.

[80] J. Lyklema. *Fundamentals of Interface and Colloid Science*. Academic Press, 2005.

[81] V. A. Marchenko and E. Y. Kruslov. *Homogenization of Partial Differential Equations*. Birkhäuser, 2006.

[82] A. Marciniak-Czochra and M. Ptashnyk. "Derivation of a macroscopic receptor-based model using homogenization techniques". In: *SIAM Journal on Mathematical Analysis* 40.1 (2008), pp. 215–237.

[83] N. Masmoudi and M. L. Tayeb. "Diffusion limit of a semiconductor Boltzmann-Poisson system". In: *SIAM Journal on Mathematical Analysis* 38.6 (2007), pp. 1788–1807.

[84] G. Matthess, A. Pekdeger, and J. Schroeter. "Persistence and transport of bacteria and viruses in groundwatera conceptual evaluation". In: *Journal of Contaminant Hydrology* 2.2 (1988), pp. 171–188.

[85] P. Meakin. "Fractal aggregates". In: *Adv. Colloid Interface Sci.* 28 (1987), pp. 249–331.

[86] C. C. Mei and B. Vernescu. *Homogenization Methods for Multiscale Mechanics*. World Scientific, 2010.

[87] I. Metzmacher, F. Radu, M. Bause, P. Knabner, and W. Friess. "A model describing the effect of enzymatic degradation on drug release from collagen minirods". In: *European Journal of Pharmaceutics and Biopharmaceutics* 67.2 (2007), pp. 349–360.

[88] S. G. Michlin. *Konstanten in einigen Ungleichungen der Analysis*. Vol. 35. Teubner-Texte zur Mathematik, 1981.

[89] K. Milinković, J. T. Padding, and M. Dijkstra. "Hydrodynamic Rayleigh-Taylor-like instabilities in sedimenting colloidal mixtures". In: *Soft Matter* 7.23 (2011), pp. 11177–11186.

[90] A. Muntean, E. N. M. Cirillo, O. Krehel, and M. Böhm. "Pedestrians moving in dark: Balancing measures and playing games on lattices". In: *Collective Dynamics from Bacteria to Crowds: An Excursion Through Modeling, Analysis and Simulation*. Ed. by A. Muntean and F. Toschi. Vol. 553. CISM Courses and Lectures. Berlin: Springer Verlag, 2014, pp. 75–104.

[91] A. Muntean and M. Neuss-Radu. "A multiscale Galerkin approach for a class of nonlinear coupled reaction–diffusion systems in complex media". In: *Journal of Mathematical Analysis and Applications* 371.2 (2010), pp. 705–718.

[92] A. Muntean and T. Van Noorden. "Corrector estimates for the homogenization of a locally periodic medium with areas of low and high diffusivity". In: *European Journal of Applied Mathematics* 24.05 (2013), pp. 657–677.

[93] H. Murakawa. "A linear scheme to approximate nonlinear cross-diffusion systems". In: *ESAIM: Mathematical Modelling and Numerical Analysis* 45 (06 2011), pp. 1141–1161.

[94] M. Neuss-Radu. "Some extensions of two-scale convergence". In: *Comptes Rendus de l'Académie des Sciences. Série 1, Mathématique* 322.9 (1996), pp. 899–904.

[95] G. Nguetseng. "A general convergence result for a functional related to the theory of homogenization". In: *SIAM Journal on Mathematical Analysis* 20.3 (1989), pp. 608–623.

[96] W.-M. Ni. "Diffusion, cross-diffusion, and their spike-layer steady states". In: *Notices of the AMS* 45.1 (1998), pp. 9–18.

[97] C. Nikolopoulos. "A model for melting of an inhomogeneous material during modulated temperature differential scanning calorimetry". In: *Applied Mathematical Modelling* 28.5 (2004), pp. 427–444.

[98] L. Nirenberg. "On elliptic partial differential equations". In: *Ann. Scuola Norm. Sup. Pisa* 13 (1959), pp. 115–162.

[99] T. L. van Noorden, I. S. Pop, A. Ebigbo, and R. Helmig. "An upscaled model for biofilm growth in a thin strip". In: *Water Resources Research* 46.6 (2010).

[100] J. M. Nordbotten and M. A. Celia. *Geological Storage of CO2: Modeling Approaches for Large-Scale Simulation*. Willey, 2012.

[101] S. Peng and R. Williams. "Direct measurement of floc breakage in flowing suspensions". In: *Journal of colloid and interface science* 166.2 (1994), pp. 321–332.

[102] W. Peukert, H. Schwarzer, and F. Stenger. "Control of aggregation in production and handling of nanoparticles". In: *Chemical Engineering and Processing* 44.2 (2005), pp. 245–252.

[103] S. Pop. "Regularization Methods in the Numerical Analysis of some Degenerate Parabolic Equations". PhD thesis. University of Heidelberg, 1998.

[104] V. Privman, H. L. Frisch, N. Ryde, and E. Matijević. "Particle adhesion in model systems. Part 13. Theory of multilayer deposition". In: *J. Chem. Soc., Faraday Trans.* 87.9 (1991), pp. 1371–1375.

[105] S. Qamar, I Angelov, M. Elsner, A Ashfaq, A Seidel-Morgenstern, and G Warnecke. "Numerical approximations of a population balance model for coupled batch preferential crystallizers". In: *Applied Numerical Mathematics* 59.3 (2009), pp. 739–753.

[106] N. Ray, A. Muntean, and P. Knabner. "Rigorous homogenization of a Stokes–Nernst–Planck–Poisson system". In: *Journal of Mathematical Analysis and Applications* 390.1 (2012), pp. 374–393.

[107] N. Ray, T. van Noorden, F. Radu, W. Friess, and P. Knabner. "Drug release from collagen matrices including an evolving microstructure". In: *ZAMM – Zeitschrift für Angewandte Mathematik und Mechanik* 93.10-11 (2013), pp. 811–822.

[108] N. Ray. "Colloidal Transport in Porous Media Modeling and Analysis". PhD thesis. University of Erlangen-Nuremberg, 2013.

[109] H. Reerink and J. Overbeek. "The rate of coagulation as a measure of the stability of silver iodide sols". In: *Discussions of the Faraday Society* 18 (1954), pp. 74–84.

[110] J. M. Rosenholm, C. Sahlgren, and M. Lindén. "Towards multifunctional, targeted drug delivery systems using mesoporous silica nanoparticles–opportunities & challenges". In: *Nanoscale* 2.10 (2010), pp. 1870–1883.

[111] S. Rothstein, W. Federspiel, and S. Little. "A unified mathematical model for the prediction of controlled release from surface and bulk eroding polymer matrices". In: *Biomaterials* 30.8 (2009), pp. 1657–1664.

[112] P. Schaaf and J. Talbot. "Surface exclusion effects in adsorption processes". In: *The Journal of Chemical Physics* 91.7 (1989), pp. 4401–4409.

[113] N. Shigesada, K. Kawasaki, and E. Teramoto. "Spatial segregation of interacting species". In: *Journal of Theoretical Biology* 79.1 (1979), pp. 83–99.

[114] M. Smith, G. Thomas, R. White, and D Ritonga. "Transport of Escherichia coli through intact and disturbed soil columns". In: *Journal of Environmental Quality* 14.1 (1985), pp. 87–91.

[115] M. Smoluchowski. "Versuch einer mathematischen Theorie der Koagulationskinetik kolloider Lösungen". In: *Z. Phys. Chem* 92 (1917), pp. 129–168.

[116] J. Soares and P. Zunino. "A mixture model for water uptake, degradation, erosion and drug release from polydisperse polymeric networks". In: *Biomaterials* 31.11 (2010), pp. 3032–3042.

[117] P. Spicer and S. Pratsinis. "Coagulation and fragmentation: Universal steady-state particle-size distribution". In: *AIChE Journal* 42.6 (1996), pp. 1612–1620.

[118] V. Ssemaganda, K. Holstein, and G. Warnecke. "Uniqueness of steady-state solutions for thermodynamically consistent Becker-Döring models". In: *Journal of Mathematical Physics* 52.8 (2011), p. 083304.

[119] W. Stumm. "Chemical interaction in particle separation". In: *Environ. Sci. Techn.* 11.12 (1977), pp. 1066–1070.

[120] S. Swanton. "Modelling colloid transport in groundwater; the prediction of colloid stability and retention behaviour". In: *Advances in Colloid and Interface Science* 54 (1995), pp. 129–208.

[121] V. Thomée. *Galerkin Finite Element Methods for Parabolic Problems*. Vol. 25. Springer Verlag, 1997.

[122] K. U. Totsche and I. Kögel-Knabner. "Mobile organic sorbent affected contaminant transport in soil". In: *Vadose Zone Journal* 3.2 (2004), pp. 352–367.

[123] K. Totsche, P. Knabner, and L. Kögel-Knabner. "The modeling of reactive solute transport with sorption to mobile and immobile sorbents: 2. Model discussion and numerical simulation". In: *Water Resources Research* 32.6 (1996), pp. 1623–1634.

[124] V. K. Vanag and I. R. Epstein. "Cross-diffusion and pattern formation in reaction–diffusion systems". In: *Physical Chemistry Chemical Physics* 11.6 (2009), pp. 897–912.

[125] E. Verwey, J. Overbeek, and K. van Nes. *Theory of the Stability of Lyophobic Colloids: the Interaction of Sol Particles having an Electric Double Layer*. Elsevier New York, 1948.

[126] E. Zeidler. *Nonlinear Functional Analysis and its Applications*. Springer Verlag, 1986.

[127] V. V. Zhikov. "On an extension of the method of two-scale convergence and its applications". In: *Sb. Math.* 191 (2000), p. 973.

Summary

Aggregation and fragmentation in reaction-diffusion systems posed in heterogeneous domains

Colloidal particles play an important role in a multitude of technological and biological processes. A main issue which influences the colloidal dynamics within a porous medium, e.g. the soil, are the processes of flocculation and fragmentation. Its accurate description in the context of advection-diffusion-reaction equations is not only of great impact since the microstructure of the porous medium depends on the attachment of flocculated particle clusters but also because contaminant transport is dictated by the dynamics of colloidal particles. Our research focuses on flocculation by investigating the effects of aggregation and fragmentation for a class of reaction diffusion systems posed in heterogeneous media.

At the microscopic level, we consider a system of non-linearly coupled partial differential equations to describe the transport (diffusion, convection, Soret and Dufour terms...) of colloidal particles as well as their interactions. In this thesis, the interactions are of two types:

(1) the classical Smoluchowski interactions;

(2) the deposition of the population of the biggest size colloids to the micropore surface.

The system is mathematically challenging due to the strong coupling induced by the presence of the thermal gradients, which makes our problem resembling very much the cross-diffusion and chemotaxis systems. Taking into consideration arrays of periodically-arranged microstructures (pores, perforations,...), we study the global solvability of our system posed at the microstructure level, and then use formal and rigorous homogenization asymptotics to scale it up to a macroscopic observable scale.

The resulting upscaled system of evolution equations has effective, computable coefficients that remember the volume (and, in the locally-periodic case, also the shape) of the microstructure. We verify the validity of the model by checking its forecast power against experimental data for column experiments by Elimelech and collaborators (cf. [60]).

To bring more microstructural information in our multiscale view on the materials and on the processes taking place there, we prepare a framework where one can use theoretical estimates (for instance, the corrector estimates for the homogenization procedure) to design controllable multiscale approximation schemes (based on MsFEM, for instance).

The thesis puts the rigorous mathematical foundations of a numerical multiscale framework able ultimately to detect the nonlocal effects induce by heating on diffusing and interacting populations of colloidal particles.

Index

List of Publications

1. O. Krehel, A. Muntean and P. Knabner. On modeling and simulation of flocculation in porous media, *Proceedings of XIX International Conference on Water Resources. (pp. 1-8)*, 2012.
2. O. Krehel, A. Muntean and T. Aiki. A thermo-diffusion system with Smoluchowski interactions: well-posedness and homogenization. *submitted to Networks and Heterogeneous Media*.
3. O. Krehel, A. Muntean and P. Knabner. Multiscale modeling of colloidal dynamics in porous media including aggregation and deposition. *submitted to Transport in Porous Media*.
4. O. Krehel and A. Muntean. Error control for the FEM approximation of an upscaled thermo-diffusion system with Smoluchowski interactions. *submitted to Numerische Mathematik*.
5. P.L. Curşeu, O. Krehel, J.H.M. Evers, A. Muntean. Cognitive Distance, Absorptive Capacity and Group Rationality: A Simulation Study. *submitted to PLOS ONE*.
6. A. Muntean, E.N.M. Cirillo, O. Krehel and M. Böhm. Pedestrians moving in the dark: Balancing measures and playing games on lattices, *Collective Dynamics from Bacteria to Crowds. (pp. 75-103), Springer Verlag*, 2014.
7. List of deal.II contributors: `http://dealii.org/authors.html`.

Acknowledgments

This thesis records the research I conducted as member of Applied Mathematics I, Department of Mathematics at the Friedrich Alexander University Erlangen-Nuremberg, Germany, throughout 2010-2012, and as member of CASA – Centre for Analysis, Scientific computing and Applications, Department of Mathematics and Computer Science, Eindhoven University of Technology throughout 2012-2014 within the Fronts and Interfaces in Science and Technology project. I would like to express my gratitude to all those who supported me throughout this work.

First of all, I would like to express my appreciation and gratitude to my supervisors Dr. habil. Adrian Muntean (Eindhoven) and Prof. Dr. Peter Knabner (Erlangen) for giving me the opportunity to work on the project as well as for their counsel and support. I am also thankful to my promotor Prof. Dr. Mark Peletier both for interesting discussions and his help in planning of my thesis.

I would like to thank my collaborators, Prof. Dr. Toyohiko Aiki (Tokyo), Dr. Emilio Cirillo (Rome), Prof. Dr. Petru L. Curşeu (Tilburg) and Prof. Dr. Kai U. Totsche (Jena) for sharing their expertises with me. I thank also Dr. Omar Lakkis, Dr. Chandrasekhar Venkataraman, Prof. Dr. Jan Zeman and Dr. Yuko Nagase for interesting discussions and helpful pointers in my research.

I am thankful to my colleagues from AM I for their help and support, especially to Nadja, Florian, Matthias, Fabian, Eduard, Simona, Estelle, Nicolae, and Serge. I thank Prof. Dr. Günther Grün and Dr. Alexander Prechtel as well as the secretaries Astrid and Cornelia for taking care of the administrative issues. The same big thanks I extend to my colleagues from CASA, especially to Patrick, Joep, Tasnim and Alessandro. I thank Prof. Dr. Sorin Pop and Dr. Georg Prokert for their useful advice and interesting discussions. I thank the secretaries of CASA, Marése and Enna, for all the administrative work.

I would like to thank my office mates throughout my PhD time for the pleasant and productive atmosphere. Thank you, Fabian, Joachim, Nicolae, Stefan, Tasnim, Patrick, Giovanni, and Joep.

I thank my friends and family for keeping me in good mood throughout this time. I thank my parents for supporting my scientific career and for providing me access to best education, letting me choose my own path.

Curriculum Vitae

Oleh Krehel was born at Lviv, Ukraine on April 29^{th}, 1986. He finished his Bachelor degree at Ivan Franko National University in Lviv, Ukraine in 2008. In 2010, he finished his M. Sc. in Applied Mathematics at the University of Hamburg, Germany with distinction.

In October 2010, he started his doctoral research in the Department of Applied Mathematics at the Friedrich-Alexander University of Erlangen-Nuremberg under the supervision of Prof. Dr. P. Knabner. In October 2012, he continued his research under the supervision of Dr.habil. A. Muntean and Prof. Dr. M.A. Peletier, the results of which are presented in this thesis.